

EUROPEAN SPACE AGENCY
CONTRACT REPORT

The work described in this report was done under ESA contract.
Responsibility for the contents resides in the author or organisation that prepared it.

Survey of Total Ionising Dose Tolerance of Power Bipolar Transistors and Silicon Carbide Devices for JUICE

TN6.4
SEE Test Report for
SiC Schottky Diode C4D40120D

Manufacturer: Cree

Date code/Lot code:
W13714 (UCL/GANIL/JULIC) and W14816 (CERN)

Report no.	Version	Date	NEO no.
069/2018	2.0	2019-06-07	NEO-14-086
Author	Coauthors	Checked by	Project
Michael Steffens +49 2251 18-222 michael.steffens@int.fraunhofer.de	--	Simone Schmitz	Survey of Total Ionising Dose Tolerance of Power Bipolar Transistors and Silicon Carbide Devices for JUICE (AO/1-7859/14/NL/SW)
Customer	Project management		
European Space Agency (ESA), contract number 4000113976/15/NL/RA	Project Coordinator: Stefan Höffgen (INT) ESA Technical Project Officer: Marc Poizat (ESA/ESTEC)		



Document Approval

Project	AO/1-8148/14/NL/SFe
Project Title	Survey of total ionising dose tolerance of power bipolar transistors and Silicon Carbide devices for JUICE
Doc ID	D6.4
Document Title	TN6.4 SEE Test Report for SiC Schottky Diode C4D40120D8
Issue.Revision	2.0
Date	2019-06-07

Prepared by	
	Name: Michael Steffens, INT

Approved by	
	Name: Stefan Höffgen, INT

Accepted by	
	Name: Marc Poizat, ESTEC

Version history

Table 1: Revision history

Version	Date	Changed by	Changes
0.1	2019-03-13	Steffens	Initial draft, Sections 1-5, Appendices A+B
1.0	2019-05-10	Steffens	Initial Release
2.0	2019-06-07	Steffens	Fixed header in Appendices, Added remark on total fluences in tests at CERN (Section 2.2 and 8.5)

Table of contents

Document Approval	2
1 Introduction	8
2 Summary	10
3 Sample preparations	14
4 Setup and Measurements	18
5 Tests at UCL.....	25
6 Tests at JULIC	31
7 Tests at GANIL.....	35
8 Tests at CERN	39
A Fraunhofer INT.....	44
B Appendix: Tests at UCL.....	47
C Appendix: Tests at JULIC	58
D Appendix: Tests at GANIL.....	63
E Appendix: Tests at CERN	74

List of figures

Figure 1: Safe operating voltage across the campaigns	11
Figure 2: Cross sections at $V_{GS} = 0$ V for each campaign.	12
Figure 3: The ESD package with the samples	14
Figure 4: Sample marking	15
Figure 5: DUT decapsulation.	16
Figure 6: Functional tests after paralene coating	17
Figure 7: Die pictures.....	17
Figure 8: Intended Test program	18
Figure 9: Detection Circuit	19
Figure 10: Test board layout	19
Figure 11: UCL: Measurement equipment/setup (including equipment for MOSFET/JFET tests) .	21
Figure 12: GANIL: Measurement equipment/setup (including equipment for MOSFET/JFET tests)	22
Figure 13: CERN: Measurement equipment/setup.....	23
Figure 14: JULIC: Measurement equipment/setup (including equipment for MOSFET/JFET tests)	24
Figure 15: UCL vacuum chamber with electrical feedthroughs.	25
Figure 16: Plot of LETs and Ranges in Silicon Carbide at UCL.	27
Figure 17: Overview of results: Heavy Ions at UCL.....	29
Figure 18: Beam line and irradiation site at the JULIC injector cyclotron, FZ Jülich	31
Figure 19: Schematic setup of the beam exit window at JULIC and the ionization chamber.....	32
Figure 20: The initial proton energy	32
Figure 21: Overview of results: Protons at JULIC	34
Figure 22: Test setup at GANIL.....	35
Figure 23: Results: Heavy Ions at GANIL.	37
Figure 24: Beam line and irradiation site at the H8 beam line, CERN.	39
Figure 25: Results: Heavy Ions at CERN.....	42
Figure 26: Run# 083, C4D40120D, Al-250, 1.1×10^4 ions/cm ² , DUT 11.1, VD= 600.0 V.....	48
Figure 27: Run# 084, C4D40120D, Al-250, 3.0×10^5 ions/cm ² , DUT 11.2, VD= 500.0 V.....	48
Figure 28: Run# 085, C4D40120D, Al-250, 9.8×10^3 ions/cm ² , DUT 12.1, VD= 500.0 V.....	49
Figure 29: Run# 086, C4D40120D, Al-250, 3.0×10^5 ions/cm ² , DUT 12.2, VD= 400.0 V.....	49
Figure 30: Run# 087, C4D40120D, Al-250, 3.0×10^5 ions/cm ² , DUT 12.2, VD= 450.0 V.....	50
Figure 31: Run# 088, C4D40120D, C-131, 3.0×10^5 ions/cm ² , DUT 13.1, VD= 600.0 V.....	50
Figure 32: Run# 089, C4D40120D, C-131, 3.0×10^5 ions/cm ² , DUT 13.1, VD= 750.0 V.....	51
Figure 33: Run# 090, C4D40120D, C-131, 3.0×10^5 ions/cm ² , DUT 13.1, VD= 900.0 V.....	51
Figure 34: Run# 091, C4D40120D, C-131, 3.0×10^5 ions/cm ² , DUT 13.1, VD= 1050.0 V.....	52
Figure 35: Run# 092, C4D40120D, C-131, 6.6×10^3 ions/cm ² , DUT 13.2, VD= 1050.0 V.....	52
Figure 36: Run# 093, C4D40120D, C-131, 3.1×10^5 ions/cm ² , DUT 14.1, VD= 900.0 V.....	53
Figure 37: Run# 096, C4D40120D, Cr-513, 1.0×10^5 ions/cm ² , DUT 14.1, VD= 300.0 V	53
Figure 38: Run# 097, C4D40120D, Cr-513, 1.0×10^5 ions/cm ² , DUT 14.1, VD= 400.0 V	54
Figure 39: Run# 098, C4D40120D, Cr-513, 3.1×10^5 ions/cm ² , DUT 14.2, VD= 300.0 V	54
Figure 40: Run# 099, C4D40120D, Kr-769, 1.0×10^5 ions/cm ² , DUT 14.2, VD= 100.0 V.....	55
Figure 41: Run# 100, C4D40120D, Kr-769, 1.0×10^5 ions/cm ² , DUT 14.2, VD= 200.0 V.....	55
Figure 42: Run# 101, C4D40120D, Kr-769, 1.0×10^5 ions/cm ² , DUT 14.2, VD= 250.0 V.....	56
Figure 43: Run# 102, C4D40120D, Kr-769, 1.0×10^5 ions/cm ² , DUT 15.1, VD= 250.0 V.....	56
Figure 44: Run# 103, C4D40120D, Kr-769, 3.1×10^5 ions/cm ² , DUT 15.2, VD= 200.0 V.....	57
Figure 45: Run# 038, C4D40120D, p, 6.7×10^9 p/cm ² , DUT 1.1, VD= 1200.0 V	61
Figure 46: Run# 039, C4D40120D, p, 1.1×10^{11} p/cm ² , DUT 1.2, VD= 900.0 V	61
Figure 47: Run# 040, C4D40120D, p, 1.1×10^{11} p/cm ² , DUT 2.1, VD= 900.0 V	62
Figure 48: Run# 041, C4D40120D, p, 1.1×10^{11} p/cm ² , DUT 2.2, VD= 900.0 V	62

Figure 49: SRIM2013 simulations of the Ganil Xenon tests on SiC	63
Figure 50: Run# 108, C4D40120D, Xe 0 mmAl, 150 mm Air, 3.0e+05 ions/cm ² , DUT 16.1, VD= 200.0 V	65
Figure 51: Run# 109, C4D40120D, Xe 0 mmAl, 150 mm Air, 3.0e+05 ions/cm ² , DUT 16.2, VD= 150.0 V	65
Figure 52: Run# 110, C4D40120D, Xe 0 mmAl, 150 mm Air, 3.0e+05 ions/cm ² , DUT 17.1, VD= 150.0 V	66
Figure 53: Run# 112, C4D40120D, Xe 0 mmAl, 150 mm Air, 3.0e+05 ions/cm ² , DUT 17.1, VD= 200.0 V	66
Figure 54: Run# 113, C4D40120D, Xe 0 mmAl, 150 mm Air, 3.0e+05 ions/cm ² , DUT 16.2, VD= 300.0 V	67
Figure 55: Run# 114 C4D40120D, Xe 0 mmAl, 150 mm Air, 3.0e+05 ions/cm ² , DUT 17.2, VD= 175.0 V	67
Figure 56: Run# 115, C4D40120D, Xe 0 mmAl, 150 mm Air, 6.0e+05 ions/cm ² , DUT 18.1, VD= 175.0 V	68
Figure 57: Run# 116, C4D40120D, Xe 500 mmAl, 180 mm Air, 6.0e+05 ions/cm ² , DUT 18.1, VD= 100.0 V	68
Figure 58: Run# 117, C4D40120D, Xe 500 mmAl, 180 mm Air, 6.0e+05 ions/cm ² , DUT 18.1, VD= 150.0 V	69
Figure 59: Run# 118, C4D40120D, Xe 500 mmAl, 180 mm Air, 6.0e+05 ions/cm ² , DUT 18.2, VD= 200.0 V	69
Figure 60: Run# 119, C4D40120D, Xe 400 mmAl, 95 mm Air, 6.0e+05 ions/cm ² , DUT 19.1, VD= 150.0 V	70
Figure 61: Run# 120, C4D40120D, Xe 400 mmAl, 95 mm Air, 6.0e+05 ions/cm ² , DUT 19.1, VD= 175.0 V	70
Figure 62: Run# 121, C4D40120D, Xe 400 mmAl, 95 mm Air, 6.0e+05 ions/cm ² , DUT 19.1, VD= 200.0 V	71
Figure 63: Run# 122, C4D40120D, Xe 400 mmAl, 95 mm Air, 6.0e+05 ions/cm ² , DUT 19.2, VD= 175.0 V	71
Figure 64: Run# 123, C4D40120D, Xe 500 mmAl, 180 mm Air, 6.0e+05 ions/cm ² , DUT 19.2, VD= 125.0 V	72
Figure 65: Run# 124, C4D40120D, Xe 500 mmAl, 180 mm Air, 6.0e+05 ions/cm ² , DUT 20.1, VD= 125.0 V	72
Figure 66: SRIM2013 simulations of Xenon ions of 10 GeV/n energy on Si and SiC	74
Figure 67: Run# 028, C4D40120D, Xe 0 °, 3.1e+04 ions/cm ² , DUT 1.1, VD= 1200.0 V.....	76
Figure 68: Run# 029, C4D40120D, Xe 0 °, 8.0e+03 ions/cm ² , DUT 1.2, VD= 1000.0 V.....	76
Figure 69: Run# 030, C4D40120D, Xe 0 °, 8.1e+03 ions/cm ² , DUT 1.2, VD= 1100.0 V.....	77
Figure 70: Run# 031, C4D40120D, Xe 0 °, 8.0e+03 ions/cm ² , DUT 1.2, VD= 1150.0 V.....	77
Figure 71: Run# 032, C4D40120D, Xe 0 °, 1.6e+04 ions/cm ² , DUT 1.2, VD= 1200.0 V.....	78
Figure 72: Run# 033, C4D40120D, Xe 0 °, 8.0e+03 ions/cm ² , DUT 1.2, VD= 1300.0 V.....	78
Figure 73: Run# 034, C4D40120D, Xe 0 °, 2.8e+03 ions/cm ² , DUT 2.1, VD= 1250.0 V.....	79
Figure 74: Run# 035, C4D40120D, Xe 0 °, 1.5e+04 ions/cm ² , DUT 2.2, VD= 1200.0 V.....	79
Figure 75: Run# 050, C4D40120D, Xe 42 °, 3.0e+03 ions/cm ² , DUT 3.1, VD= 1150.0 V.....	79
Figure 76: Run# 051, C4D40120D, Xe 42 °, 2.7e+03 ions/cm ² , DUT 3.1, VD= 1200.0 V.....	80
Figure 77: Run# 052, C4D40120D, Xe 42 °, 2.7e+03 ions/cm ² , DUT 3.1, VD= 1250.0 V.....	80
Figure 78: Run# 053, C4D40120D, Xe 42 °, 2.7e+03 ions/cm ² , DUT 3.1, VD= 1300.0 V.....	80
Figure 79: Run# 054, C4D40120D, Xe 42 °, 2.6e+03 ions/cm ² , DUT 3.1, VD= 1350.0 V.....	81
Figure 80: Run# 055, C4D40120D, Xe 42 °, 2.7e+03 ions/cm ² , DUT 3.1, VD= 1400.0 V.....	81
Figure 81: Run# 056, C4D40120D, Xe 42 °, 2.7e+03 ions/cm ² , DUT 3.1, VD= 1450.0 V.....	81
Figure 82: Run# 057, C4D40120D, Xe 42 °, 2.7e+03 ions/cm ² , DUT 3.1, VD= 1500.0 V.....	82
Figure 83: Run# 058, C4D40120D, Xe 42 °, 2.9e+03 ions/cm ² , DUT 3.2, VD= 1200.0 V.....	82
Figure 84: Run# 059, C4D40120D, Xe 42 °, 2.7e+03 ions/cm ² , DUT 3.2, VD= 1250.0 V.....	82

Figure 85: Run# 060, C4D40120D, Xe 42 °,, 2.8e+03 ions/cm2 , DUT 3.2, VD= 1300.0 V.....	83
Figure 86: Run# 061, C4D40120D, Xe 42 °,, 2.8e+03 ions/cm2 , DUT 3.2, VD= 1350.0 V.....	83
Figure 87: Run# 062, C4D40120D, Xe 42 °,, 2.8e+03 ions/cm2 , DUT 3.2, VD= 1400.0 V.....	83
Figure 88: Run# 063, C4D40120D, Xe 42 °,, 2.9e+03 ions/cm2 , DUT 3.2, VD= 1450.0 V.....	84
Figure 89: Run# 064, C4D40120D, Xe 42 °,, 5.5e+03 ions/cm2 , DUT 3.2, VD= 1500.0 V.....	84

List of tables

Table 1: Revision history	2
Table 2: Summary	10
Table 3: Sample shipment.....	14
Table 4: Sample marking:	15
Table 5: Measurement parameters.....	20
Table 6: UCL: Measurement equipment and instrumentation.....	21
Table 7: GANIL: Measurement equipment and instrumentation	22
Table 8: CERN: Measurement equipment and instrumentation.....	22
Table 9: JULIC: Measurement equipment and instrumentation.....	24
Table 10: UCL: Ion energies, LETs and ranges in Silicon Carbide covered by 10 µm Paralene: ...	26
Table 11: UCL: Irradiation steps of SiC Schottky Diode C4D40120D.	28
Table 12: Results: Heavy Ions at UCL - Calculated cross sections Calculated with the formulae in ESCC25100 with CL=0.95 and flux uncertainty of 10% (approx. worst case)	30
Table 13: Results of simulations of the LET with package thickness.	33
Table 14: JULIC: Irradiation steps of SiC Schottky Diode C4D40120D.	34
Table 15: Results: Heavy Ions at UCL - Calculated cross sections Calculated with the formulae in ESCC25100 with CL=0.95 and flux uncertainty of 10% (approx. worst case)	34
Table 16: GANIL: Beam characteristics.....	36
Table 17: GANIL: Irradiation steps of SiC Schottky Diode C4D40120D.....	36
Table 18: Results: Heavy Ions at GANIL - Calculated cross sections	37
Table 19: CERN: Irradiation steps of SiC Schottky Diode C4D40120D.....	41
Table 20: Results: Heavy Ions at CERN - Calculated cross sections	42
Table 21: Mold material of example C2M0080120D. Values indicated with * are estimates.....	59
Table 22: Results of GRAS simulations of the LET with package thickness.....	59
Table 23: Intermediate results of MULASSIS simulations of the proton energy with package thickness.	59
Table 24: Results of SRIM simulations of the LET with package thickness.....	60
Table 25: GANIL: Beam characteristics.....	63

1 Introduction

1.1 Scope

The Fraunhofer Institute for Technological Trend Analysis (INT) carried out a series of Single Event Effects tests with protons and heavy ions on SiC Schottky Diode C4D40120D from Cree for the ESA project "Survey of Total Ionizing Dose Tolerance of Power Bipolar Transistors and Silicon Carbide Devices for JUICE" (ESA-TOPSIDE, AO/1-8148/14/NL/SFe) under contract number 4000113976/15/NL/RA.

This reports documents the preparation, execution and the results of these tests.

1.2 Applicable Documents

- [AD1] ITT/AO/1-8148/14/NL/SFe "Statement of work: Survey of Total Ionizing Dose Tolerance of Power Bipolar Transistors and Silicon Carbide Devices for JUICE"
- [AD2] Proposal for ITT/AO/1-8148/14/NL/SFe, Fraunhofer INT

1.3 Reference Documents

- [1] Website of Fraunhofer INT: <http://www.int.fraunhofer.de>
- [2] Guidelines for Evaluating and Expressing the Uncertainty of NIST Measurement Results, B.N. Taylor and C.E. Kuyatt, NIST Technical Note 1297, 1994, <http://www.nist.gov/pml/pubs/tn1297/index.cfm>.
- [3] ESCC Basic Specification No. 25100, issue 2, October 2014
- [4] Datasheet of SiC Schottky Diode C4D40120D, "C4D40120D Silicon Carbide Schottky Diode Z-Rec® Rectifier", Cree, Rev. E
- [5] TN3.4 "SEE (HI) Test Plan C4D40120D (Schottky Diode)", Issue 1, Revision 4, 2018-04-15
- [6] TN3.10 "SEE (p) Test Plan C4D40120D (Schottky Diode)", Issue 1, Revision 1, 2017-07-25
- [7] Casey et. al., "Schottky Diode Derating for Survivability in a Heavy Ion Environment", IEEE TNS vol. 62, no.6, pp. 2482-2489 (2015)
- [8] Website of the HIF Facility at UCL: <http://www.cyc.ucl.ac.be/HIF/HIF.php>, last accessed: 2019-01-17
- [9] SRIM 2013, www.srim.org, detailed in Ziegler et. Al., "SRIM - The stopping and range of ions in matter (2010)", Nuclear Instruments and Methods in Physics Research Section B, Volume 268, Issue 11-12, p. 1818-1823.016-12-08)
- [10] Website of SPENVIS, <https://www.spennis.oma.be/>
- [11] Website of the PSTAR database at NIST, <https://physics.nist.gov/PhysRefData/Star/Text/PSTAR.html>
- [12] Website of the GANIL facility for irradiation of electronic components: <https://www.ganil-spiral2.eu/en/industrial-users-2/applications-industrielles/irradiation-of-electronic-components/>
- [13] Website of the H8 beam line at CERN: sba.web.cern.ch/sba/BeamsAndAreas/resultbeam.asp?beamline=H8

- [14] García Alía et al., “Ultraenergetic Heavy-Ion Beams in the CERN Accelerator Complex for Radiaiton Effects Testing”, IEEE TNS, vol. 66, No. 1, p. 458, 2018. DOI: 10.1109/TNS.2018.2883501
- [15] Fernánzet-Martinez et al., “Characterization of the Ultra-High Energy Xe beam of the CERN NAH8 line”, Report for users – ongoing analysis

2 Summary

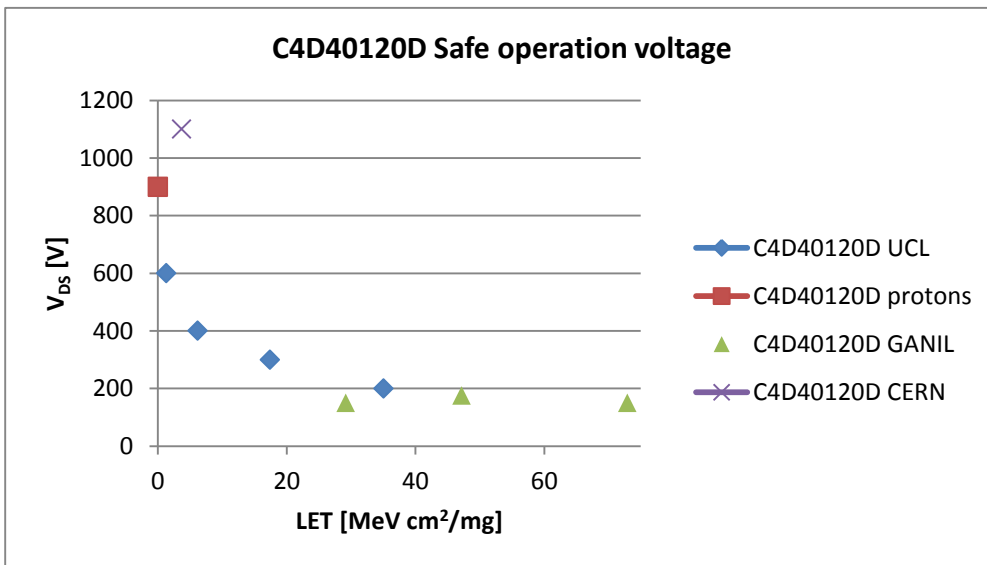
Table 2: Summary

Test Report Number	069/2018
Project (INT)	NEO-14-086
Customer	European Space Agency (ESA), contract number 4000113976/15/NL/RA
Contact	Project Coordinator: Stefan Höffgen (INT) ESA Technical Project Officer: Marc Poizat (ESA/ESTEC)
ESA project / contract number	AO/1-8148/14/NL/SFe 4000113976/15/NL/RA
Device under test	C4D40120D
Family	SiC Schottky Diode
Technology	1.2kV Schottky Rectifier
Package	TO247-3
Date code / Wafer lot	W13714 (UCL/GANIL/JULIC) and W14816 (CERN)
SN	UCL: #11, #12, #13, #14, #15 GANIL: #16, #17, #18, #19, #20 CERN: #1, #2, #3 (delivery #2) JULIC: #1, #2 (previously Gamma irradiated)
Manufacturer	Cree
Irradiation test house	Fraunhofer INT
Radiation source	UCL, CERN and GANIL: Heavy Ions, JULIC: Protons
Irradiation facility	UCL, CERN, GANIL, JULIC
Generic specification	ESCC 25100 Iss. 2
Detail specification	MIL-STD-750-1 w/CHANGE 5, Method 1080.1
Test plan	TN3.4 "SEE (HI) Test Plan C4D40120D (Schottky Diode)", Issue 1, Revision 4, 2018-04-15 TN3.10 "SEE (p) Test Plan C4D40120D (Schottky Diode)", Issue 1, Revision 1, 2017-07-25
Single/Multiple Exposure	Multiple
Parameters tested	Reverse current
Dates	UCL: 2018-04-16 – 2018-04-17 CERN: 2017-11-30 – 2017-12-01

	GANIL: 2018-06-06 – 2018-06-07 JULIC: 2017-09-19 – 2017-09-20
--	--

2.1 Overview of results

Figure 1: Safe operating voltage across the campaigns



The heavy ion tests at UCL with the SiC Schottky Diode C4D40120D were performed with 4 different LETs at a reduced target fluence of 3E5 ions/cm². Considering the rather low number of devices, that number of LETs was only achievable by testing each of the two diodes per package separately, thus effectively doubling the number of available devices. We see no correlation that diode #2 in any package is more likely to fail if diode #1 already failed.

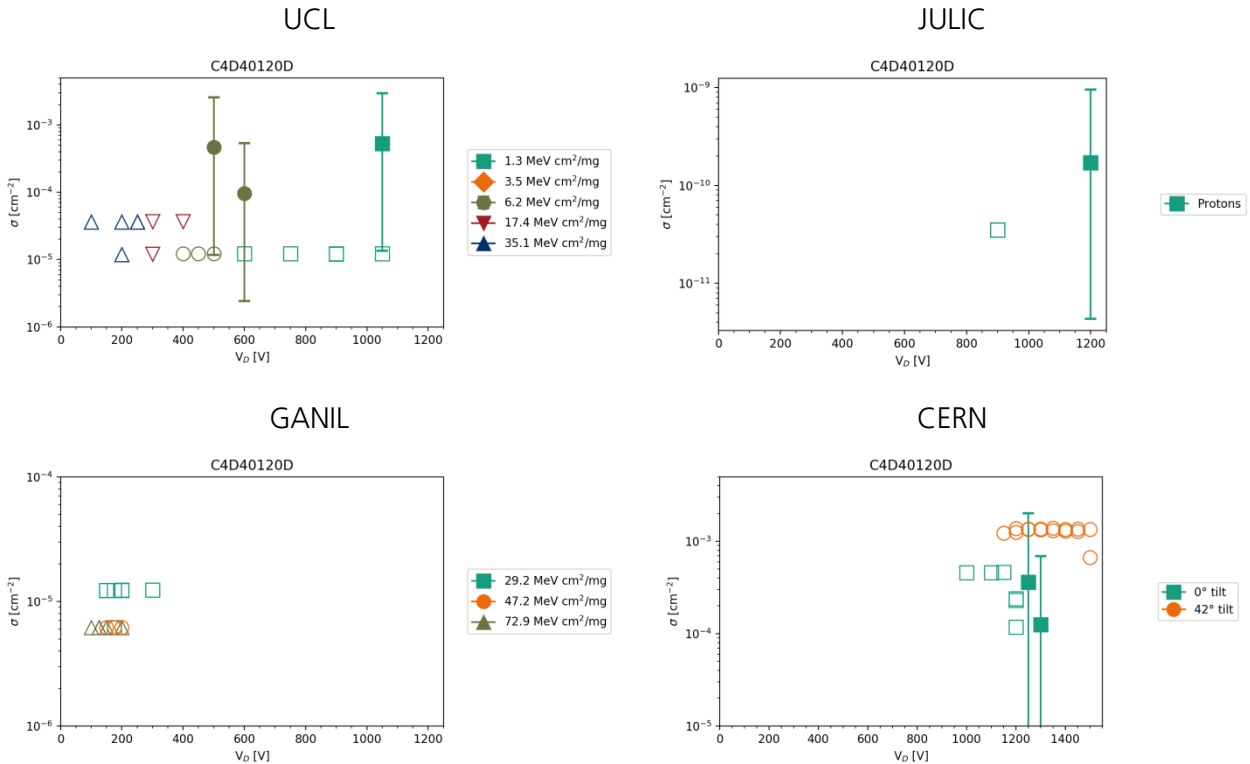
The voltage achievable for a safe operation up to the target fluence decreases from 900 V with carbon ions (LET = 1.3 MeV cm²/mg) down to 200 V with Krypton (LET = 35.1 MeV cm²/mg). LETs are given in SiC according to Table 10. Results at 250 V with Krypton show a pronounced increase of the leakage current. To define the safe operating voltage we count these as failed.

The voltage achievable for a safe operation with the GANIL Xenon ions decrease down to 125 V at these larger LETs and the proton, UCL and GANIL results give roughly an overall trend of the minimum voltage for safe operation.

Tests at CERN were performed with DUTs from a different lot. A striking difference to the previous tests is the increased voltage of safe operation of 1100 V. However when looking at all devices tested at CERN, all of them show a similar behaviour. Lot-to-lot variability might thus not be an explanation for this.

Additionally, in tests with tilted devices at CERN the DUTs could be operated at voltages much larger than the nominal rating.

Figure 2: Cross sections at $V_{GS} = 0$ V for each campaign. Filled symbols mark the cross section in case of device failures and error bars mark the upper lower limits. Open symbols mark the cross section upper limit in case no failure was observed during a run.



2.2 Comments

- **All campaigns:**
 - Huge sensitivity in conjunction with a limited number of devices led to major deviations from the intended test plan.
 - Destructive events could not be mitigated.
- **Tests at JULIC:**
 - Tests were performed with packaged DUTs.
 - Test devise were previously tested with Co-60 to 1 Mrad(Si).
- **Tests at GANIL:**
 - Some errors in the log files from GANIL with runs #114 and #115 (see Table 18 on page 37)
- **Tests at CERN:**
 - Tests were performed with packaged DUTs.

- The effective fluences across the tests were $<3.2E4$ ions/cm². This very low fluence might be an explanation for the increased “safe operation” levels observed in these tests compared to the other test campaigns.
- Most device failures occurred at the first spill of beam. Properly deducing the fluence of failure and thus the cross sections of the devices is not possible in these cases, so the cross sections in case of failures given for the CERN results should only be seen as a rough order of magnitude.
- Additional tests with tilted devices were performed. In these the DUTs could be operated at higher voltages without failures than at normal incidence.

3 Sample preparations

3.1 Sample shipment

A total of 30 Samples were procured by INT at a commercial supplier (Mouser Electronics) for the conduction of these tests for ESA. The parcel contained devices with one identification code (W13714) and was used for the campaigns at UCL, GANIL and JULIC. For the campaign at CERN 20 additional samples were procured, but samples from the same batch were no longer available. For that campaign the identification code was W14816. Due to the devices being so-called “commercial-off-the-shelf” (COTS) devices, it is not clear whether this identifies the wafer or just the packaging).

Table 3: Sample shipment

Samples ordered	Samples received	Samples sent back
December 2015	December 2015	still at INT (partially used for other tests in this project)
November 2017	November 2017	still at INT

Figure 3: The ESD package with the samples



3.2 Sample identification/ marking

The samples were soldered to adapter pins, to ease the mounting to the board, exchanging, plugging and storage of the samples.

The samples were colour marked to differentiate the samples between each other and to separate the samples of the different campaigns or types.

Figure 4: Sample marking



Table 4: Sample marking: Due to a limited number of samples, the DUTs tested with protons were previously used for a 1 Mrad(Si) TID campaign. Only DUTs used in the tests of this report are shown.

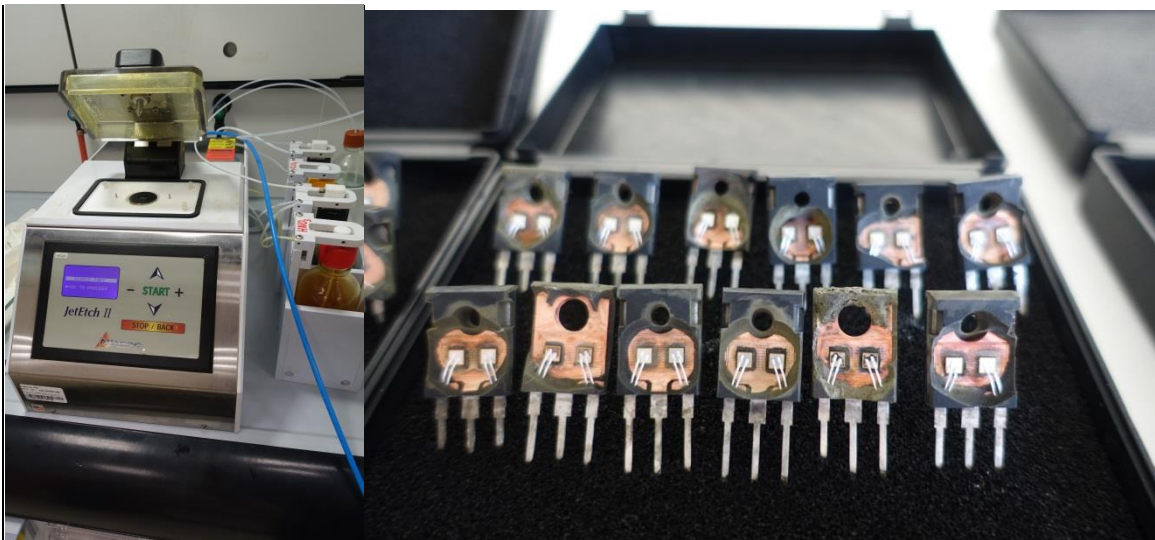
Condition	S/N	Color Code	Comment
W13714			
UCL	11	[Red]	decap, coated
	12	[Red]	decap, coated
	13	[Red]	decap, coated
	14	[Red]	decap, coated
	15	[Red]	decap, coated
GANIL	16	[Red]	decap, coated
	17	[Red]	decap, coated
	18	[Red]	decap, coated
	19	[Red]	decap, coated
	20	[Red]	decap, coated
JULIC	1	[Red]	non-decap, previously used for TID
	2	[Red]	non-decap, previously used for TID
W14816			
CERN	1	[Red]	non-decap
	2	[Red]	non-decap
	3	[Yellow]	non-decap

3.3 Sample decapsulation and preparation

In preparation for the heavy ion test campaign at UCL and GANIL, the DUTs were decapsulated and parylene coated.

DUT decapsulation was performed at INT using a Nisene JetEtch II (Figure 5). The JetEtch II uses sprays of acid, in our case a 2:1 mixture of sulfuric to nitric acid, to remove the capping layers covering the die and the active region of the device without inducing mechanical stress on the device. Decapsulation was performed with the device already soldered onto their respective socket adapters.

Figure 5: DUT decapsulation. Left side: Nisene JetEtch II at INT. Right side: batch of decapsulated C4D40120D



For etching, sulfuric acid at a flow of 5 ml/min was applied for 360 s at a temperature of 90°C.

After decapsulation the functionality of all DUTs was checked. Due to the missing insulation provided by the package material, only tests at low voltage to prevent corona discharges were performed. All 12 decapsulated devices passed these functional tests and were considered for the coating process.

Parylene coating was performed by the “Advanced Chip & Wire Bonding” group, department “System Integration and Interconnection Technologies (SIIT)”, at Fraunhofer IZM in Berlin.

Tests of the reverse current performed at INT after receiving the coated samples, are shown in Figure 6. Two diodes are in each package and these were tested separately. All devices passed this test and were considered for the SEE tests.

Figure 6: Functional tests after paralene coating

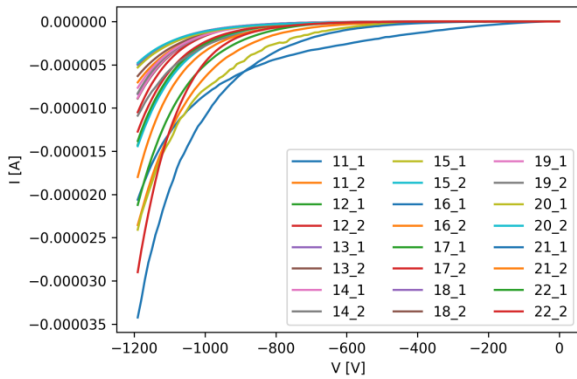
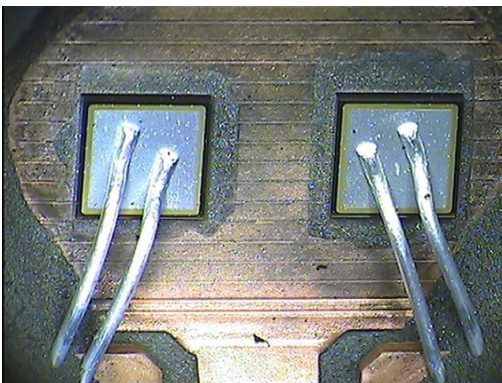
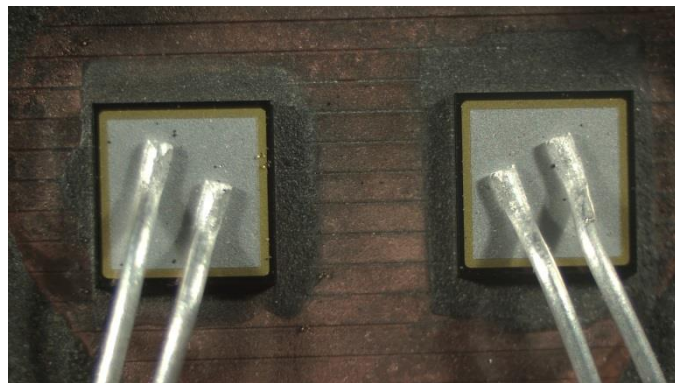


Figure 7: Die pictures. Images were taken with different optical microscopes. The camera used before the tests has a lower quality and resolution.



DUT #12 before tests at UCL



DUT #12 after tests at UCL (Top: left diode, bottom: right diode)

Figure 7 shows microscopic images of one DUT (#12) after parylene coating and after the tests at UCL wherein this DUT showed destructive failure. The surface of the DUT does not show signs indicating this destructive failure.

3.4 Sample safekeeping

The samples were stored in an Electro-Static Discharge (ESD) box (Figure 5) to handle them safely during the test, the interim storage after the last measurement and the final shipment.

4 Setup and Measurements

The test approach and setup covered in this section is mostly independent of the facility.

The tests performed with Heavy ions or protons aimed primarily at determining the safe operating voltage range rather than getting detailed cross sections for each setting and LET. This is mostly due to the high sensitivity of most of the SiC devices studied in this project to even moderate LETs.

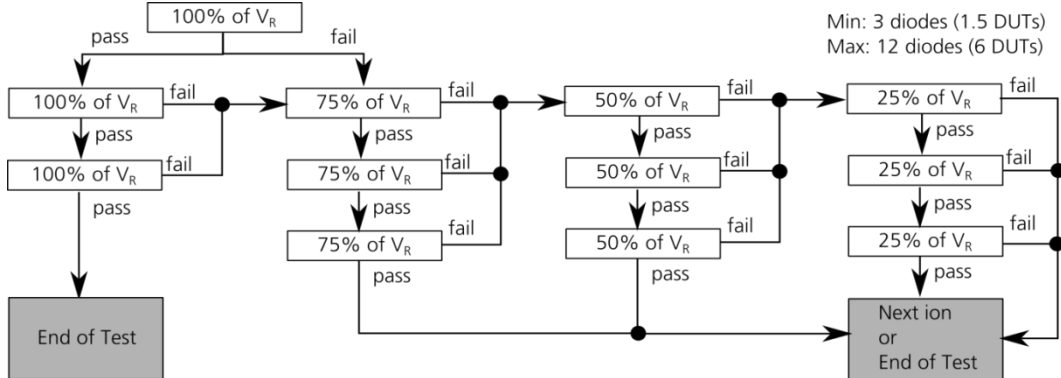
Due to a limited number of devices and having destructive failures which could not be mitigated, the required number of 3 samples to check the pass compliance of each test is not reached in any case.

4.1 Intended test program

The test logic is shown in Figure 8. As there are no applicable test standards or MIL test methods concerning Schottky diode SEE tests, the intended test logic follows mostly the approach for silicon Schottky diodes of Casey et. al. [7].

However during the tests and due to the high sensibility of the SiC diodes, this test program was in the end not followed.

Figure 8: Intended Test program



After each test step, a post-irradiation-stress-test is planned with the reverse voltage swept to its maximum rating.

4.2 Test Board and Detection Circuit

A custom-build printed-circuit board (Figure 10) was manufactured to

- bias the samples according to the circuit-layout of the irradiation test plan [5] [6]
- fix the samples at the radiation source
- switch between the samples and connect the respectively active sample to the external setup
- detect destructive events

To reduce the number of parts required for testing, the two diodes in each DUT are biased separately (Figure 9). No mitigation of destructive events is foreseen.

Figure 9: Detection Circuit

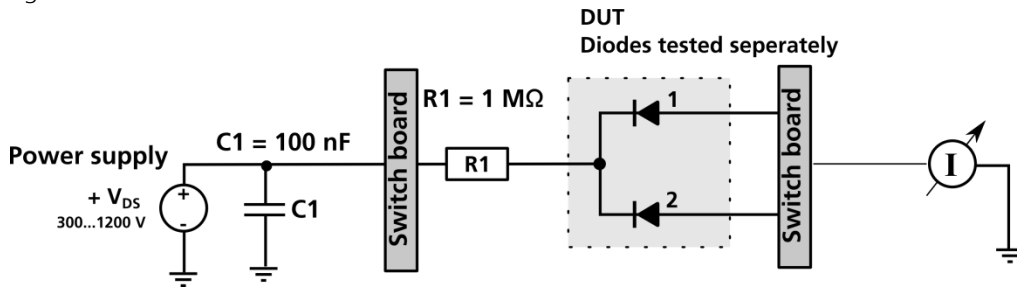
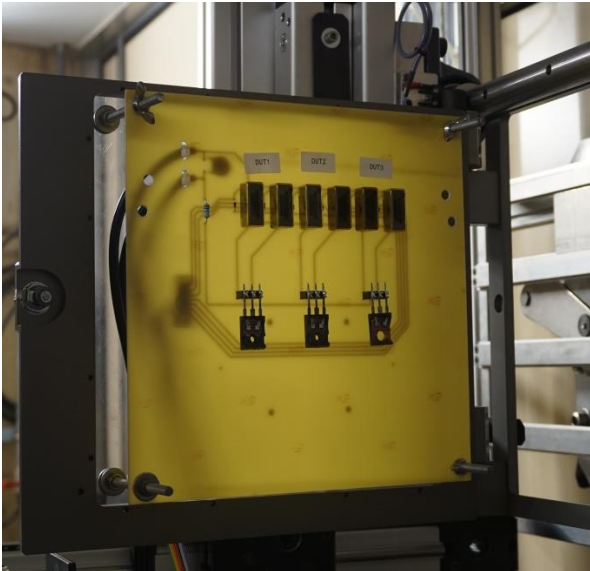


Figure 10: Test board layout Top left side: proton tests at JULIC, Top right side: Heavy ion tests at UCL, bottom left: Heavy ion tests at GANIL





The boards used for the Heavy Ion and proton tests are functionally identical, but the proton board featured additional holes for four ionization chambers. The DUT was then positioned off-center from the beam, such that all ionization chambers and the DUT position are at the same distance from the center, thus allowing to calculate the proton flux at the DUT position without a fixed installation at the facility which would allow to do that. As a drawback, only one DUT position on the board could be used at a time.

For protons the board was at a distance of 1.8 m from the beam line exit window. Due to interaction in air and the exit window, the proton beam with initial energy 45 MeV was then broadened and reduced in energy to approx. 39 MeV.

The DUTs were exposed to the protons in package, thus when passing the package and hitting the sensitive volume of the devices, the proton energy is further reduced.

Calculations of the LETs in SiC are shown in the respective sections of the campaigns.

4.3 Measurement parameters

Parameters are continuously monitored during the runs. V_D is only indicated at the respective runs, I_D are shown in the appendices.

Table 5: Measurement parameters. Based on [4], taken from [5][6]

No.	Characteristics	Symbol	Remark
1	Reverse Voltage	V_D	Set according to test flow
2	Reverse Current	I_D	Monitored, typ. 35 μ A @ 1200 V, max. 200 μ A @ 1200 V

4.4 Measurement equipment

The test equipment is shown in Table 6 - Table 9 and Figure 11 - Figure 14.

The due date of the calibration can change from campaign to campaign if a new calibration was performed in the time between.

Table 6: UCL: Measurement equipment and instrumentation

Equipment	Manufacturer	Model	INT-Code	Calibr. due	Measurement
High Power System Source Meter	Keithley	2657A	E-SMU-012	03/2018	V_b, I_b
Data Acquisition/Switch unit	Agilent	34970A	E-SMF-002	n/a	Switch matrix
Triple Output Power Supply	Agilent	E3631A	E-PS3-002	n/a	Power supply of relays

Figure 11: UCL: Measurement equipment/setup (including equipment for MOSFET/JFET tests)

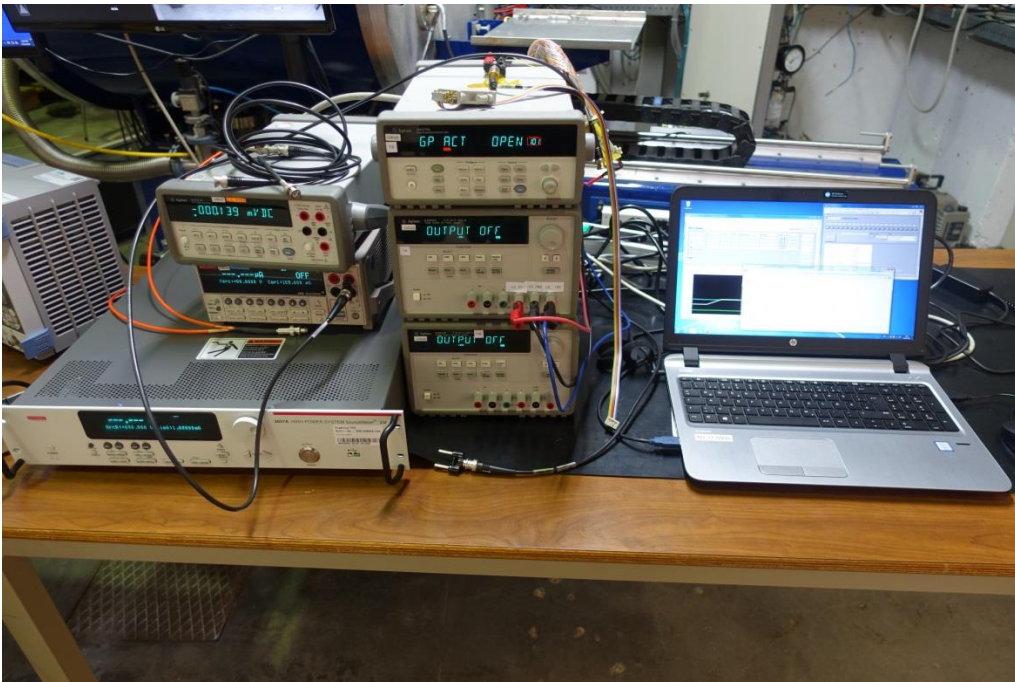


Table 7: GANIL: Measurement equipment and instrumentation

Equipment	Manufacturer	Model	INT-Code	Calibr. due	Measurement
High Power System Source Meter	Keithley	2657A	E-SMU-012	03/2020	V_D, I_D
Data Acquisition/Switch unit	Agilent	34970A	E-SMF-002	n/a	Switch matrix
Triple Output Power Supply	Agilent	E3631A	E-PS3-001	n/a	Power supply of of relais

Figure 12: GANIL: Measurement equipment/setup (including equipment for MOSFET/JFET tests)



Table 8: CERN: Measurement equipment and instrumentation

Equipment	Manufacturer	Model	INT-Code	Calibr. due	Measurement
High Power System Source Meter	Keithley	2657A	E-SMU-012	03/2020	V_D, I_D

Equipment	Manufacturer	Model	INT-Code	Calibr. due	Measurement
Data Acquisition/Switch unit	Agilent	34970A	E-SMF-002	n/a	Switch matrix
Triple Output Power Supply	Agilent	E3631A	E-PS3-001	n/a	Power supply of relais
Step motor	ISEL	LES4	--	n/a	Moving samples along 1 direction
Linear guide	ISEL	IT116 G	--	n/a	Moving samples along 1 direction

Figure 13: CERN: Measurement equipment/setup.

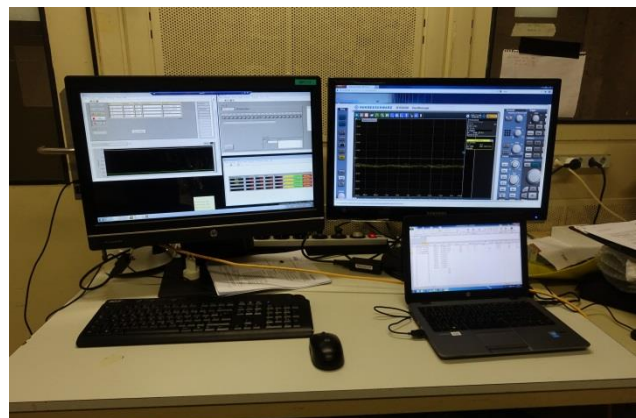
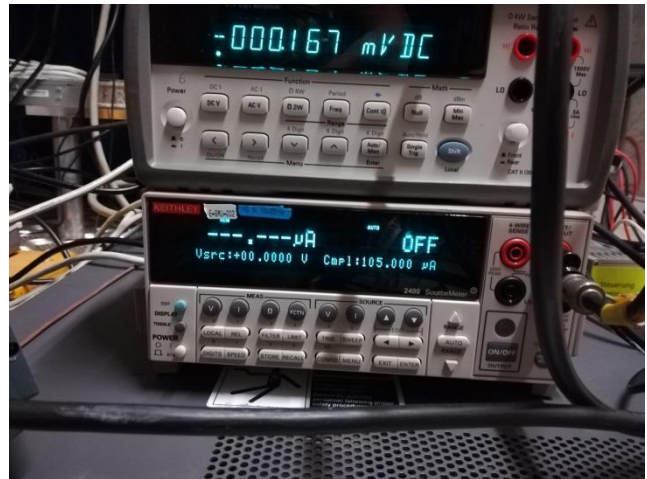
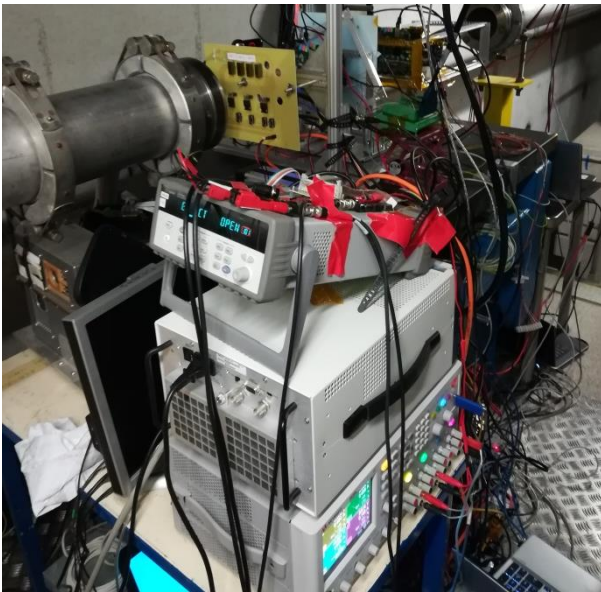
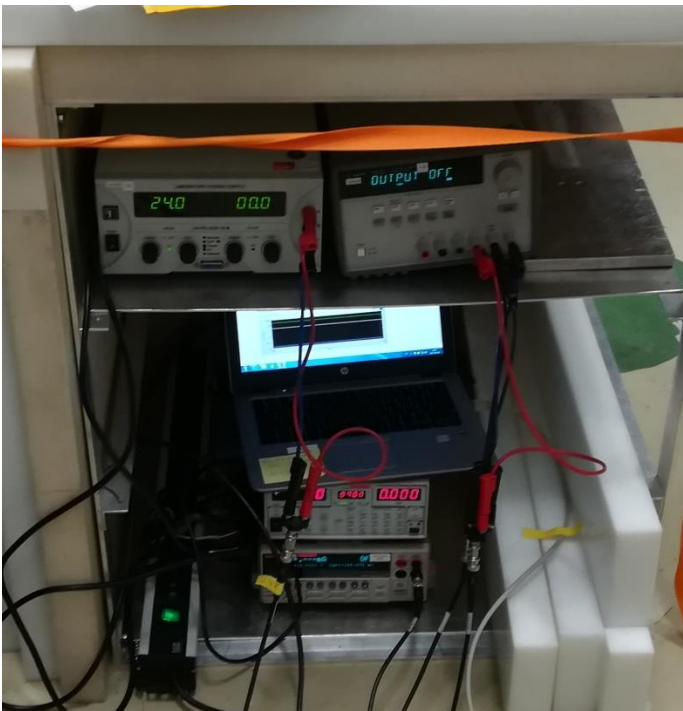


Table 9: JULIC: Measurement equipment and instrumentation

Equipment	Manufacturer	Model	INT-Code	Calibr. due	Measurement
5 kV Power supply	Keithley	2290E-5	E-PS1-030	10/2017	V_D, I_D
Laboratory Power Supply	EA	EA-PS-3032-10B	E-PS1-001	n/a	Control of relays

As only one DUT was on the board, no switch matrix was included in the setup, and the power supplies were only used to power the relays, not for switching between DUTs.

Figure 14: JULIC: Measurement equipment/setup (including equipment for MOSFET/JFET tests)



4.5 Measurement procedures

Bias conditions of diode were fixed for each step. When no destructive events occurred during a run, a post-irradiation-stress test was scheduled. In some instances across the campaigns, that test might not have been performed. These instances are commented in the respective sections.

5 Tests at UCL

5.1 Facility

The main heavy ion test was performed at the HIF facility of the CYCLONE cyclotron of the Université catholique de Louvain (UCL) in Louvain-la-Neuve.

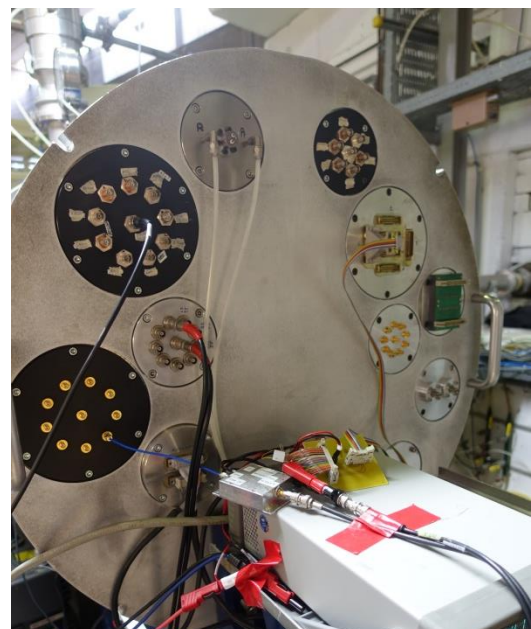
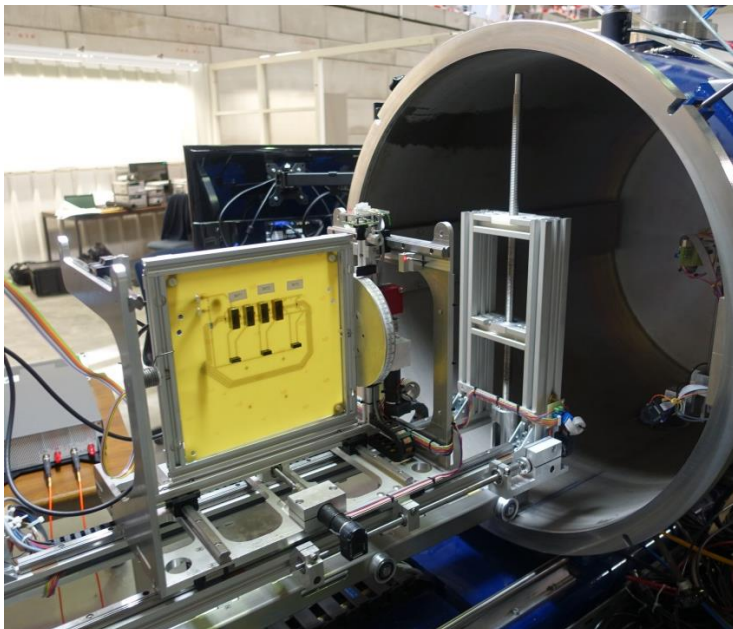
The facility can provide selected heavy ion beams from Carbon to Xenon in a particle cocktail with mass/charge ratio of approx. $M/Q=3.3$, allowing to switch from ion species to ion species quickly within the cocktail.

The experimental setup at the facility consists of the main vacuum chamber with a sample holder, which is moveable in x- and y-direction and can be tilted along one axis.

Feedthroughs can be used to connect boards within the enclosure with outside instrumentation (Figure 15).

Users can start and stop the irradiation from the user station next to the test chamber, other beam parameters like the particle flux can only be set by an operator.

Figure 15: UCL vacuum chamber with electrical feedthroughs. Two SHV cable feedthroughs, one DB9 feedthrough and one SMA feedthrough were used to connect the board with the outside instrumentation.



5.2 Beam parameters

The resulting total energies of the respective ions, as well as their LET and range in Silicon are provided by UCL [8]. However this data is not valid for Silicon Carbide.

SRIM 2013 [9] simulations by Fraunhofer INT show the respective values for the heavy ion beams provided by UCL under normal incidence in Silicon Carbide covered by a 10 μm Paralene layer. Detailed data and a comparison to the data in blank Silicon Carbide is included in the test plan [5].

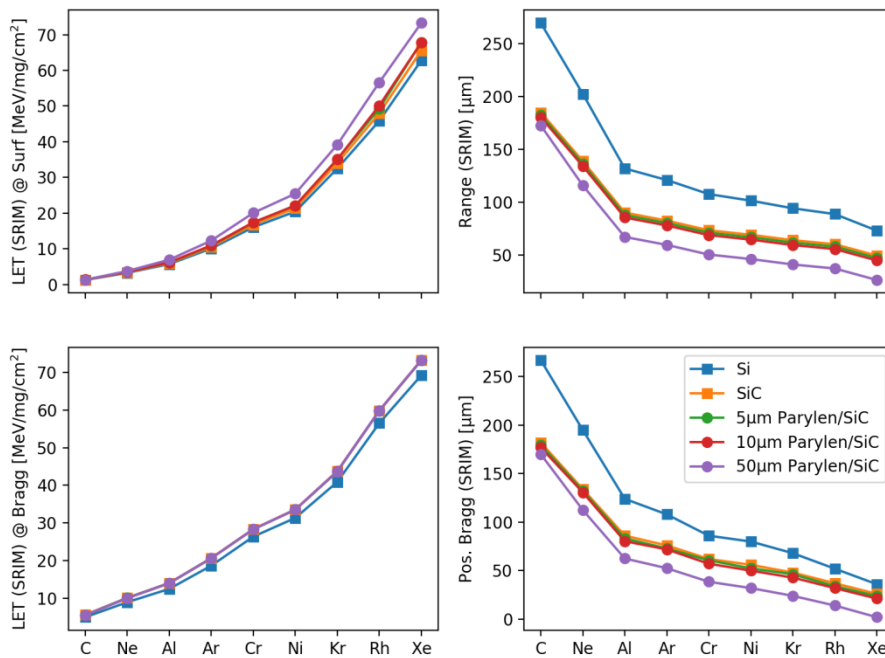
Tests with the C4D40120D were only performed with ions marked in bold letters in Table 10.

Table 10: UCL: Ion energies, LETs and ranges in Silicon Carbide covered by 10 μm Paralene: Shown are the ions available at UCL [8]. LETs highlighted in bold font were actually used. LET and range data are based on SRIM2013 [9] simulations done at Fraunhofer INT.

Ion	Energy [MeV]	LET ^{SRIM} @ Surface [MeV cm ² /mg]	Range ^{SRIM*} [μm]	LET ^{SRIM} @ Bragg Peak [MeV cm ² /mg]	Depth of Bragg Peak* [μm]
C	131	1.33	180.22	5.49	176.90
Ne	238	3.49	134.13	10.02	130.70
Al	250	6.20	85.42	13.99	80.30
Ar	379	10.95	77.91	20.63	71.90
Cr	513	17.41	68.74	28.34	57.10
Ni	582	22.09	64.53	33.55	50.00
Kr	769	35.06	59.36	43.77	42.80
Rh	972	50.14	55.57	59.84	32.00
Xe	995	67.81	44.79	73.27	21.20

* Range and position of Bragg peak is given within the Silicon Carbide layer.

Figure 16: Plot of LETs and Ranges in Silicon Carbide at UCL. Additional data with Paralene layers and data for Silicon are included. Thin Paralene layers have limited impact.



5.3 Geometry

The board is attached to the moveable board holder (Figure 15) which can be fully retracted from the chamber for ease of access. Tests are then performed with the chamber sealed and evacuated.

5.4 Irradiation steps

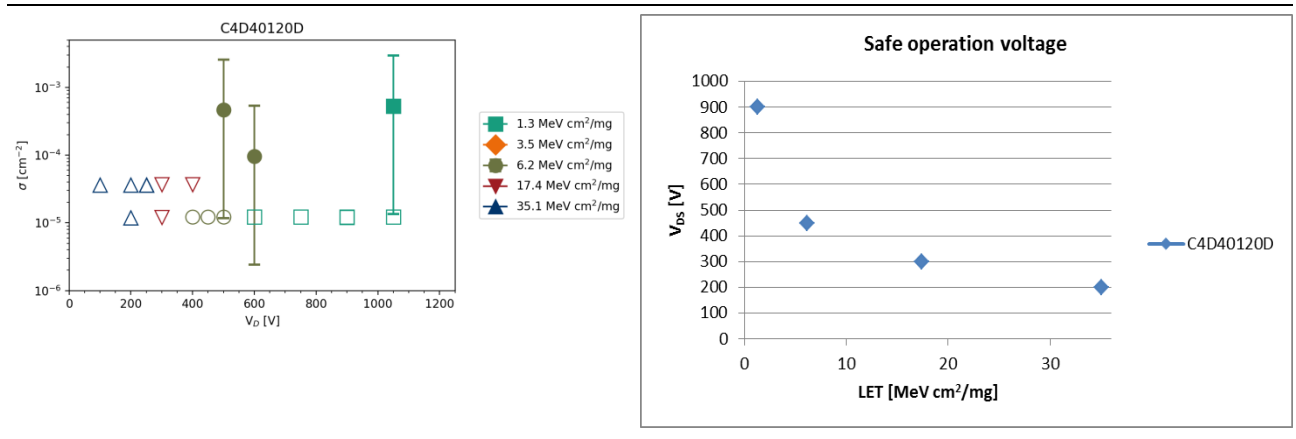
The log file of the tests performed at UCL can be found in Appendix B.B.1 shows an overview over the test indicating pass and fail results. A detailed evaluation of the results is shown in Section 5.5.

Table 11: UCL: Irradiation steps of SiC Schottky Diode C4D40120D. Numbers indicate the DUT serial number from Table 4. Table cells without numbers indicate that no run was performed under these conditions. Green or red background color indicate PASS or FAIL respectively. If a DUT fails at some voltage, all higher voltages are also indicated as fail. Yellow color (if applicable) indicates mixed results (e.g. 1 DUT passing, 1 DUT failing at the same level) or non-conclusive results with the device showing some damage not clearly attributable to a fail.

V _R [V]	C		Ne		Al		Cr		Kr	
	1.3	3.5	6.2	17.4	35.1					
	in-situ	Post	in-situ	Post	in-situ	Post	in-situ	Post	in-situ	Post
100									14.2	
200									14.2, 15.2	
250									14.2, 15..1	
300							14.1, 14.2			
400					12.2		14.1			
450					12.2					
500					11.2, 12.1					
600	13.1				11.1					
750	13.1									
900	13.1, 14.1									
1050	13.1,13..2									
1200										

5.5 Results

Figure 17: Overview of results: Heavy Ions at UCL. The first three images show the cross section results for various settings of V_{GS} . Filled symbols mark the cross section in case of device failures and error bars mark the upper lower limits. Open symbols mark the cross section upper limit in case no failure was observed during a run. The bottom right image shows the safe operating voltage at $V_{GS} = 0 V$.



The heavy ion tests at UCL with the SiC Schottky Diode C4D40120D were performed with 4 different LETs at a reduced target fluence of $3E5$ ions/cm². A device which passes a run up to $3E5$ ions/cm² without errors has an upper limit of the cross section of $\sigma_{upper} = 1.23E-5$ cm² assuming 95%CL and 10% flux uncertainty.

To save some time, several runs were performed at even lower total fluence of $1E5$ ions/cm². However after a destructive event at some voltage a run to $3E5$ ions/cm² was always performed to confirm the lower voltage level.

Considering the rather low number of devices, that number of LETs was only achievable by testing each of the two diodes per package separately, thus effectively doubling the number of available devices. We see no correlation that diode #2 in any package is more likely to fail if diode #1 already failed.

The voltage achievable for a safe operation up to the target fluence decreases from 900 V with carbon ions (LET = 1.3 MeV cm²/mg) down to 200 V with Krypton (LET = 35.1 MeV cm²/mg). LETs are given in SiC according to Table 10. Results at 250 V with Krypton show a pronounced increase of the leakage current. To define the safe operating voltage we count these as failed.

Within the runs we see some indication, that there may be an intermediate voltage range beyond that safe operation voltage in which destructive events are less likely, but instead lead to steps of the leakage current of the device.

Table 12: Results: Heavy Ions at UCL - Calculated cross sections Calculated with the formulae in ESCC25100 with CL=0.95 and flux uncertainty of 10% (approx. worst case)

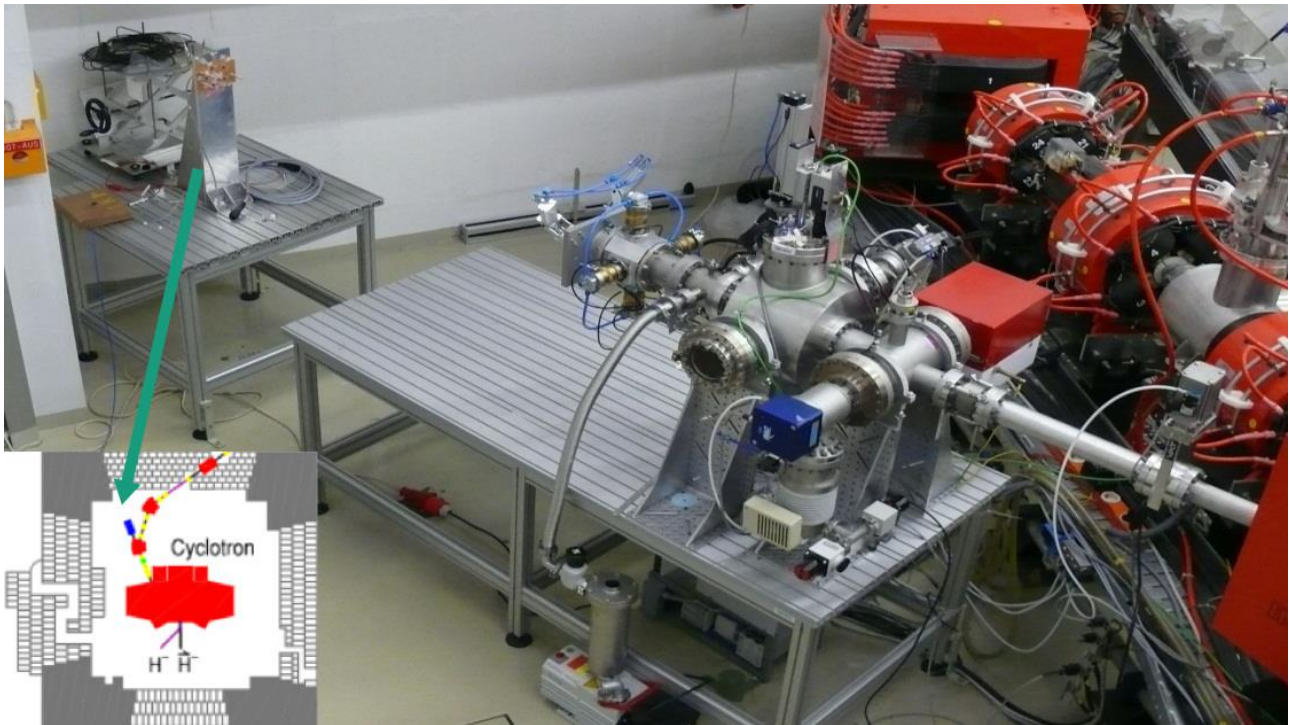
#	Ion	DUT #	V	Failure fluence [cm ⁻²]	σ lower [cm ²]	σ [cm ²]	σ upper [cm ²]	Effect	Comment
83	Al	11.1	600	1.04e+04	2.43e-06	9.62e-05	5.36e-04	FAIL	Several Events with jumps in leakage current observed Destructive failure at indicated fluence
84	Al	11.2	500	3.01e+05	0	0	1.22e-05	--	Several Events with jumps in leakage current observed
85	Al	12.1	500	2.16e+03	1.17e-05	4.63e-04	2.58e-03	FAIL	Destructive failure at indicated fluence
86	Al	12.2	400	3.02e+05	0	0	1.22e-05	--	--
87	Al	12.2	450	3.02e+05	0	0	1.22e-05	--	Several Events with jumps in leakage current observed
88	C	13.1	600	3.01e+05	0	0	1.22e-05	--	--
89	C	13.1	750	3.02e+05	0	0	1.22e-05	--	--
90	C	13.1	900	3.02e+05	0	0	1.22e-05	--	One Event with jump in leakage current observed
91	C	13.1	1050	3.02e+05	0	0	1.22e-05	--	Very frequent events with jumps in leakage current observed.
92	C	13.2	1050	1.88e+03	1.35e-05	5.32e-04	2.96e-03	FAIL	Destructive failure at indicated fluence
93	C	14.1	900	3.05e+05	0	0	1.21e-05	--	--
94	Cr	14.1	300					--	Device not in beam
95	Cr	14.1	300					--	Device not in beam
96	Cr	14.1	300	1.01e+05	0	0	3.65e-05	--	Slight continuous increase of leakage current
97	Cr	14.1	400	1.01e+05	0	0	3.65e-05	--	Pronounced continuous increase of leakage current
98	Cr	14.2	300	3.06e+05	0	0	1.21e-05	--	Slight continuous increase of leakage current
99	Kr	14.2	100	1.01e+05	0	0	3.64e-05	--	--
100	Kr	14.2	200	1.01e+05	0	0	3.64e-05	--	--
101	Kr	14.2	250	1.02e+05	0	0	3.63e-05	FAIL?	Pronounced continuous increase of leakage current
102	Kr	15.1	250	1.02e+05	0	0	3.63e-05	FAIL?	Pronounced continuous increase of leakage current
103	Kr	15.2	200	3.09e+05	0	0	1.19e-05	--	--

6 Tests at JULIC

6.1 Facility

Proton tests were performed at the JULIC injector cyclotron of the Forschungszentrum Jülich (FZJ, Research Centre Jülich). JULIC is the injector cyclotron of the Cooler Synchrotron COSY.

Figure 18: Beam line and irradiation site at the JULIC injector cyclotron, FZ Jülich



The initial energy of the proton beam is fixed to 45.0 MeV inside the cyclotron (vacuum). Usually the device under test (DUT) is placed at 1.8 m distance from the exit window of the beam. After passing the exit window of 1 mm aluminium and the air the mean proton energy is reduced to 39.3 MeV at the surface of DUT (Figure 19 and Figure 20). The maximum current of the beam is 10 μA (i.e. $6.24 \cdot 10^{13}$ p+/s). The beam has a Gaussian profile with a FWHM of about 7 cm at the surface of the DUTs.

The dose is measured online with Farmer Ionisation Chambers 30010 (measurement volume of 0.6 cm³) from PTW and an electrometer Multidos T10004 from PTW. Typically this type of ionisation chamber (IC) is used as an absolute dose-meter in high energy photon, electron, or proton-radiation therapy. The ionisation chambers are calibrated with a Co-60 gamma reference field against national standards by the manufacturer. The PMMA cap of the chamber further reduces the energy to 30.5 MeV inside the chamber.

The dose D given by the IC is related to the particle fluence Φ by the linear energy transfer (LET):

$$D = \frac{1}{\rho} \cdot \underbrace{\frac{dE}{dx}}_{LET} \cdot \Phi$$

The conversion factor is obtained by a numerical simulation by MULASSIS (Geant4). For the experimental setup a fluence $\Phi = 10^{10}$ p⁺/cm² at the exit window produces a dose $D = 24.38(15)$ Gy(air) in the ionization chamber. Alternatively, the LET (also called stopping power) of protons in different materials can be looked up at [11].

Figure 19: Schematic setup of the beam exit window at JULIC and the ionization chamber. The DUT is placed in same distance as the IC.

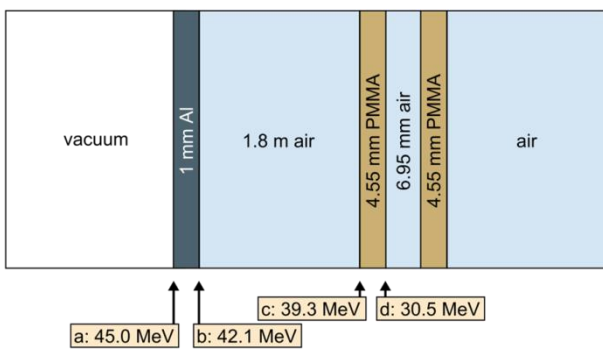
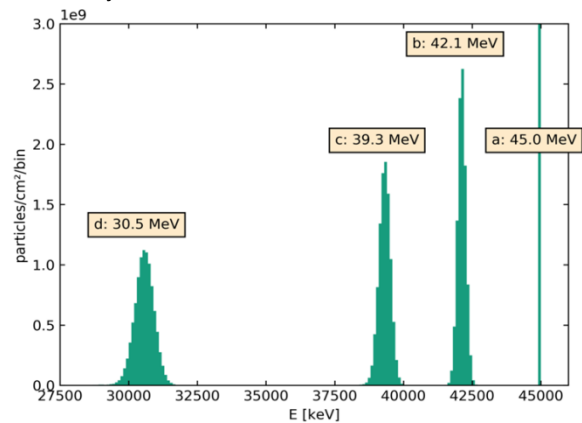


Figure 20: The initial proton energy of 45.0 MeV gets reduced to 39.3 MeV at the position of the IC/DUT. The PMMA cap of the chamber further reduces the energy to 30.5 MeV, calculation by MULASSIS (Geant4) on SPENVIS[10].



For the current tests, packaged Silicon Carbide devices were irradiated with the protons. Thus to calculate the LET on the die, additional simulations were performed with GRAS (Geant4).

6.2 Beam parameters

To receive the impact in terms of proton energy and LET on the Silicon Carbide die with packaged DUTs, radiation transport simulations have to be made. Simulations were performed with GRAS and a combination of MULASSIS and SRIM. Details on the approach and intermediate results are given in Appendix C.1. We see more of an impact on package thickness and nearly no impact of the package material. Thus here we will give a summary of the results just by thickness of the package.

Table 13: Results of simulations of the LET with package thickness. Details on the approach and intermediate results are given in Appendix C.1

Thickness	0.5 mm		1 mm		2 mm		3 mm	
LET _{GRAS} [MeV cm ² /mg]	0.012		0.008		0.005		0.003	
LET _{SRIM} [MeV cm ² /mg]	0.013		--		--		0.016	
Atomic recoil	Silicon	Carbon	Silicon	Carbon	Silicon	Carbon	Silicon	Carbon
Peak LET _{SRIM} [MeV cm ² /mg] at max. recoil	12.30	5.81	12.16	5.81	11.86	5.80	11.31	5.80
Range [μm]	2.01	6.6	1.96	6.3	1.84	5.7	1.72	5.1

While the results from GRAS and SRIM are not identical, the proton induced LET is well below 0.02 MeV cm²/mg in any case. The LETs of the recoil nuclei in SiC vary strongly with the LET of Si at or below 12.3 MeV cm²/mg and the LET of C around 5.8 MeV cm²/mg. For the overall data evaluation we identify the proton data with an LET of 0.01 MeV cm²/mg.

The thickness of the actual package of the DUTs is around 2 mm.

6.3 Geometry

The DUT was positioned off-center from the beam, such that all ionization chambers and the DUT position are at the same distance from the center, thus allowing to calculate the proton flux at the DUT position without a fixed installation at the facility which would allow to do that. As a drawback, only one DUT position on the board could be used at a time. The beam still was incident normally (90°) to the surface of the DUT.

6.4 Irradiation steps

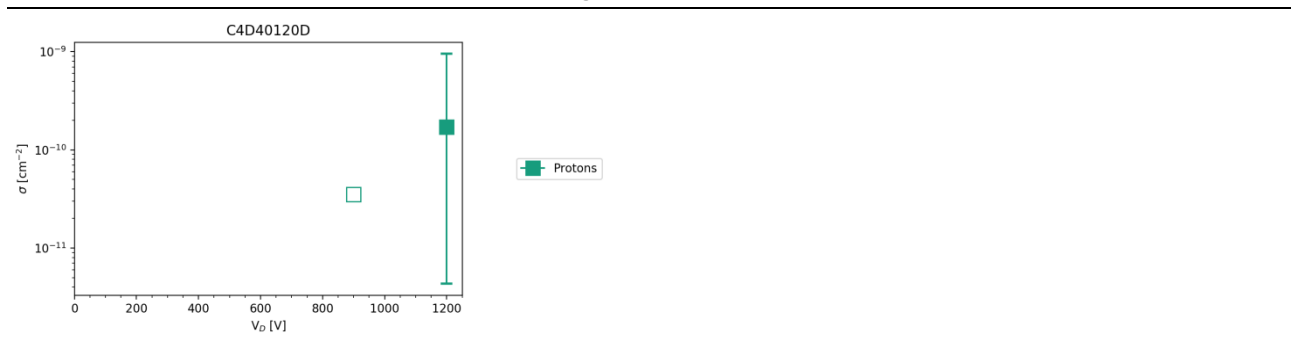
The log file of the tests performed at JULIC can be found in Appendix C. Table 14 shows an overview over the test indicating pass and fail results. A detailed evaluation of the results is shown in Section 6.5

Table 14: JULIC: Irradiation steps of SiC Schottky Diode C4D40120D. Numbers indicate the DUT serial number from Table 4. Table cells without numbers indicate that no run was performed under these conditions. Green or red background color indicate PASS or FAIL respectively. If a DUT fails at some voltage, all higher voltages are also indicated as fail. Yellow color (if applicable) indicates mixed results (e.g. 1 DUT passing, 1 DUT failing at the same level) or non-conclusive results with the device showing some damage not clearly attributable to a fail.

V _R [V]	Proton	
	E _{init} = 45 MEV	
	in-situ	POST
900	1.2, 2.1, 2.2	1.2, 2.1, 2.2
1200	1.1	

6.5 Results

Figure 21: Overview of results: Protons at JULIC. The test at 900 V was verified with 3 diodes (in 2 packages). Filled symbols mark the cross section in case of device failures and error bars mark the upper lower limits. Open symbols mark the cross section upper limit in case no failure was observed during a run.



Tests with this device were verified with 3 diodes at 900 V and a fluence of approx. 1e11 p/cm² per run. There were no voltages tested between 900 V and 1200 V, but the safe operating voltage is at least as high as found in the heavy ion tests with carbon (LET = 1.3 MeV cm²/mg) in Section 5.

Table 15: Results: Heavy ions at UCL - Calculated cross sections Calculated with the formulae in ESCC25100 with CL=0.95 and flux uncertainty of 10% (approx. worst case)

#	Ion	DUT #	V_DS, V	Failure fluence [cm-2]	σ lower [cm2]	σ [cm2]	σ upper [cm2]	Effect	Comment
38	p	1.1	1200	5.84E+09	4.33E-12	1.71E-10	9.53E-10	FAIL	Destructive failure at indicated fluence
39	p	1.2	900	1.05E+11	0	0	3.51E-11	--	--
40	p	2.1	900	1.05E+11	0	0	3.5E-11	--	--
41	p	2.2	900	1.05E+11	0	0	3.5E-11	--	--

7 Tests at GANIL

7.1 Facility

GANIL offers the irradiation of electric components with heavy ions over a wide LET range.

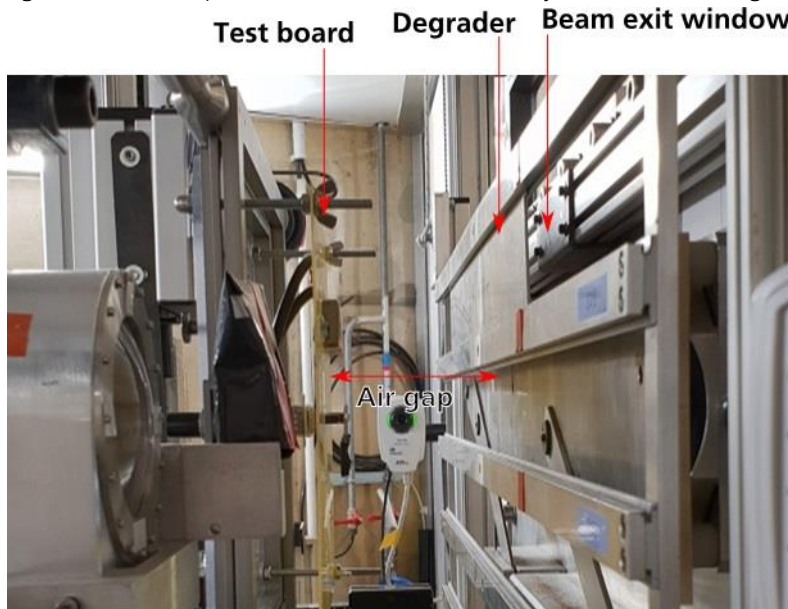
Additional heavy ion tests were performed at the G4 cave at GANIL, Caen, France.

The facility can provide selected heavy ion beams from Argon to Lead with a larger kinetic energy per nucleon than is available e.g. at UCL. The available ion at the time of our tests was Xenon.

The experimental tests at the facility take place in air and the setup consists of a sample holder, which is moveable in x-,y- and z-direction and variable degraders that can be put between the beam exit window and the DUT. By inclusion or variation of the degrader and by varying the air gap between exit window and DUT, the LET in Silicon can be tuned from approx. 26.5 MeV cm²/mg to 64.3 MeV cm²/mg and the corresponding ranges of the ions in Silicon go from 685 μm to 35 μm over that LET range.

DUT aligned is done with the help of a laser system.

Figure 22: Test setup at GANIL. Ion LETs can be set by variation of the degrader and the air gap.



7.2 Beam parameters

The resulting total energies of the respective ions, as well as their LET and range in Silicon are provided by GANIL [12]. However this data is not valid for Silicon Carbide.

SRIM 2013 [9] simulations by Fraunhofer INT in Table 16 show the respective surface LET values for the Xenon beam provided by GANIL under normal incidence in Silicon Carbide covered by a 10 μm Paralene layer with the air gap and degrader settings used in the experiments. For comparison, the values in Silicon provided by GANIL are included in the table. The devices used for these tests were de-identified, so packages were not included in the simulations.

Table 16: GANIL: Beam characteristics. Values in Silicon are provided by GANIL [12], Values in SiC are calculated by INT

Degrader [mm Al]	Air gap [mm]	LET (Si) (MeV.cm ² /mg)	Range (Si) [μm]	LET _{SURF} (SiC) [MeV.cm ² /mg]	Range (SiC) [μm]
0	150	27.76	640.33	29.2	430
0.4	95	42.03	226.23	47.2	141
0.5	180	60.12	65.68	72.9	30

7.3 Geometry

The board is attached to the moveable board holder (Figure 22). Tests are then performed in air.

7.4 Irradiation steps

The tests at GANIL with the C4D40120D were performed near the end of the beam time and only limited data could be taken. No PIGS tests were performed.

Table 17: GANIL: Irradiation steps of SiC Schottky Diode C4D40120D. Numbers indicate the DUT serial number from Table 4. Table cells without numbers indicate that no run was performed under these conditions. Green or red background color indicate PASS or FAIL respectively. If a DUT fails at some voltage, all higher voltages are also indicated as fail. Yellow color (if applicable) indicates mixed results (e.g. 1 DUT passing, 1 DUT failing at the same level) or non-conclusive results with the device showing some damage not clearly attributable to a fail.

		Xe, 0 mm Al, 150 mm Air		Xe, 0.4 mm Al, 95 mm Air		Xe, 0.5 mm Al, 180 mm Air	
V_DS [V]	V_GS [V]	29.2		47.2		72.9	
		in-situ	POST	in-situ	POST	in-situ	POST
100	0					18.1	18.1
125						19.2, 20.1	19.2, 20.1
150		16.2, 17.1	16.2, 17.1	19.1	19.1	18.1	18.1
175		17.2, 18.1	18.1, 17.2	19.1, 19.2	19.2		

200	16.1, 17.1	16.1, 17.1	19.1	19.1	18.2	18.2
300	16.2	16.2				
1200						

The log file of the tests performed at GANIL can be found in Appendix D. Table 17 shows an overview over the test indicating pass and fail results. A detailed evaluation of the results is shown in Section 7.5.

7.5 Results

In all tests with this device up to voltages of 300 V, no destructive SEE was observed when the DUT was in beam. However at several occasions, the DUT failed the POST test performed afterwards. Also, significant degradation was seen at the higher voltages (200 – 300 V depending on LET).

The safe operating voltage was chosen to fit the settings, where the DUT passed the POST tests.

Figure 23: Results: Heavy Ions at GANIL. The cross section results for various settings of V_D . Filled symbols mark the cross section in case of device failures and error bars mark the upper lower limits. Open symbols mark the cross section upper limit in case no failure was observed during a run.

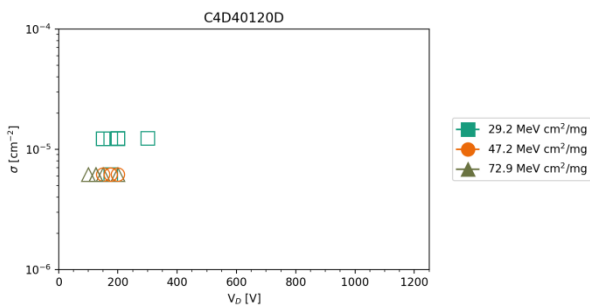


Table 18: Results: Heavy Ions at GANIL - Calculated cross sections Calculated with the formulae in ESCC25100 with $CL=0.95$ and flux uncertainty of 10% (approx. worst case)

#	Ion	Al [μm]	Air [mm]	DUT #	V_{DS} , V	Failure fluence [cm ⁻²]	σ lower [cm ²]	σ [cm ²]	σ upper [cm ²]	Effect	Comment
108	Xe	0	150	16.1	200	3.00E+05	0	0	1.23E-05	Degr.	Slight degradation during irradiation. DUT fails POST test.
109	Xe	0	150	16.2	150	3.00E+05	0	0	1.23E-05	--	--

110	Xe	0	150	17.1	150	3.00E+05	0	0	1.23E-05	--	--
112	Xe	0	150	17.1	200	3.00E+05	0	0	1.23E-05	Degr.	Slight degradation during irradiation. DUT fails POST test.
113	Xe	0	150	16.2	300	3.00E+05	0	0	1.23E-05	Degr.	Significant degradation during irradiation. DUT fails POST test.
114	Xe	0	150	17.2	175	3.00E+05	0	0	1.23E-05	--	Information on this run is missing from the log file. The total fluence is thus taken from our notes during the campaign.
115	Xe	0	150	18.1	175	6.00E+05	0	0	6.15E-06	--	This run was credited as run #114 in the GANIL logfile. Subsequent runs are correct in the logfile.
116	Xe	500	180	18.1	100	6.00E+05	0	0	6.15E-06	--	--
117	Xe	500	180	18.1	150	6.00E+05	0	0	6.15E-06	--	DUT fails POST test. No observable effect during irradiation.
118	Xe	500	180	18.2	200	6.00E+05	0	0	6.15E-06	Degr.	Significant degradation during irradiation. DUT fails POST test.
119	Xe	400	95	19.1	150	6.00E+05	0	0	6.15E-06	--	--
120	Xe	400	95	19.1	175	6.00E+05	0	0	6.15E-06	--	No POST test performed
121	Xe	400	95	19.1	200	6.00E+05	0	0	6.15E-06	Degr.	Slight degradation during irradiation. DUT fails POST test.
122	Xe	400	95	19.2	175	6.00E+05	0	0	6.15E-06	--	--
123	Xe	500	180	19.2	125	6.00E+05	0	0	6.15E-06	--	--
124	Xe	500	180	20.1	125	6.00E+05	0	0	6.15E-06	--	--

8 Tests at CERN

8.1 Facility

Tests at CERN took place at the H8 beam line [13] from the T4 target of the SPS North Experimental Area with a Xenon beam of 30 or 40 GeV/n. The opportunity to test at this beam line was given in a joint effort from ESA and CERN [14].

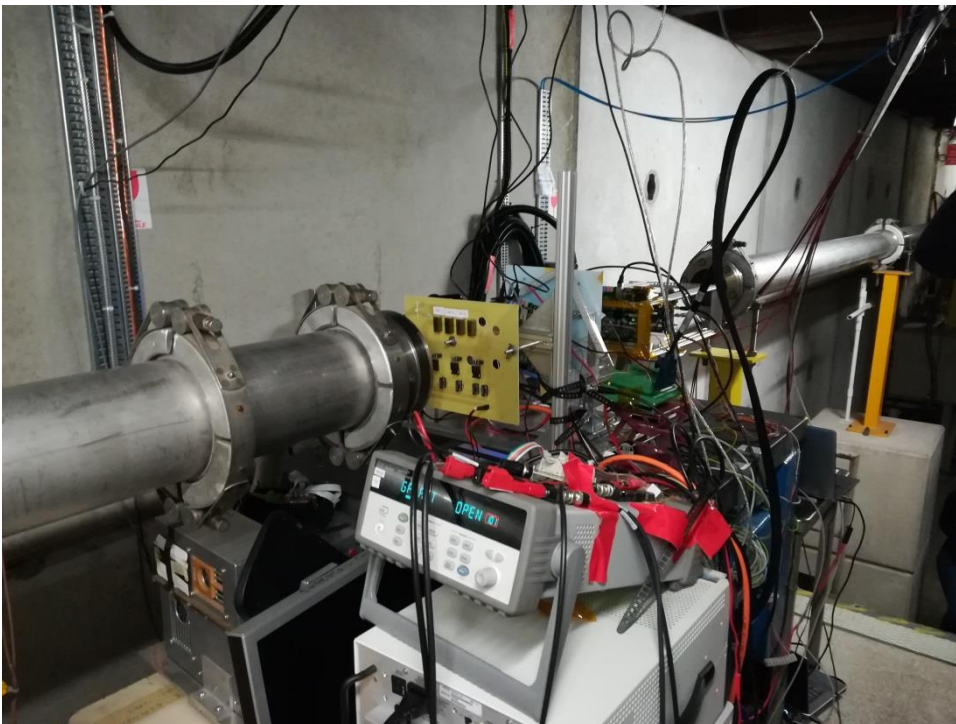
The ion beam is ultra-energetic and thus highly penetrating, which has several practical advantages for testing:

- The test can take place in air
- The DUTs do not need to be de-lidded
- Multiple test boards can be placed successively in the beam.

The INT test board was positioned first in line during all the tests, so energy reduction and thus LET modifications by other boards in the beam line does not occur.

The test site is not specifically intended for SEE tests of electronics, therefore additional infrastructure like a moveable frame holder are not installed.

Figure 24: Beam line and irradiation site at the H8 beam line, CERN.



8.2 Beam parameters

The beam was delivered in spills of approx. 8 s length at an interval of 30 – 50 s [14][15]. While the time-average flux is thus relatively low in the range of $1 - 2 \cdot 10^3$ ions/(cm²·s), the actual flux during the spill time is much higher.

The dosimetry on-site was recorded by CERN and preliminarily available during the campaign. The translation from the dosimeter readout to the actual particle flux and fluence was available after the campaign [15].

The total fluences given in Appendix E are based on the timestamps of the individual runs and the dosimetry information provided by CERN. Most device failures occurred at the first spill of beam. Properly deducing the fluence of failure and thus the cross sections of the devices is not possible in these cases, so the cross sections in case of failures given in Section 8.5 should only be seen as a rough order of magnitude.

The calculation of the LET for particles of these energies cannot be done easily e.g. with SRIM due to the interactions with matter at these energies. The LET values for silicon were simulated with FLUKA by Rubén García Alía et al. and reported [14] There different LET values were considered, one unrestricted value taking into account all ionization caused by the beam (approx. 6.3 MeV cm²/mg) and a volume-restricted value covering the area of a 9.3 MeV/n Silicon particle track (approx. 3.7 MeV cm²/mg). Comparisons with the ESA SEU [14] indicate that the volume-restricted LET is a more proper expression for the particle LET in Silicon.

We adopt the LET value of 3.7 MeV cm²/mg for our tests although these were determined in Silicon and we would require the value in SiC. While we cannot show or prove this assumption here, indicative simulations with SRIM using 10 GeV/n Xenon ions (maximum possible energy) are shown in the appendix E.1.

Additional runs were performed with the DUT tilted by 42° to the beam (angle determined by measurement). As in general the concept of effective LET is not valid for power devices [3] and all data collected at these settings further implicate that assuming a larger LET than at 0° incidence is invalid, we cannot properly give an expression of LET for these runs.

8.3 Geometry

The test board was attached to a frame holder on a motor unit, allowing to shift the board along one axis. Three DUTs could be installed on the board and irradiated separately. For the PIGS or POST tests, the DUTs were moved out of the beam, which ran continuously except when installing new DUTs.

First, the beam was incident normally on the DUTs. In addition, tests with the DUT at 42° to the beam were performed. For this the whole motor unit was turned at an 42° angle as tilting would not be possible with the frame holder and motor.

8.4 Irradiation steps

Table 19: CERN: Irradiation steps of SiC Schottky Diode C4D40120D. Numbers indicate the DUT serial number from Table 4. Table cells without numbers indicate that no run was performed under these conditions. Green or red background color indicate PASS or FAIL respectively. If a DUT fails at some voltage, all higher voltages are also indicated as fail. Yellow color (if applicable) indicates mixed results (e.g. 1 DUT passing, 1 DUT failing at the same level) or non-conclusive results with the device showing some damage not clearly attributable to a fail.

V_DS [V]	Xe, 0°		Xe, 42°	
	in-situ	PIGS	in-situ	PIGS
900				
950				
1000	1.2			
1050				
1100	1.2			
1150	1.2		3.1	
1200	1.1, 1.2, 2.2		3.1, 3.2	
1250	2.1		3.1, 3.2	
1300	1.2		3.1, 3.2	
1350			3.1, 3.2	
1400			3.1, 3.2	
1450			3.1, 3.2	
1500			3.1, 3.2	3.2

8.5 Results

At normal incidence of the ions, the tests with the C4D40120D at CERN failed repeatedly at 1200 V and passed 1150 V once. At 1200 V, failure is however not immediate but occurs stepwise most likely whenever a new spill of ions is incoming. At 1150 V the measurement shows some increase of current but hardly to separate from the noise in the data. So the latter is assigned the safe operation voltage, however no POST tests were performed leaving a chance that the devices may have failed already at lower voltages.

At first glance there is a difference to the previous tests in the increased voltage of safe operation of 1050 V. This value was 900 V with the lowest LET at UCL and with protons. At UCL the next highest test voltage where the device failed was at 1050 V, and with protons even at 1200 V. Thus when taking this into account the UCL data would still be conflicting with the findings at CERN.

Tests at CERN were performed with DUTs from a different lot as the previous tests, so lot-to-lot variability could also play a role.

Additional tests were performed with the DUT at an 42° angle to the beam. According to ESCC25100, using an effective LET when tilting is not valid for SEB or SEGR tests of power devices. Given the ultra-energetic ions in this tests, it is safe to assume that the sensitive volume is still penetrated fully in these tests. An effective LET at 42° would however in any case give a 1.34-times larger LET and thus having a larger safe operating voltage is the opposite of the naïve expectation. The C4D40120D did not show desctructive events or degradation up to 1500 V, hugely above the rated voltage. No post tests were performed up to 1500 V, but the one performed at 1500 V passed.

The effective fluences across the tests were <3.2E4 ions/cm². This very low fluence might be an explanation for the increased “safe operation” levels observed in these tests compared to the other test campaigns.

Figure 25: Results: Heavy Ions at CERN. The cross section results for various settings of V_{DS} . Filled symbols mark the cross section in case of device failures and error bars mark the upper lower limits. Open symbols mark the cross section upper limit in case no failure was observed during a run.

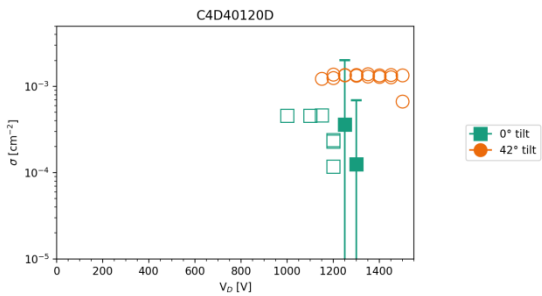


Table 20: Results: Heavy Ions at CERN - Calculated cross sections Calculated with the formulae in ESCC25100 with CL=0.95 and flux uncertainty of 10% (approx. worst case)

#	Ion	Tilt [°]	DUT #	V_{DS} , V	Failure fluence [cm ⁻²]	σ lower [cm ²]	σ [cm ²]	σ upper [cm ²]	Effect	Comment
028	Xe	0	1.1	1200	3.14E+04	0	0	1.18E-04	FAIL	Increases of current potentially with same periodicity as beam spills.
029	Xe	0	1.2	1000	8.03E+03	0	0	4.60E-04	--	No POST test
030	Xe	0	1.2	1100	8.05E+03	0	0	4.58E-04	--	No POST test
031	Xe	0	1.2	1150	8.00E+03	0	0	4.61E-04	--	Measurements show some increase of current but hardl to truly separate from the noise in the data. No POST test
032	Xe	0	1.2	1200	1.61E+04	0	0	2.30E-04	FAIL	Nearly instantaneous failure, increases of current potentially with same periodicity as beam spills.
033	Xe	0	1.2	1300	8.03E+03	3.15E-06	1.25E-04	6.94E-04	--	Additional test with already failed DUT. But shows approx. 1 order of magnitude higher current that in previous test.
034	Xe	0	2.1	1250	2.77E+03	9.13E-06	3.61E-04	2.01E-03	FAIL	Immediate destructive failure. No

										stepwise increase.
035	Xe	0	2.2	1200	1.54E+04	0	0	2.39E-04	FAIL	Increases of current potentially with same periodicity as beam spills.
050	Xe	42	3.1	1150	2.99E+03	0	0	1.24E-03	--	No POST tests
051	Xe	42	3.1	1200	2.69E+03	0	0	1.37E-03	--	No POST tests
052	Xe	42	3.1	1250	2.75E+03	0	0	1.34E-03	--	No POST tests
053	Xe	42	3.1	1300	2.72E+03	0	0	1.36E-03	--	No POST tests
054	Xe	42	3.1	1350	2.64E+03	0	0	1.40E-03	--	No POST tests
055	Xe	42	3.1	1400	2.75E+03	0	0	1.34E-03	--	No POST tests
056	Xe	42	3.1	1450	2.72E+03	0	0	1.36E-03	--	No POST tests
057	Xe	42	3.1	1500	2.74E+03	0	0	1.35E-03	--	No POST tests
058	Xe	42	3.2	1200	2.94E+03	0	0	1.25E-03	--	No POST tests
059	Xe	42	3.2	1250	2.72E+03	0	0	1.36E-03	--	No POST tests
060	Xe	42	3.2	1300	2.76E+03	0	0	1.34E-03	--	No POST tests
061	Xe	42	3.2	1350	2.83E+03	0	0	1.30E-03	--	No POST tests
062	Xe	42	3.2	1400	2.85E+03	0	0	1.29E-03	--	No POST tests
063	Xe	42	3.2	1450	2.87E+03	0	0	1.29E-03	--	No POST tests
064	Xe	42	3.2	1500	5.52E+03	0	0	6.69E-04	--	--

A Fraunhofer INT

A.1. About the institute

The Fraunhofer Institute for Technological Trend Analysis INT provides scientifically sound assessments and counselling on the entire spectrum of technological developments. On this basis, the Institute conducts Technology Forecasting, making possible a long-term approach to strategic research planning. Fraunhofer INT constantly applies this competence in projects tailor-made for our clients.

Over and above these skills, we run our own experimental and theoretical research on the effects of ionizing and electromagnetic radiation on electronic components, as well as on radiation detection systems. To this end, INT is equipped with the latest measurement technology. Our main laboratory and large-scale appliances are radiation sources, electromagnetic simulation facilities and detector systems that cannot be found in this combination in any other civilian body in Germany.

For more than 40 years, INT has been a reliable partner for the Federal German Ministry of Defence, which it advises in close cooperation and for which it carries out research in technology analysis and strategic planning as well as radiation effects. INT also successfully advises and conducts research for domestic and international civilian clients: both public bodies and industry, from SMEs to DAX 30 companies.

Further information can be found on the website [1].

A.2. Business unit Nuclear Effects in Electronics and Optics

The Business Unit „Nuclear Effects in Electronic and Optics (NEO)“ at Fraunhofer INT investigates the effects of ionizing radiation on electronic, optoelectronic, and photonic components and systems. Its work is based on more than 40 years of experience in that field.

NEO performs irradiation tests based on international standards and advises companies regarding radiation qualification and hardening of components and systems. The knowledge obtained in years of radiation testing is also used for the development of new radiation sensor systems. These activities are performed either at irradiation facilities installed at INT or at partner institutions to which our scientists have regular access.

A multitude of modern equipment to measure electrical and optical parameters is available. Furthermore our institute runs a precision mechanical workshop and an electronic laboratory. This enables us to conduct most of the irradiation tests without help or equipment of the customer.

The activities within NEO are:

- Investigations of the effects in all kinds of radiation environments
- Performance, analysis, and evaluation of irradiation tests done at Fraunhofer INT and external facilities

- Ensuring the operability of components and systems in typical radiation environments, such as space, nuclear facilities, medicine, or accelerators
- Consulting users and manufacturers on the use of products in radiation environments by selecting, optimizing and hardening
- Measurement of the radiation effects on optical fibers and fiber Bragg gratings (FBG)
- Development of radiation sensors based on optical fibers, FBGs, oscillating crystals, UV-EPROMs, and SRAMs
- Participation in the development of international test procedures for IEC, IEEE, NATO, and IAEA
- Since 2013 all services of the business unit are certified according to ISO 9001

A.3. Irradiation facilities

Fraunhofer INT operates several irradiation facilities on site that are dedicated to perform irradiation tests. For that purpose the design and operation characteristics are highly optimised from many decades of experience and to comply with all relevant standards and test procedures.

Furthermore Fraunhofer INT accesses regularly external facilities, partly with dedicated irradiation spots for exclusive use to Fraunhofer INT.

These irradiation facilities are:

- Co-60 irradiation sources on site to simulate the effect of total dose
- Neutron generators on site to simulate the displacement damage of heavy particles
- 450 keV X-ray irradiation facility on site
- Laser induced single event test system on site
- Dedicated proton irradiation spot at the injector cyclotron of FZ Jülich to simulate the effects of solar and trapped protons
- External Co-60 irradiation sources for high dose and high dose rate irradiations

The facilities used in the context of this work will be described in detail in the following sections.

A.4. QM-Certificate



MANAGEMENT SYSTEM CERTIFICATE

Certificate No: 126306-2012-AQ-GER-DAKKS	Initial certification date: 13. February 2013	Valid: 14. February 2019 - 12. February 2022
---	--	---

This is to certify that the management system of



**Fraunhofer-Institut für
Naturwissenschaftlich-Technische
Trendanalysen INT**

Appelsgarten 2, 53879 Euskirchen, Germany

has been found to conform to the Quality Management System standard:

ISO 9001:2015

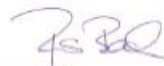
This certificate is valid for the following scope:

**Scientific research on the effects of nuclear and electromagnetic radiation
as well as application and development of methods for their characterization**

Place and date:
Essen, 14. February 2019



For the issuing office:
DNV GL - Business Assurance
Schnieringshof 14, 45329 Essen, Germany



Thomas Beck
Technical Manager

Lack of fulfillment of conditions as set out in the Certification Agreement may render this Certificate invalid.
ACCREDITED UNIT: DNV GL Business Assurance Zertifizierung und Umweltgutachter GmbH, Schnieringshof 14, 45329 Essen, Germany.
TEL: +49 201 7296-222. www.dnvgl.de/assurance

B Appendix: Tests at UCL

B.1. Logfile / Test steps

In case of device failure the fluences in this table indicate the fluence provided by the facility not the fluence until failure which may differ by some additional seconds of beam.

#	Run (UCL)	Date	Time	Ion	Device Type	Device	Position on board	DUT #	V	beam time [s]	fluence [cm-2]
83	111	17.04.	18:49	Al	Schottky	C4D40120D	#1	11.1	600	107	1.13E+04
84	112	17.04.	18:53	Al	Schottky	C4D40120D	#1	11.2	500	498	3.01E+05
85	113	17.04.	19:07	Al	Schottky	C4D40120D	#2	12.1	500	10	9.85E+03
86	114	17.04.	19:45	Al	Schottky	C4D40120D	#2	12.2	400	444	3.02E+05
87	115	17.04.	19:54	Al	Schottky	C4D40120D	#2	12.2	450	295	3.02E+05
88	116	17.04.	20:19	C	Schottky	C4D40120D	#1	13.1	600	309	3.01E+05
89	117	17.04.	20:27	C	Schottky	C4D40120D	#1	13.1	750	197	3.02E+05
90	118	17.04.	20:32	C	Schottky	C4D40120D	#1	13.1	900	151	3.02E+05
91	119	17.04.	20:36	C	Schottky	C4D40120D	#1	13.1	1050	388	3.02E+05
92	120	17.04.	20:45	C	Schottky	C4D40120D	#1	13.2	1050	7	6.59E+03
93	121	17.04.	20:48	C	Schottky	C4D40120D	#2	14.1	900	61	3.05E+05
94	122	17.04.	21:11	Cr	Schottky	C4D40120D	#2	14.1	300	11	1.06E+03
95	123	17.04.	21:12	Cr	Schottky	C4D40120D	#2	14.1	300	10	9.17E+02
96	124	17.04.	21:13	Cr	Schottky	C4D40120D	#2	14.1	300	343	1.01E+05
97	125	17.04.	21:22	Cr	Schottky	C4D40120D	#2	14.1	400	198	1.01E+05
98	126	17.04.	21:29	Cr	Schottky	C4D40120D	#2	14.2	300	62	3.06E+05
99	127	17.04.	21:43	Kr	Schottky	C4D40120D	#2	14.2	100	102	1.01E+05
100	128	17.04.	21:46	Kr	Schottky	C4D40120D	#2	14.2	200	101	1.01E+05
101	129	17.04.	21:50	Kr	Schottky	C4D40120D	#2	14.2	250	110	1.02E+05
102	130	17.04.	21:54	Kr	Schottky	C4D40120D	#1	15.1	250	93	1.02E+05
103	131	17.04.	21:58	Kr	Schottky	C4D40120D	#1	15.2	200	60	3.09E+05

B.2. Measurements

Figure 26: Run# 083, C4D40120D, Al-250, 1.1×10^4 ions/cm², DUT 11.1, $V_D = 600.0$ V

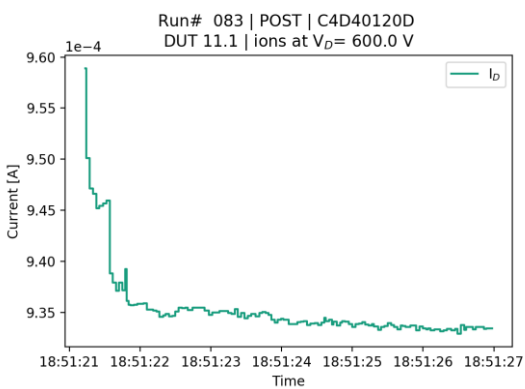
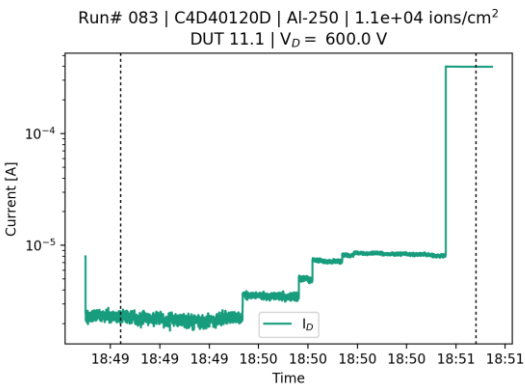
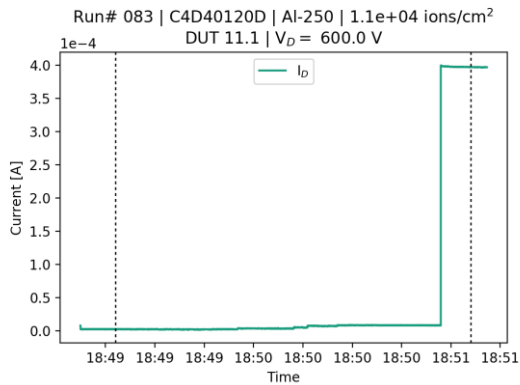


Figure 27: Run# 084, C4D40120D, Al-250, 3.0×10^5 ions/cm², DUT 11.2, $V_D = 500.0$ V

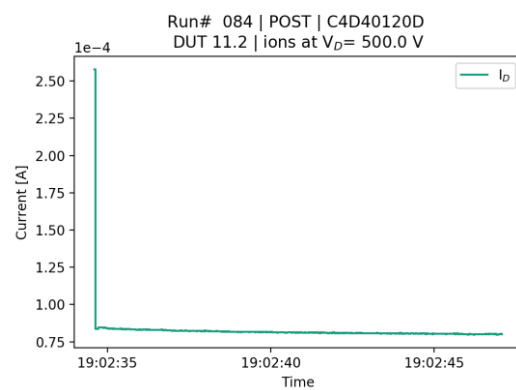
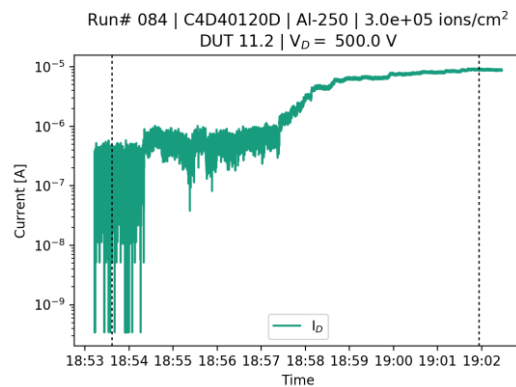
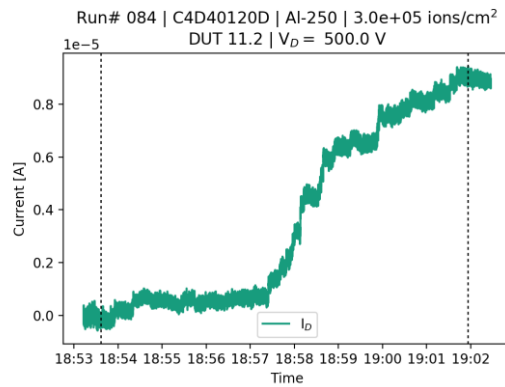


Figure 28: Run# 085, C4D40120D, Al-250, $9.8e+03$ ions/cm², DUT 12.1, $V_D = 500.0$ V

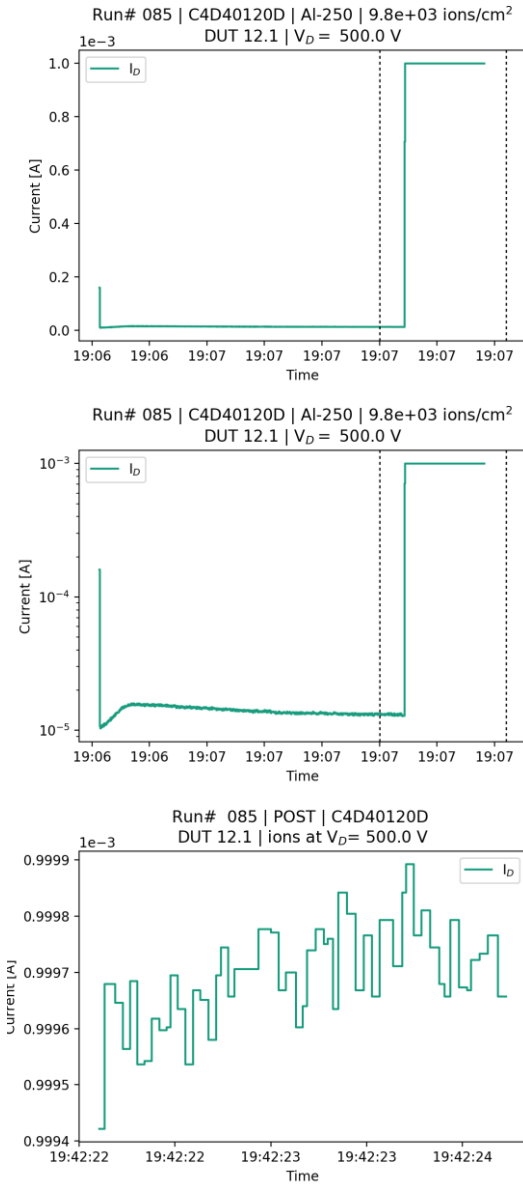


Figure 29: Run# 086, C4D40120D, Al-250, $3.0e+05$ ions/cm², DUT 12.2, $V_D = 400.0$ V

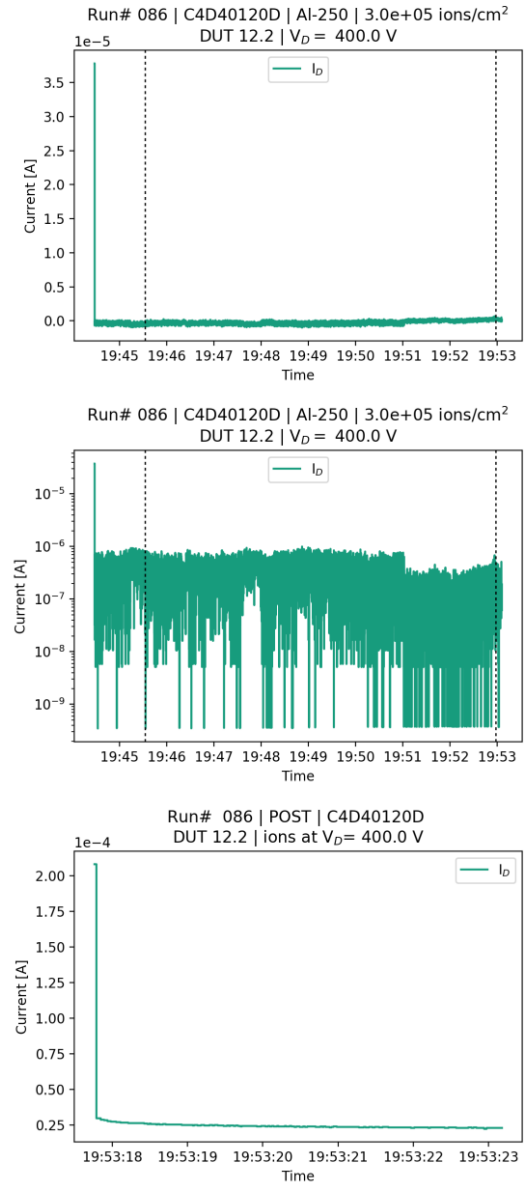


Figure 30: Run# 087, C4D40120D, Al-250, $3.0e+05$ ions/cm², DUT 12.2, $V_D = 450.0$ V

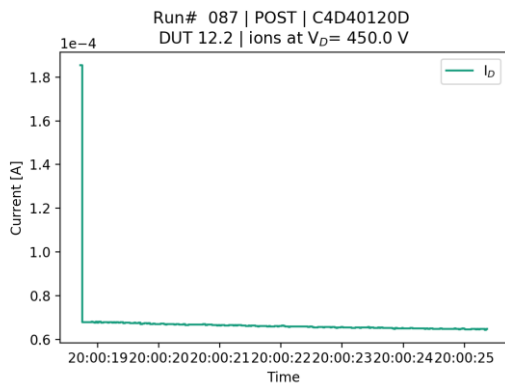
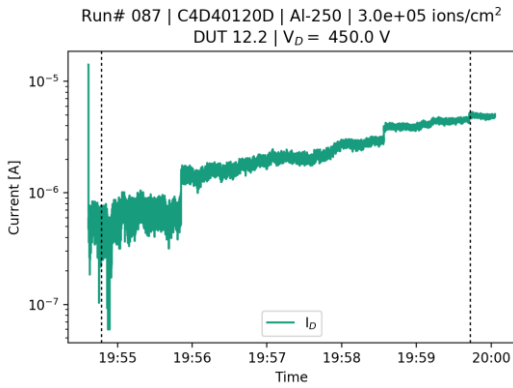
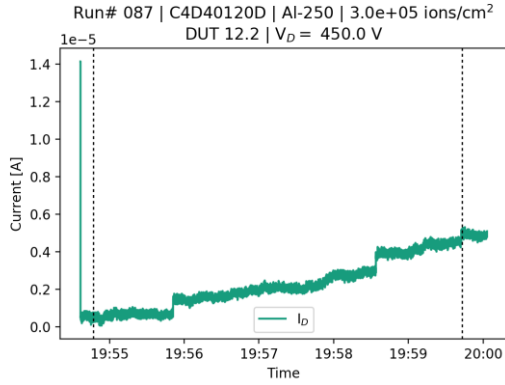


Figure 31: Run# 088, C4D40120D, C-131, $3.0e+05$ ions/cm², DUT 13.1, $V_D = 600.0$ V

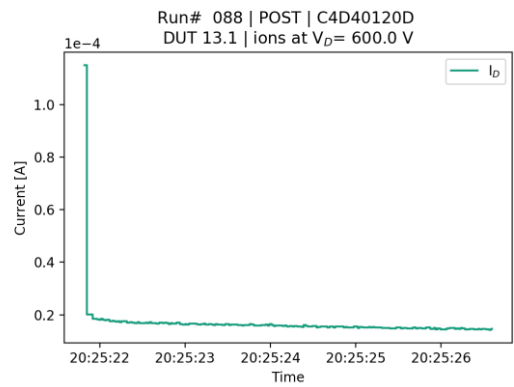
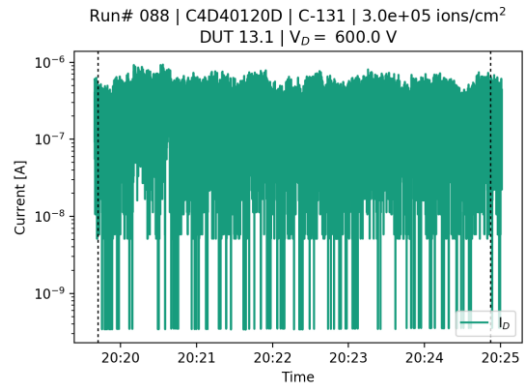
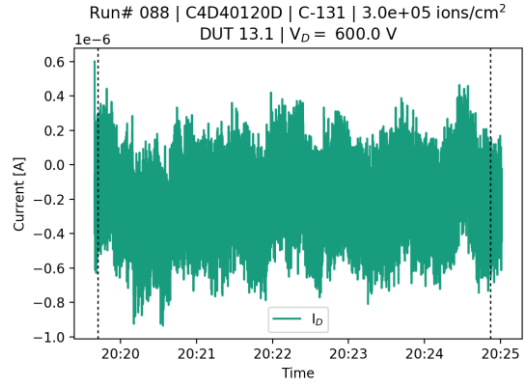


Figure 32: Run# 089, C4D40120D, C-131, $3.0e+05$ ions/cm², DUT 13.1, $V_D = 750.0$ V

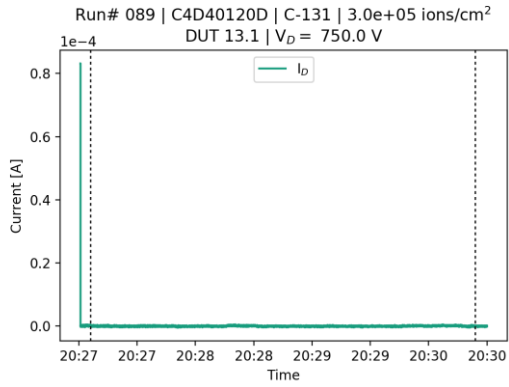


Figure 33: Run# 090, C4D40120D, C-131, $3.0e+05$ ions/cm², DUT 13.1, $V_D = 900.0$ V

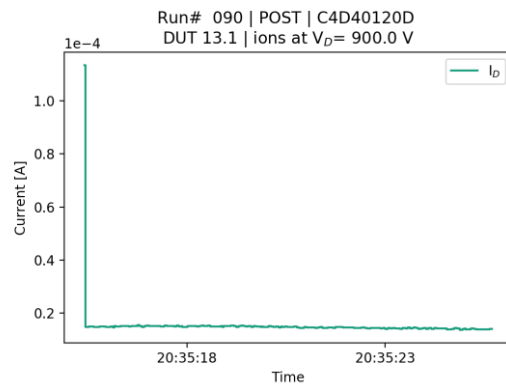
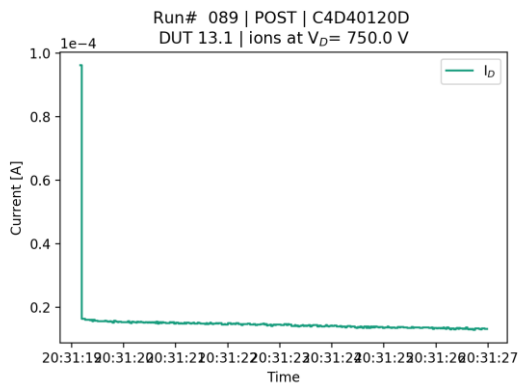
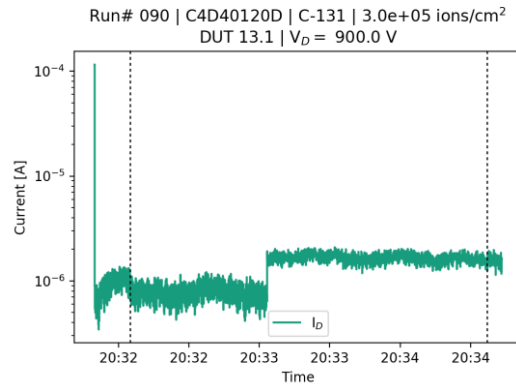
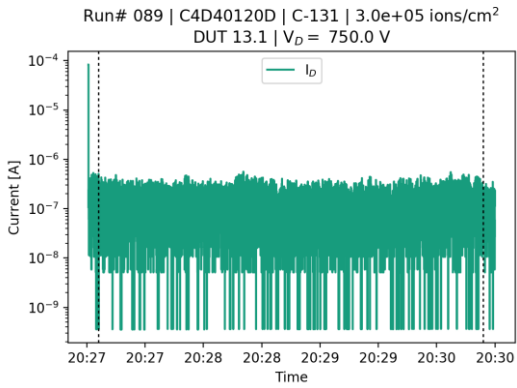
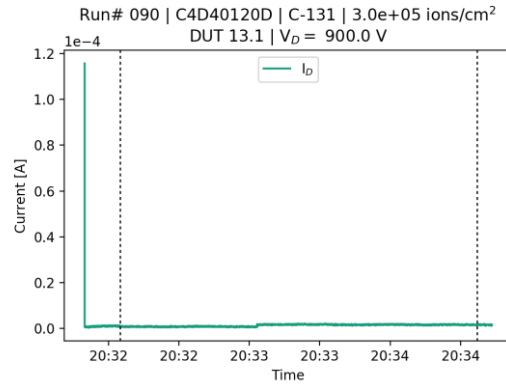


Figure 34: Run# 091, C4D40120D, C-131, 3.0×10^5 ions/cm², DUT 13.1, $V_D = 1050.0$ V

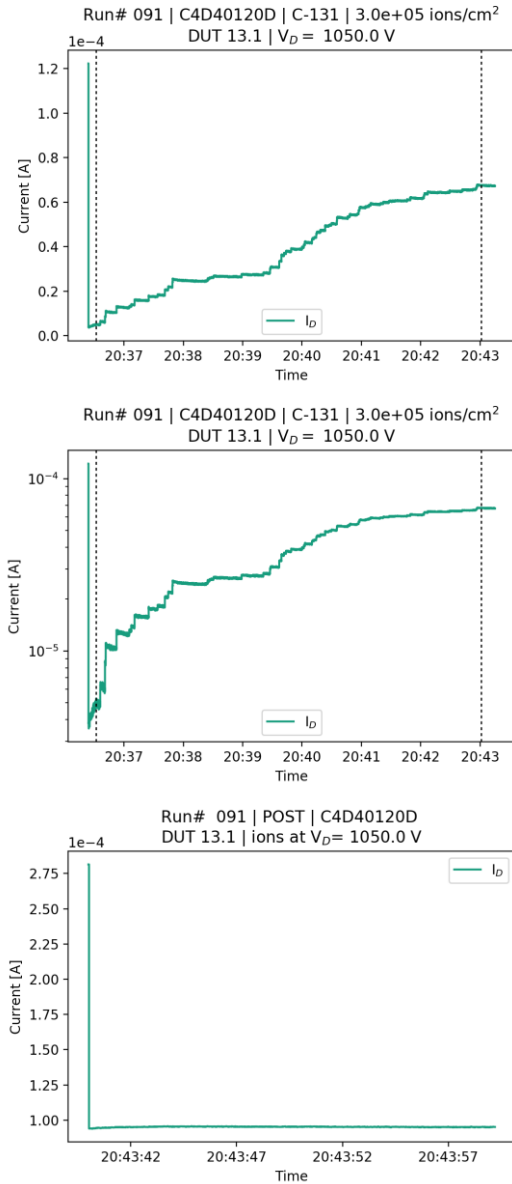


Figure 35: Run# 092, C4D40120D, C-131, 6.6×10^3 ions/cm², DUT 13.2, $V_D = 1050.0$ V

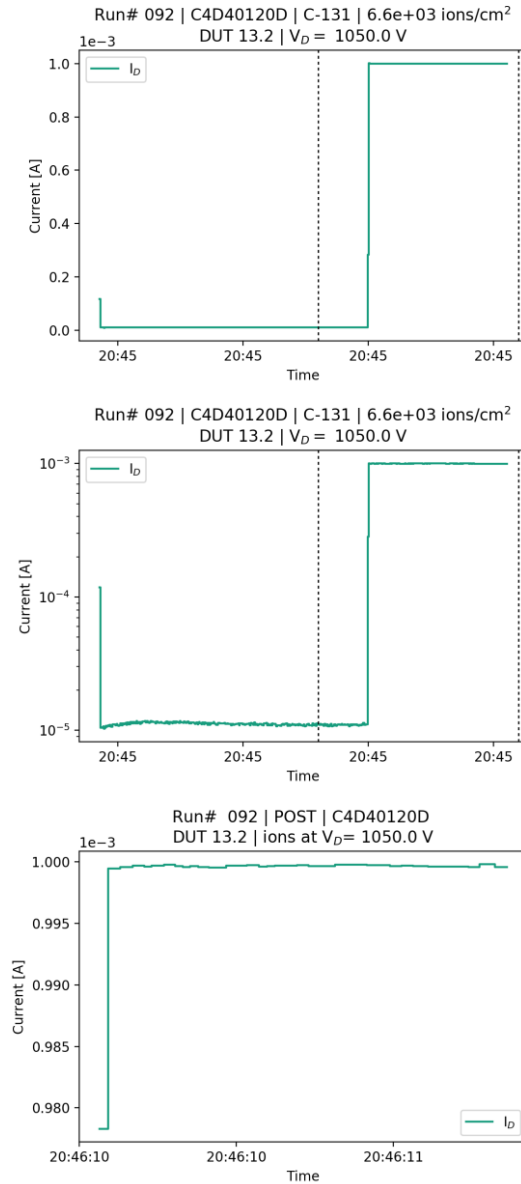


Figure 36: Run# 093, C4D40120D, C-131, 3.1×10^5 ions/cm², DUT 14.1, $V_D = 900.0$ V

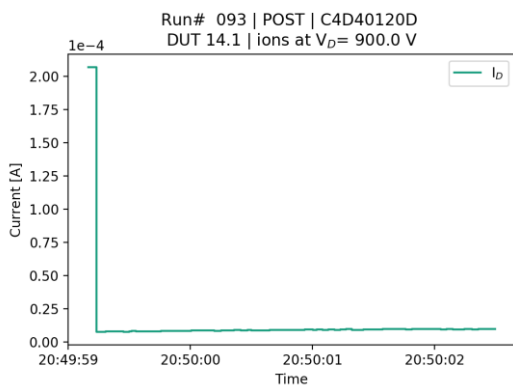
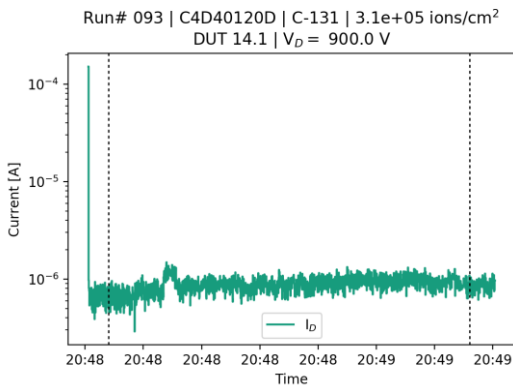
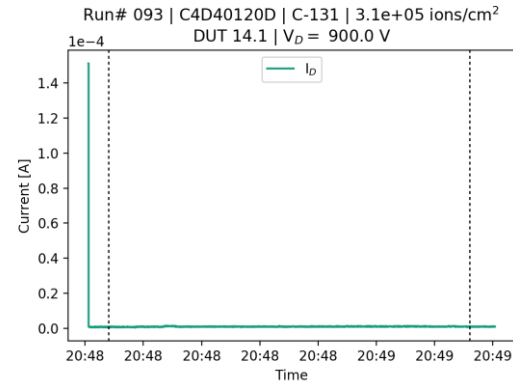


Figure 37: Run# 096, C4D40120D, Cr-513, 1.0×10^5 ions/cm², DUT 14.1, $V_D = 300.0$ V

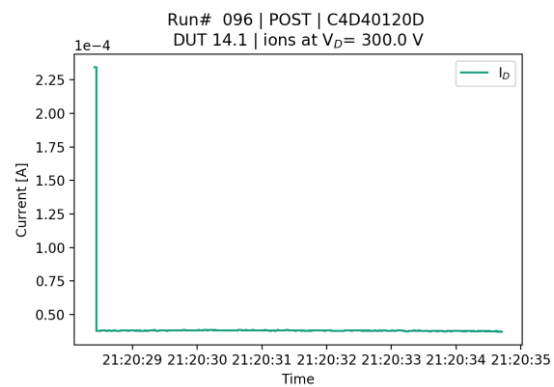
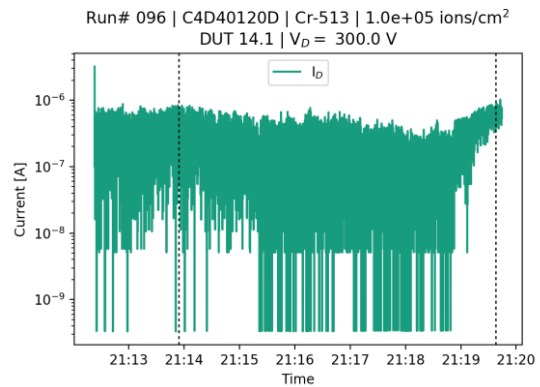
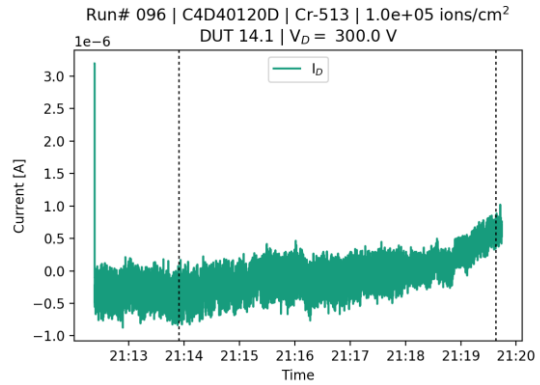


Figure 38: Run# 097, C4D40120D, Cr-513, $1.0e+05$ ions/cm², DUT 14.1, $V_D = 400.0$ V

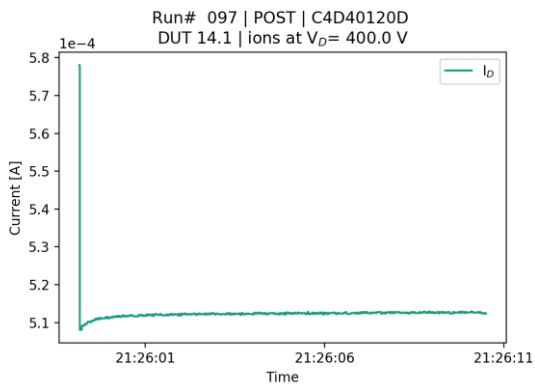
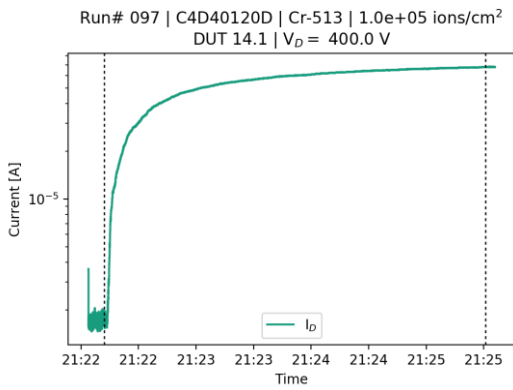
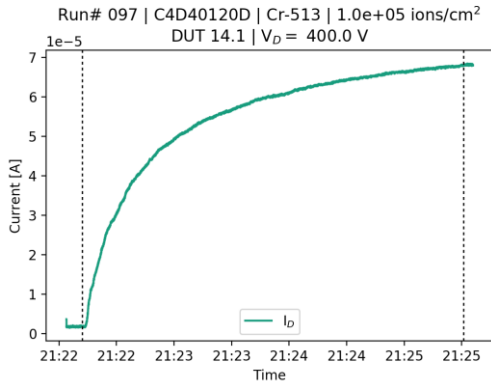


Figure 39: Run# 098, C4D40120D, Cr-513, $3.1e+05$ ions/cm², DUT 14.2, $V_D = 300.0$ V

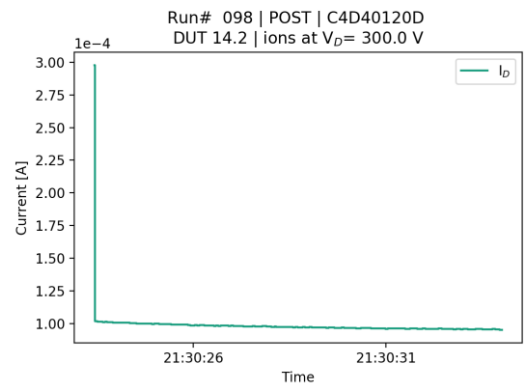
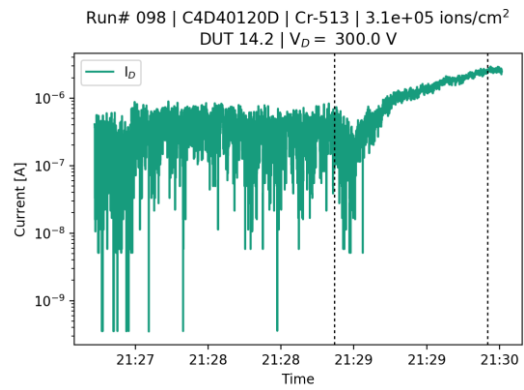
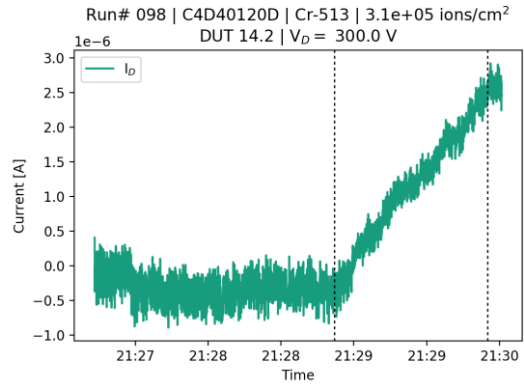


Figure 40: Run# 099, C4D40120D, Kr-769, $1.0e+05$ ions/cm², DUT 14.2, $V_D = 100.0$ V

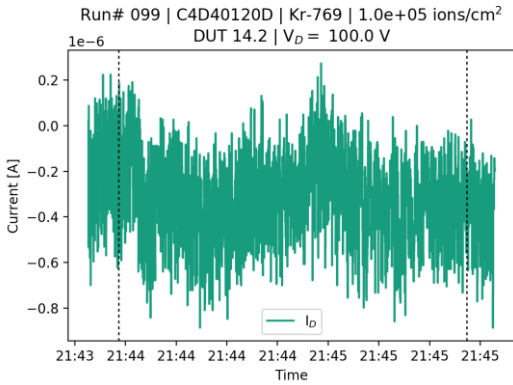


Figure 41: Run# 100, C4D40120D, Kr-769, $1.0e+05$ ions/cm², DUT 14.2, $V_D = 200.0$ V

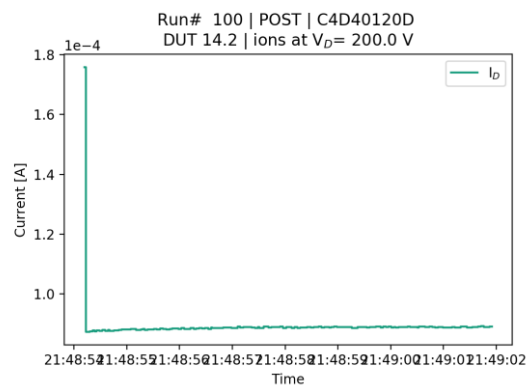
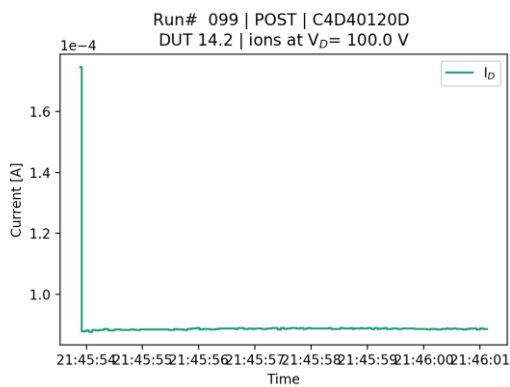
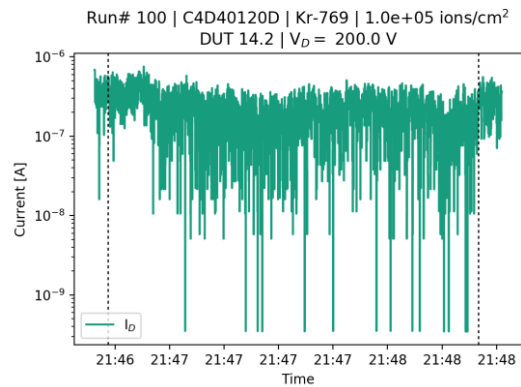
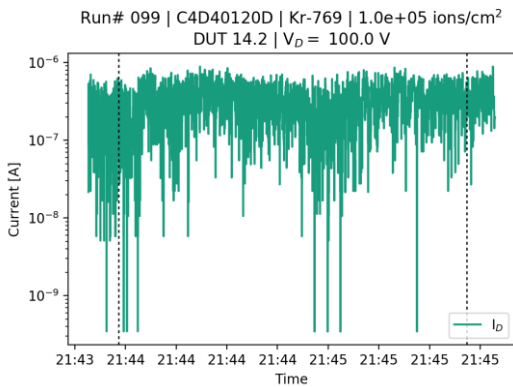
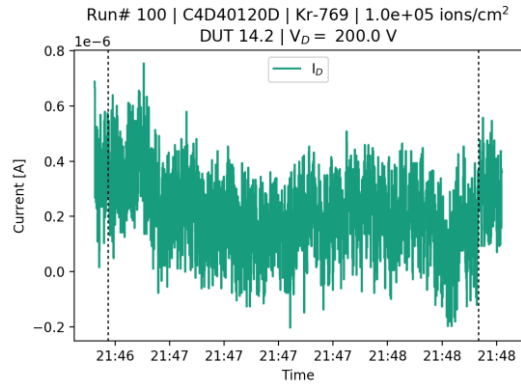


Figure 42: Run# 101, C4D40120D, Kr-769, $1.0e+05$ ions/cm², DUT 14.2, $V_D = 250.0$ V

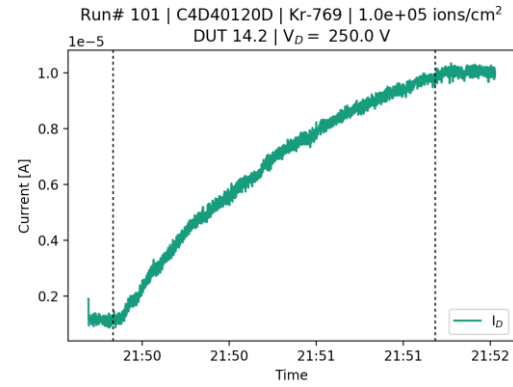


Figure 43: Run# 102, C4D40120D, Kr-769, $1.0e+05$ ions/cm², DUT 15.1, $V_D = 250.0$ V

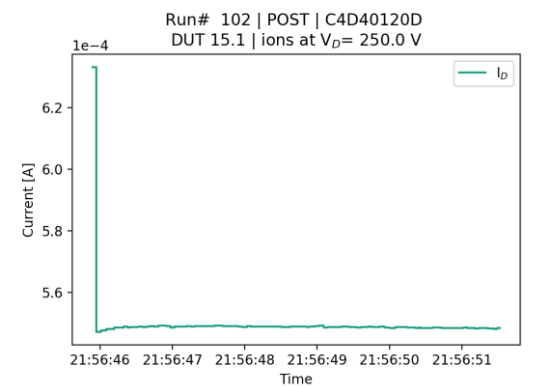
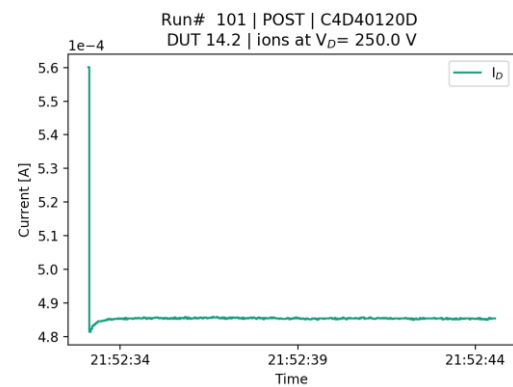
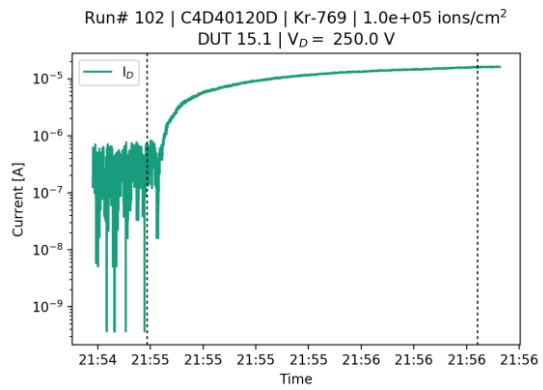
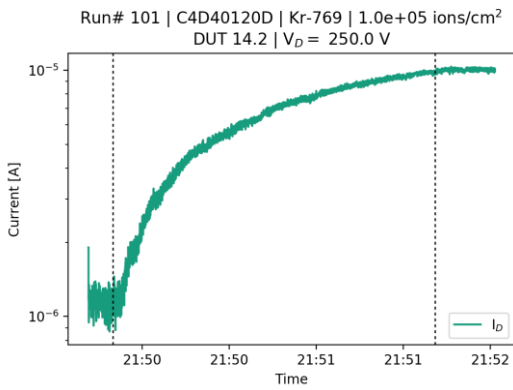
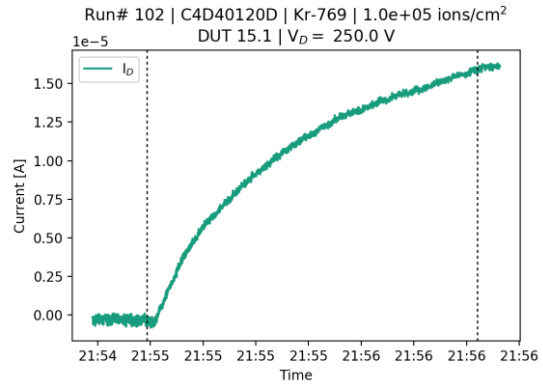
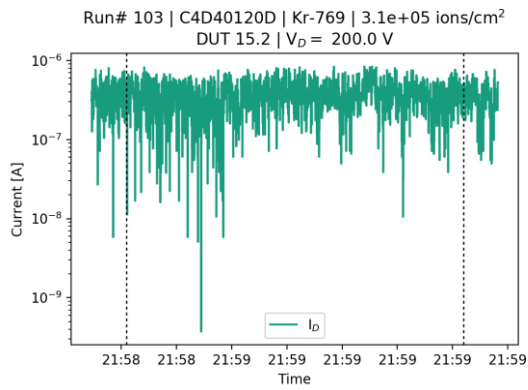
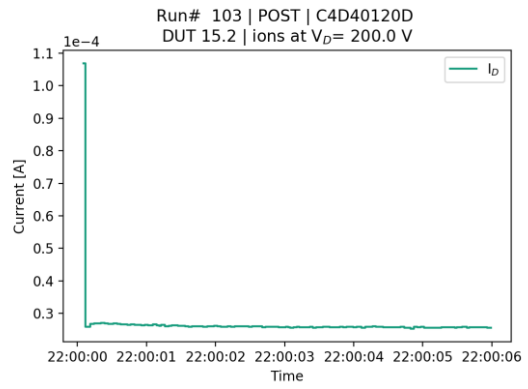
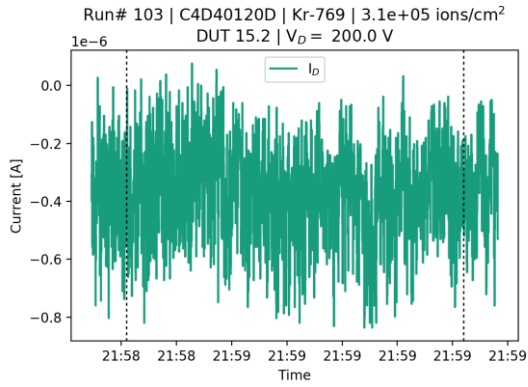


Figure 44: Run# 103, C4D40120D, Kr-769, 3.1×10^5 ions/cm², DUT 15.2, $V_D = 200.0$ V



C Appendix: Tests at JULIC

C.1. LET estimation

To receive the impact in terms of proton energy and LET on the Silicon Carbide die with packaged DUTs, radiation transport simulations have to be made:

- 1) The setup (beam exit window, air gap, package, die) were simulated with GRAS in standalone version 3.03 for $1E7$ protons. The average LET at the layer boundary from the package to the silicon carbide was evaluated by GRAS. This gives the average LET in MeV/cm. Rare events e.g. maximum recoil energy transfer, are few in these simulations. For the results in Table 13, this was then divided by the density $\rho = 3210 \text{ mg/cm}^3$ to give the LET in units of MeV cm^2/mg .
- 2) The setup (beam exit window, air gap, package, die) were simulated with MULASSIS in standalone version 1.26 for $1E7$ protons. The proton energy at the layer boundary from the package to the silicon carbide was evaluated by MULASSIS. With this proton energy, the maximum recoil energy to Silicon and Carbon atoms in SiC were calculated with $E_{ion}(E_p) = \frac{4 m_p m_{ion}}{(m_p + m_{ion})^2} \cdot E_p$. SRIM 2013 [9] simulations were then performed with the respective particles and maximum kinetic energy in Silicon Carbide. From the SRIM ionization curve the LET can then be calculated. This LET gives information on the recoils happening inside the SiC layer and is not restricted to the layer "surface" (although only extreme values were considered).

For these simulations, the 1 mm Aluminum exit window and 1.8 m of air were taken into account, such that the spread of the proton energy on the DUT package and the transport simulations through the package in the LET calculations is included. Package thickness for all materials was taken as 0.5, 1, 2 and 3 mm. The 3 mm was not simulated for Aluminum package (which was on the scale of 0.5 mm).

Alternatively the above geometry could be simulated only with SRIM. This has however some major drawbacks, when looking at a $100 \mu\text{m}$ layer at the end of the target of length $>1.8 \text{ m}$ as then only particles incident on $\pm 50 \mu\text{m}$ around the center are evaluated.

Information on the plastic package of the materials was not readily available for the use in SRIM or GRAS, as both require the atomic stoichiometry of the materials. For the sake of the Monte Carlo simulations this does not have to be chemically exact, but has to reflect the likelihood of interacting e.g. with a Silicon, if an interaction with a random nucleus takes place.

For some devices in this project, information was given in the Material Content Data Sheet. A value of 2.37 g/cm^3 was assumed for the density of the plastic mold and the stoichiometry for the example of SiC MOSFET C2M0080120D was estimated to be around Si:O:C:H = 1.6 : 3.6 : 1.2 : 1, thus the estimate for the chemical sum formula to be used in the simulations to be $\text{Si}_3\text{-O}_7\text{-C}_2\text{-H}_2$.

Table 21: Mold material of example C2M0080120D. Values indicated with * are estimates.

Name	CAS	Stoichiometry	Density [g/cm ³]	Molar mass [u]	Mass in Mold [mg]
Silicon Dioxide	7631-86-9	SiO ₂	2.6	60.0843	1640.71
Epoxy Resin	29690-82-2	C ₃₃ H ₄₂ O ₉ X ₂	1.12 *	582.68 *	189.62
Anhydride	2421-28-5	C ₁₇ H ₆ O ₇	1.57 *	322.23 *	159.68
Carbon Black	1333-86-4	C	1.7	12.01	5.99

Table 22: Results of GRAS simulations of the LET with package thickness. The GRAS results are the average "surface" LETs on the layer boundary from the package to SiC and would include error information. Error estimates are not given but are < 0.001 MeV cm²/mg in any case).

Name	LET _{GRAS} [MeV cm ² /mg]			
	0.5 mm	1 mm	2 mm	3 mm
Al	0.012	0.008	0.004	--
Si1-O2-C1-H1	0.012	0.008	0.005	0.003
Si3-O7-C2-H2	0.012	0.008	0.005	0.003
Si545-O1220-C512-H597-P3-B1	0.013	0.009	0.005	0.004

Table 23: Intermediate results of MULASSIS simulations of the proton energy with package thickness. Little variation is seen based on the package material.

Name	E(p) [MeV] at boundary Package → SiC			
	0.5 mm	1 mm	2 mm	3 mm
Al	37.72	36.08	32.64	---
Si1-O2-C1-H1	37.77	36.18	32.85	29.17
Si3-O7-C2-H2	37.80	36.24	32.97	29.38
Si545-O1220-C512-H597-P3-B1	37.77	35.75	32.83	29.15
Average	37.76	36.06	32.82	29.23
LETSRIM [MeV cm ² /mg]	0.013	--	--	0.016

Table 24: Results of SRIM simulations of the LET with package thickness. The SRIM results are the maximum LETs of the Silicon or Carbon recoil nuclei. The values given are the peak values, i.e. not necessarily at the beginning of the track, in the material. The average energies from Table 23 were taken for the recoil energies.

	Silicon				Oxygen			
	0.5 mm	1 mm	2 mm	3 mm	0.5 mm	1 mm	2 mm	3 mm
Max. Energy of Recoil Atom (180°) [MeV]	5.05	4.82	4.39	3.91	10.79	10.30	9.38	8.35
Peak LET _{SRIM} [MeV cm ² /mg] at max. recoil	12.30	12.16	11.86	11.31	5.81	5.81	5.80	5.80
Peak at track length [μm]	0	0	0	0	4.5	4.1	3.3	2.8
Range [μm]	2.01	1.96	1.84	1.72	6.6	6.3	5.7	5.1

C.2. Logfile / Test steps

In case of device failure the fluences in this table indicate the fluence provided by the facility not the fluence until failure which may differ by some additional seconds of beam.

#	Date	Time	Ion	Device Type	Device	DUT #	V_D	beam time [s]	fluence [cm ⁻²]
38	20.09.	09:49	p	Schottky	C4D40120D	1.1	1200	19	6.7e09
39	20.09.	09:55	p	Schottky	C4D40120D	1.2	900	252	1.1e11
40	20.09.	10:05	p	Schottky	C4D40120D	2.1	900	250	1.1e11
41	20.09.	10:14	p	Schottky	C4D40120D	2.2	900	253	1.1e11

C.3. Measurements

Figure 45: Run# 038, C4D40120D, p, 6.7e+09 p/cm², DUT 1.1, VD= 1200.0 V

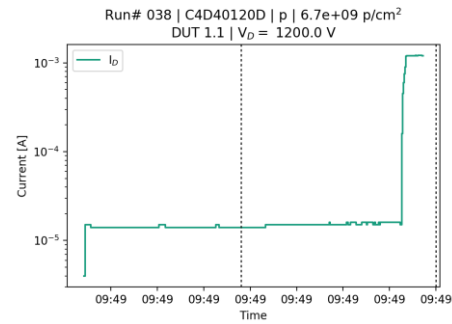
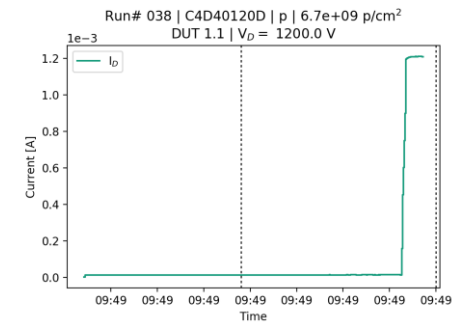
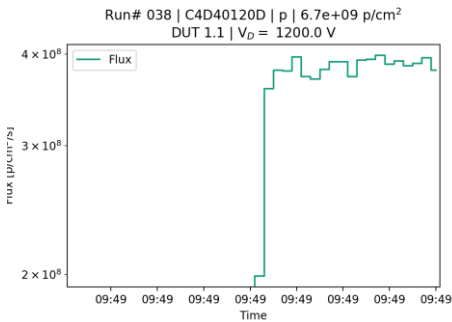


Figure 46: Run# 039, C4D40120D, p, 1.1e+11 p/cm², DUT 1.2, VD= 900.0 V

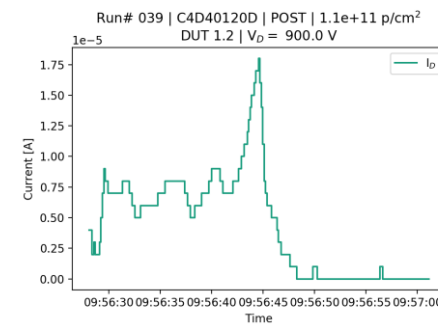
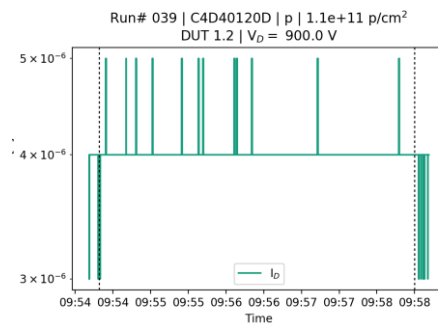
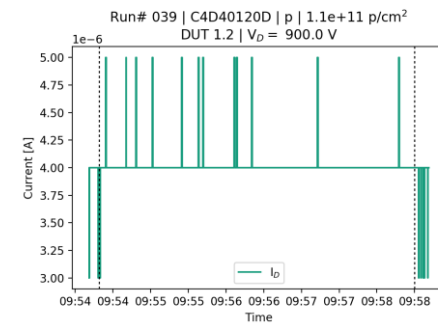
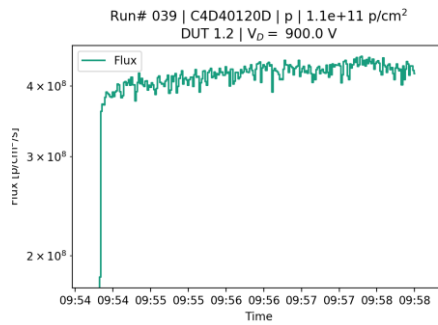


Figure 47: Run# 040, C4D40120D, p, 1.1e+11 p/cm², DUT 2.1, VD= 900.0 V

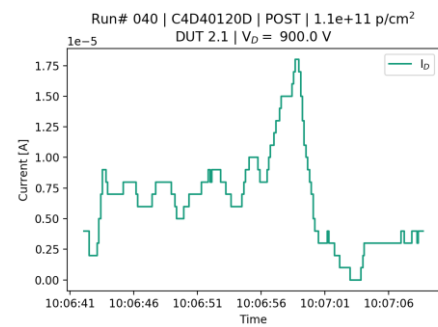
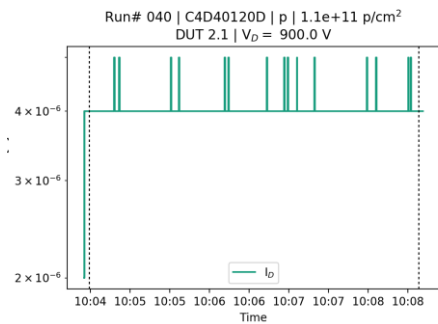
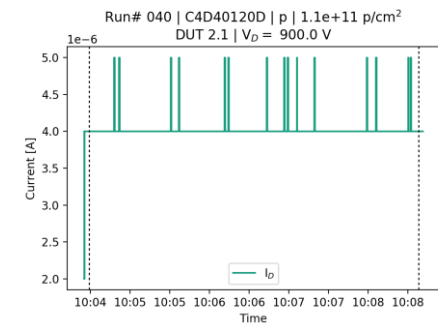
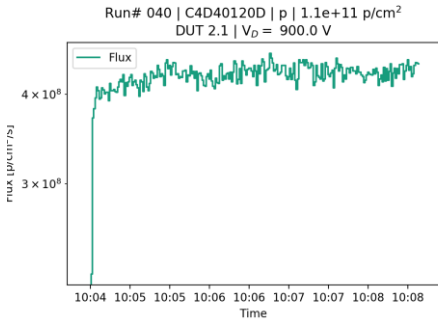
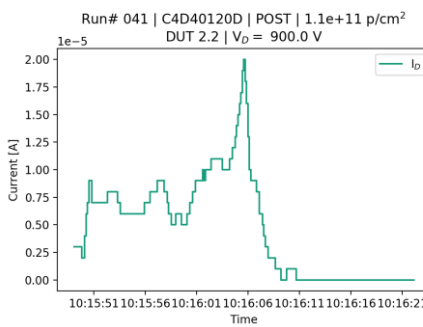
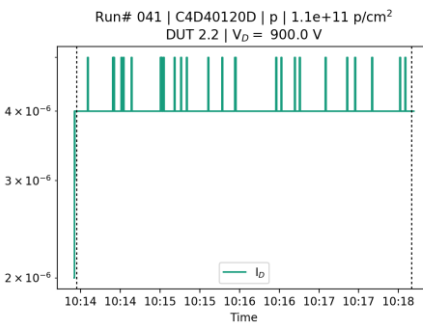
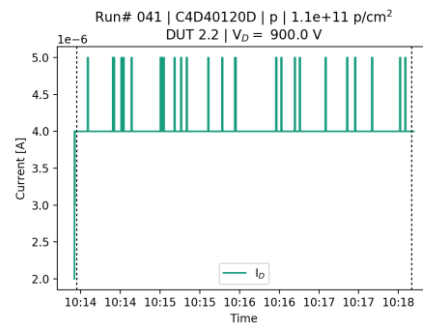
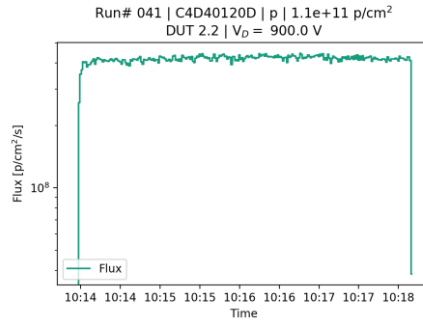


Figure 48: Run# 041, C4D40120D, p, 1.1e+11 p/cm², DUT 2.2, VD= 900.0 V



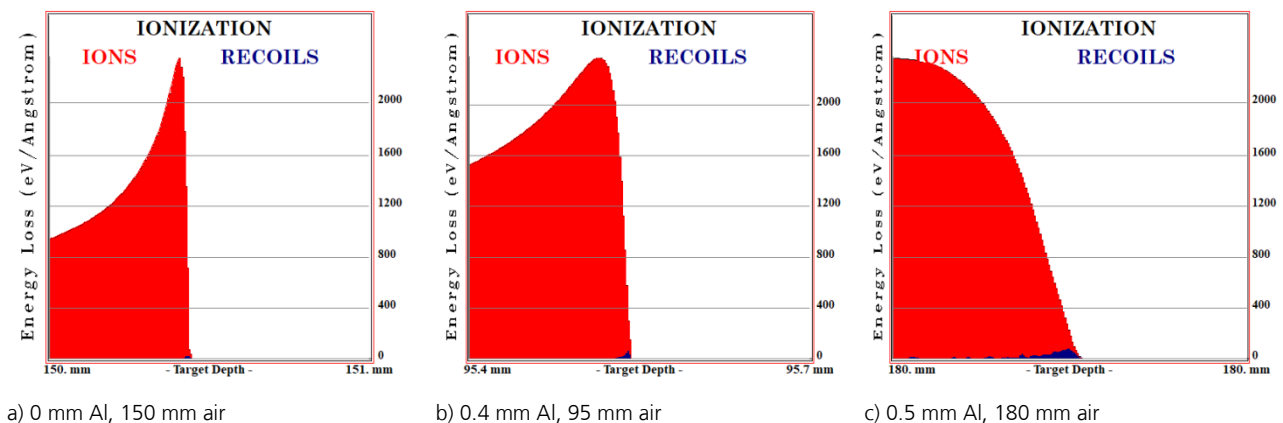
D Appendix: Tests at GANIL

D.1. LET estimation

To receive the impact in terms of LET on the Silicon Carbide die, radiation transport simulations have to be made. A major difference to the proton LET estimations, is that the tests were performed on decapsulated devices, so the package is not taken into account.

For these simulations, the 10 μm stainless steel exit window, a variable amount of air gap, and if applicable an Aluminium degrader were included in simulations with SRIM2013. The incident particles were 49.1 MeV/n Xenon ions (isotope mass = 136 u).

Figure 49: SRIM2013 simulations of the Ganil Xenon tests on SiC



The views of the ionization curves in Figure 49 start at the surface of the silicon carbide layer, so e.g. at 95.410 mm in Figure 49 b), although only one digit is displayed.

The LET in $\text{MeV cm}^2/\text{mg}$ can be directly calculated from the Energy loss in $\text{eV}/\text{\AA}$ by unit conversion ($1 \text{ eV}/\text{\AA} = 100 \text{ MeV}/\text{cm}$) and division by the SiC density of $3.21 \text{ g}/\text{cm}^3 = 3210 \text{ mg}/\text{cm}^3$.

Table 25: GANIL: Beam characteristics. Values in Silicon are provided by GANIL [12] Values in SiC are calculated by INT and given with one digit

Degrader [mm Al]	Air gap [mm]	LET (Si) ($\text{MeV}\cdot\text{cm}^2/\text{mg}$)	Range (Si) [μm]	LET _{SURF} (SiC) [$\text{MeV}\cdot\text{cm}^2/\text{mg}$]	Range (SiC) [μm]
0	150	27.76	640.33	29.2	430
0.4	95	42.03	226.23	47.2	141
0.5	180	60.12	65.68	72.9	30

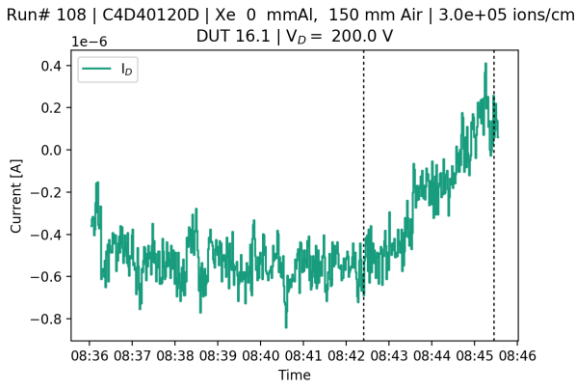
D.2. Logfile / Test steps

#	Date	Time	Ion	Al [μm]	Air [mm]	Device Type	Device	Position on board	DUT #	V_DS, V	beam time [s]	fluence [cm ⁻²]
108	06.06.	08:34	Xe	0	150	Schottky	C4D40120D	#1	16.1	200	183	3.00E+05
109	06.06.	08:46	Xe	0	150	Schottky	C4D40120D	#1	16.2	150	200	3.00E+05
110	06.06.	08:52	Xe	0	150	Schottky	C4D40120D	#2	17.1	150	187	3.00E+05
112	06.06.	09:26	Xe	0	150	Schottky	C4D40120D	#2	17.1	200	111	3.00E+05
113	06.06.	09:33	Xe	0	150	Schottky	C4D40120D	#1	16.2	300	126	3.00E+05
114	06.06.	09:47	Xe	0	150	Schottky	C4D40120D	#2	17.2	175	*	3.00E+05
115	06.06.	09:55	Xe	0	150	Schottky	C4D40120D	#3	18.1	175	125	6.00E+05
116	06.06.	10:18	Xe	500	180	Schottky	C4D40120D	#3	18.1	100	111	6.00E+05
117	06.06.	10:21	Xe	500	180	Schottky	C4D40120D	#3	18.1	150	107	6.00E+05
118	06.06.	10:27	Xe	500	180	Schottky	C4D40120D	#3	18.2	200	103	6.00E+05
119	06.06.	10:31	Xe	400	95	Schottky	C4D40120D	#1	19.1	150	107	6.00E+05
120	06.06.	10:34	Xe	400	95	Schottky	C4D40120D	#1	19.1	175	100	6.00E+05
121	06.06.	10:37	Xe	400	95	Schottky	C4D40120D	#1	19.1	200	107	6.00E+05
122	06.06.	10:40	Xe	400	95	Schottky	C4D40120D	#1	19.2	175	111	6.00E+05
123	06.06.	10:47	Xe	500	180	Schottky	C4D40120D	#1	19.2	125	111	6.00E+05
124	06.06.	10:50	Xe	500	180	Schottky	C4D40120D	#2	20.1	125	109	6.00E+05

* conflicting information in Logfile (in the rapport, run #114 was included and run #115 was missing. However after cross checking the times and information, #114 of the rapport would only fit for run #115). Fluence was noted in INT log file.

D.3. Measurements

Figure 50: Run# 108, C4D40120D, Xe 0 mmAl, 150 mm Air, $3.0e+05$ ions/cm², DUT 16.1, $V_D=200.0$ V



Run# 108 | C4D40120D | Xe 0 mmAl, 150 mm Air | $3.0e+05$ ions/cm² DUT 16.1 | $V_D=200.0$ V

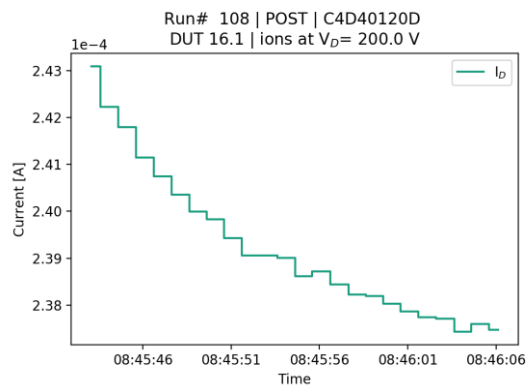
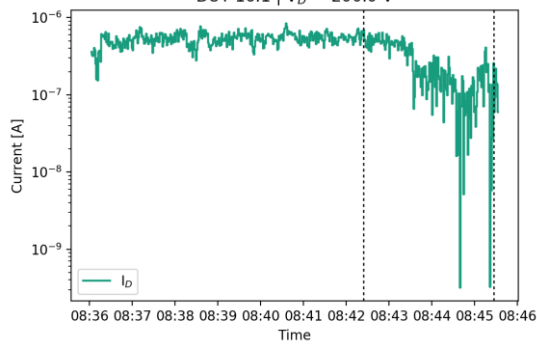
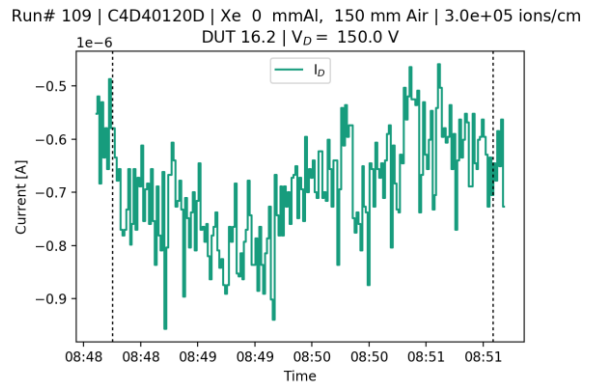


Figure 51: Run# 109, C4D40120D, Xe 0 mmAl, 150 mm Air, $3.0e+05$ ions/cm², DUT 16.2, $V_D=150.0$ V



Run# 109 | C4D40120D | Xe 0 mmAl, 150 mm Air | $3.0e+05$ ions/cm² DUT 16.2 | $V_D=150.0$ V

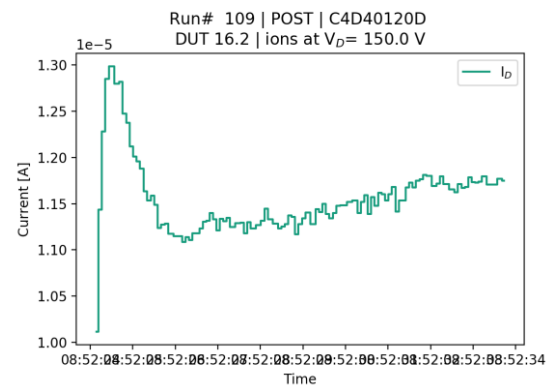
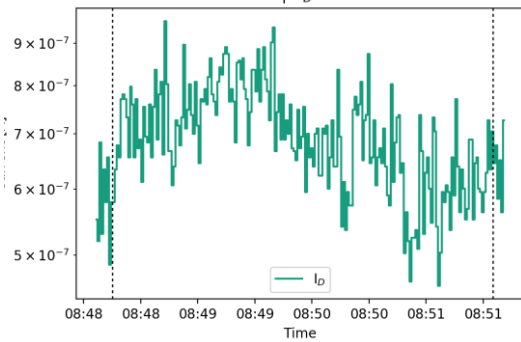
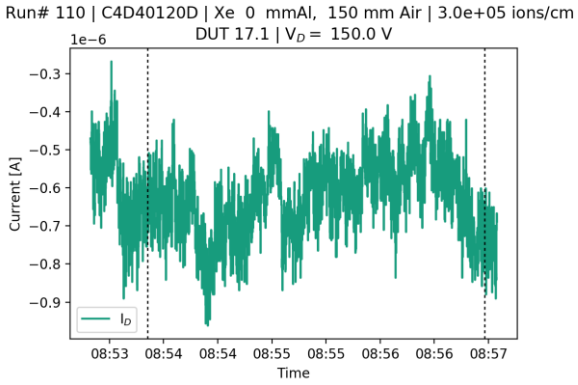


Figure 52: Run# 110, C4D40120D, Xe 0 mmAl, 150 mm Air, $3.0e+05$ ions/cm², DUT 17.1, $V_D=150.0$ V



Run# 110 | C4D40120D | Xe 0 mmAl, 150 mm Air | $3.0e+05$ ions/cm² | DUT 17.1 | $V_D=150.0$ V

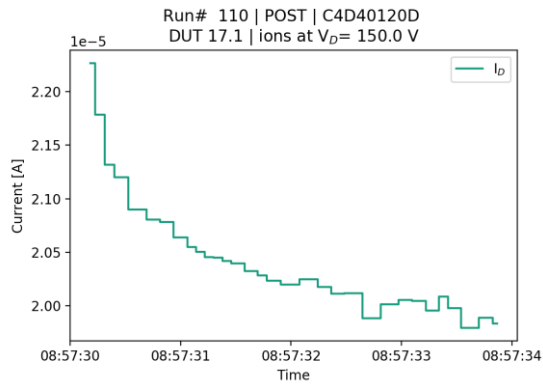
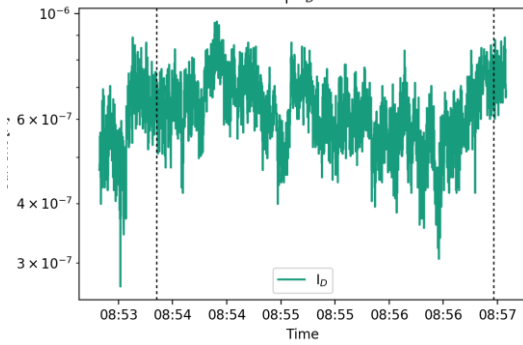
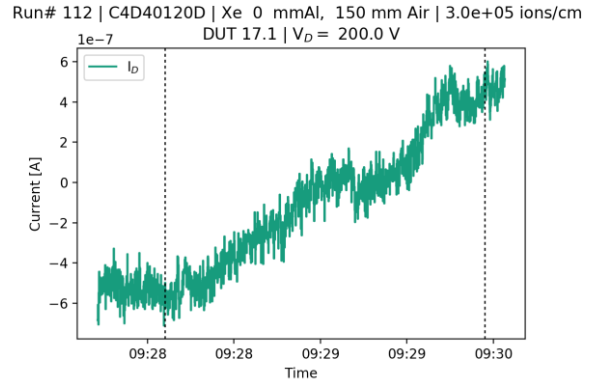


Figure 53: Run# 112, C4D40120D, Xe 0 mmAl, 150 mm Air, $3.0e+05$ ions/cm², DUT 17.1, $V_D=200.0$ V



Run# 112 | C4D40120D | Xe 0 mmAl, 150 mm Air | $3.0e+05$ ions/cm² | DUT 17.1 | $V_D=200.0$ V

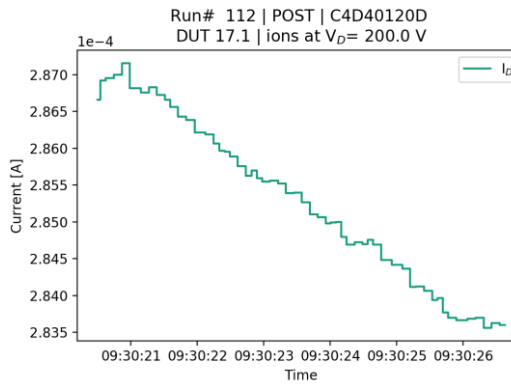
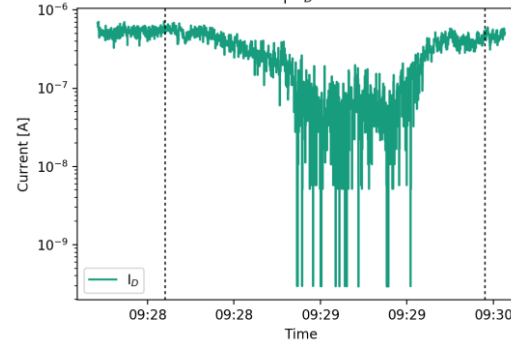
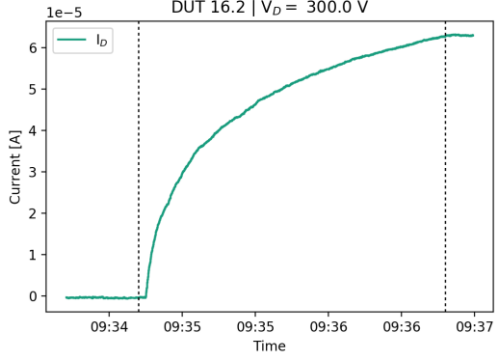


Figure 54: Run# 113, C4D40120D, Xe 0 mmAl, 150 mm Air, 3.0e+05 ions/cm², DUT 16.2, VD= 300.0 V

Run# 113 | C4D40120D | Xe 0 mmAl, 150 mm Air | 3.0e+05 ions/cm
DUT 16.2 | VD= 300.0 V



Run# 113 | C4D40120D | Xe 0 mmAl, 150 mm Air | 3.0e+05 ions/cm
DUT 16.2 | VD= 300.0 V

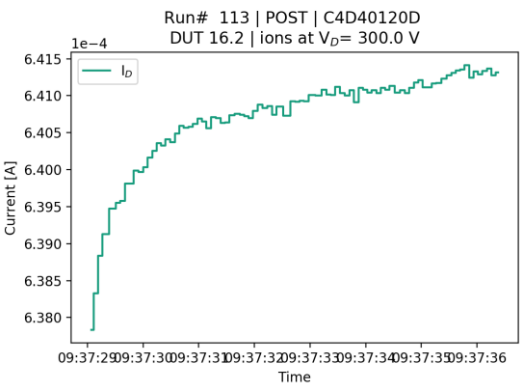
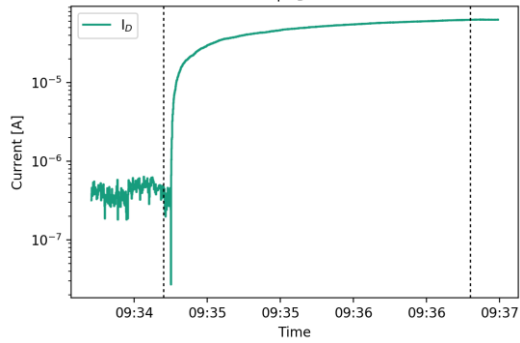
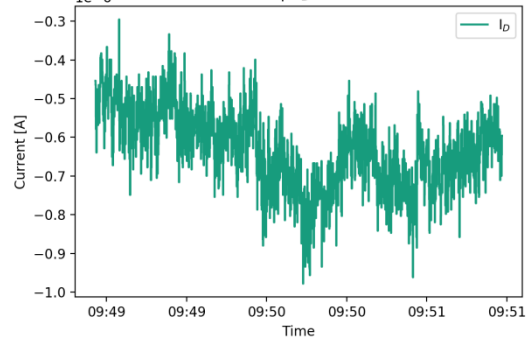


Figure 55: Run# 114 C4D40120D, Xe 0 mmAl, 150 mm Air, 3.0e+05 ions/cm², DUT 17.2, VD= 175.0 V

Run# 114 | C4D40120D | Xe 0 mmAl, 150 mm Air | 3.0e+05 ions/cm
DUT 17.2 | VD= 175.0 V



Run# 114 | C4D40120D | Xe 0 mmAl, 150 mm Air | 3.0e+05 ions/cm
DUT 17.2 | VD= 175.0 V

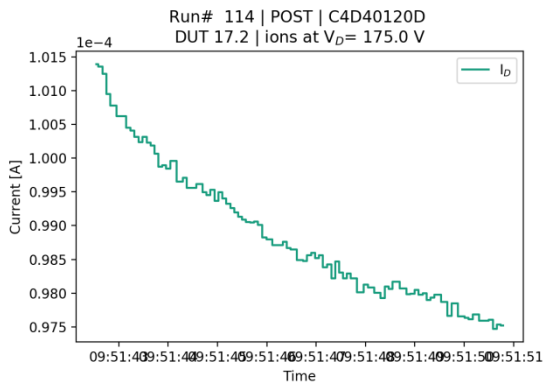
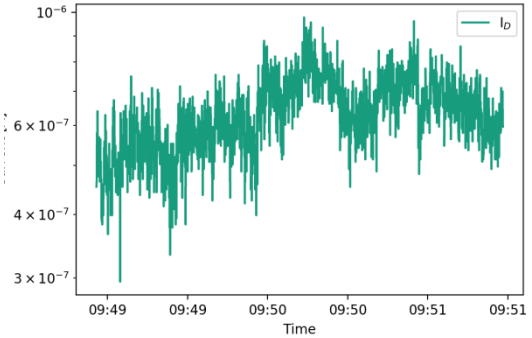
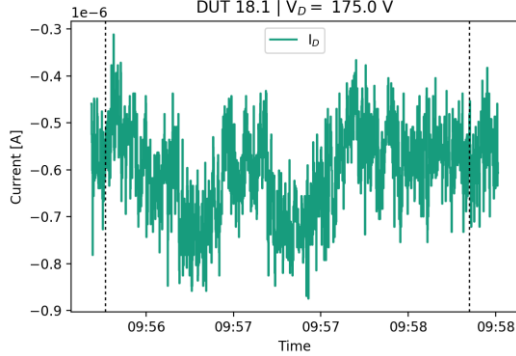
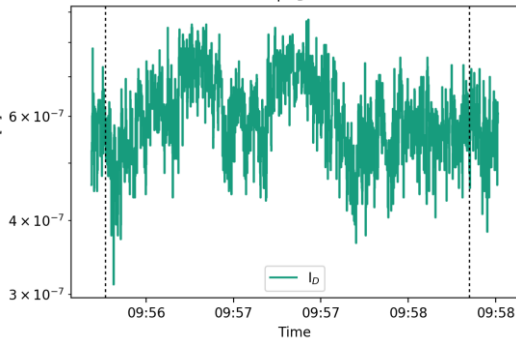


Figure 56: Run# 115, C4D40120D, Xe 0 mmAl, 150 mm Air, $6.0e+05$ ions/cm², DUT 18.1, $V_D=175.0$ V

Run# 115 | C4D40120D | Xe 0 mmAl, 150 mm Air | $6.0e+05$ ions/cm
DUT 18.1 | $V_D=175.0$ V



Run# 115 | C4D40120D | Xe 0 mmAl, 150 mm Air | $6.0e+05$ ions/cm
DUT 18.1 | $V_D=175.0$ V



Run# 115 | POST | C4D40120D
DUT 18.1 | ions at $V_D=175.0$ V

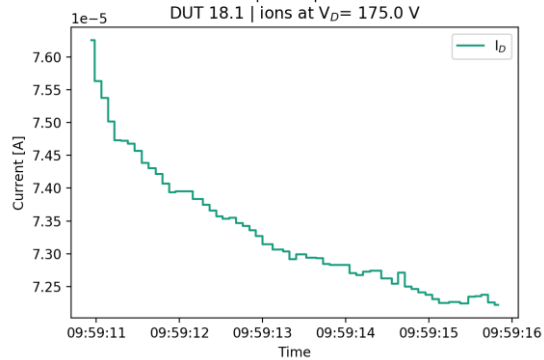
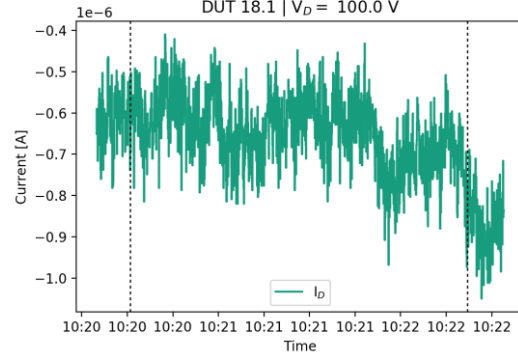
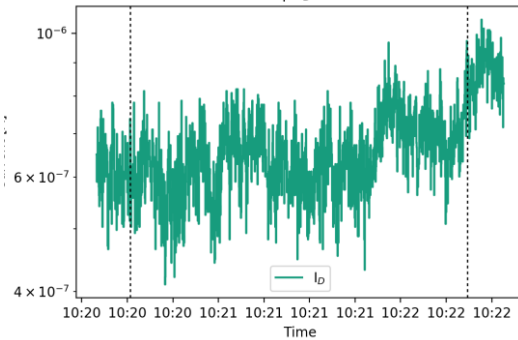


Figure 57: Run# 116, C4D40120D, Xe 500 mmAl, 180 mm Air, $6.0e+05$ ions/cm², DUT 18.1, $V_D=100.0$ V

Run# 116 | C4D40120D | Xe 500 mmAl, 180 mm Air | $6.0e+05$ ions/cm²
DUT 18.1 | $V_D=100.0$ V



Run# 116 | C4D40120D | Xe 500 mmAl, 180 mm Air | $6.0e+05$ ions/cm²
DUT 18.1 | $V_D=100.0$ V



Run# 116 | POST | C4D40120D
DUT 18.1 | ions at $V_D=100.0$ V

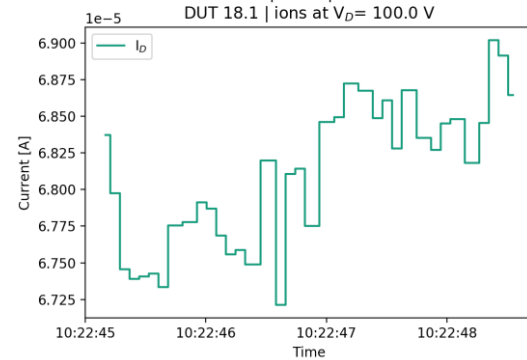
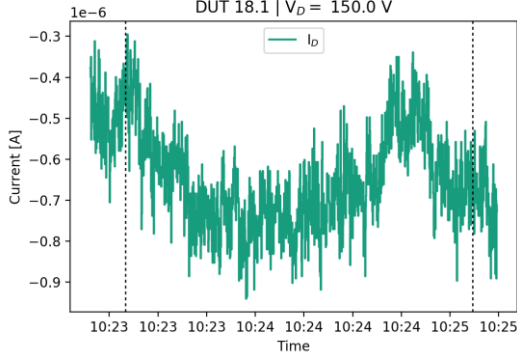
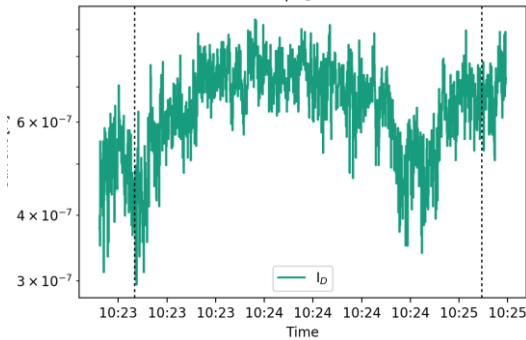


Figure 58: Run# 117, C4D40120D, Xe 500 mmAl, 180 mm Air, $6.0e+05$ ions/cm², DUT 18.1, $V_D = 150.0$ V

Run# 117 | C4D40120D | Xe 500 mmAl, 180 mm Air | $6.0e+05$ ions/cr
DUT 18.1 | $V_D = 150.0$ V



Run# 117 | C4D40120D | Xe 500 mmAl, 180 mm Air | $6.0e+05$ ions/cr
DUT 18.1 | $V_D = 150.0$ V



Run# 117 | POST | C4D40120D
DUT 18.1 | ions at $V_D = 150.0$ V

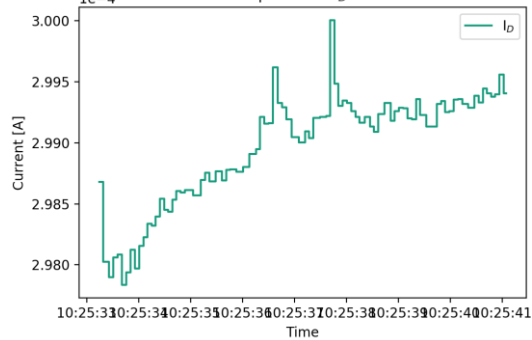
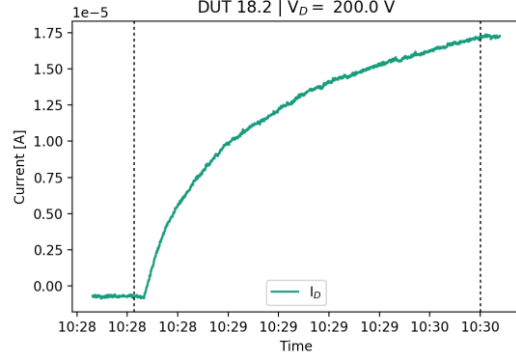
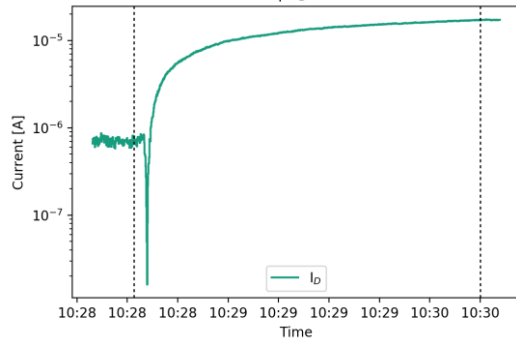


Figure 59: Run# 118, C4D40120D, Xe 500 mmAl, 180 mm Air, $6.0e+05$ ions/cm², DUT 18.2, $V_D = 200.0$ V

Run# 118 | C4D40120D | Xe 500 mmAl, 180 mm Air | $6.0e+05$ ions/cr
DUT 18.2 | $V_D = 200.0$ V



Run# 118 | C4D40120D | Xe 500 mmAl, 180 mm Air | $6.0e+05$ ions/cr
DUT 18.2 | $V_D = 200.0$ V



Run# 118 | POST | C4D40120D
DUT 18.2 | ions at $V_D = 200.0$ V

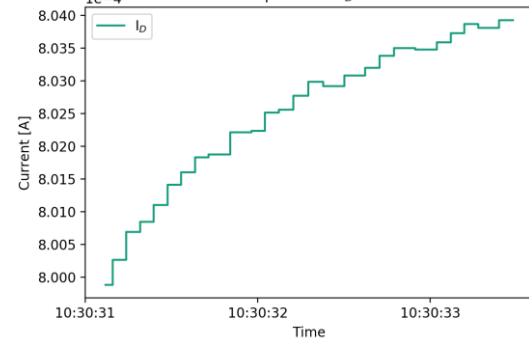
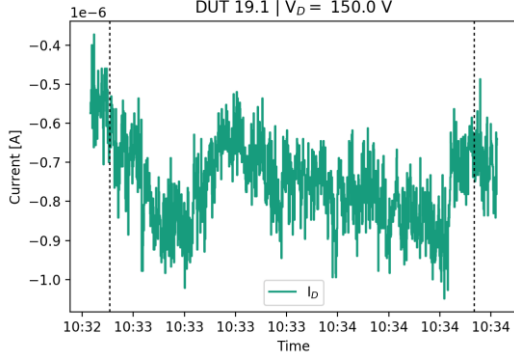


Figure 60: Run# 119, C4D40120D, Xe 400 mmAl, 95 mm Air, $6.0e+05$ ions/cm², DUT 19.1, $V_D=150.0$ V

Run# 119 | C4D40120D | Xe 400 mmAl, 95 mm Air | $6.0e+05$ ions/cr
DUT 19.1 | $V_D=150.0$ V



Run# 119 | C4D40120D | Xe 400 mmAl, 95 mm Air | $6.0e+05$ ions/cr
DUT 19.1 | $V_D=150.0$ V

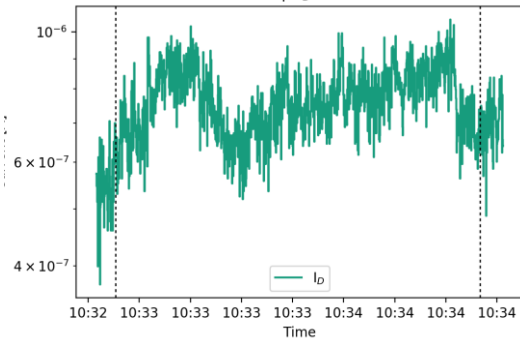
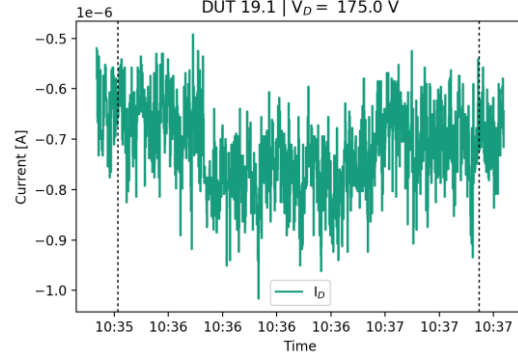
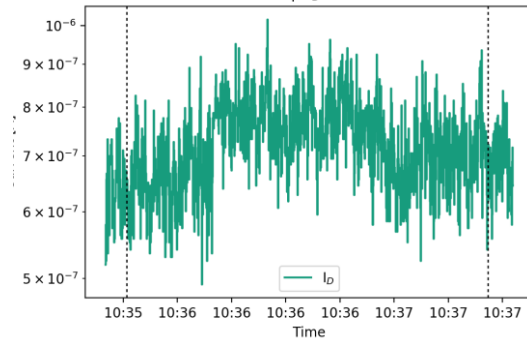


Figure 61: Run# 120, C4D40120D, Xe 400 mmAl, 95 mm Air, $6.0e+05$ ions/cm², DUT 19.1, $V_D=175.0$ V

Run# 120 | C4D40120D | Xe 400 mmAl, 95 mm Air | $6.0e+05$ ions/cr
DUT 19.1 | $V_D=175.0$ V



Run# 120 | C4D40120D | Xe 400 mmAl, 95 mm Air | $6.0e+05$ ions/cr
DUT 19.1 | $V_D=175.0$ V



Run# 119 | POST | C4D40120D
DUT 19.1 | ions at $V_D=150.0$ V

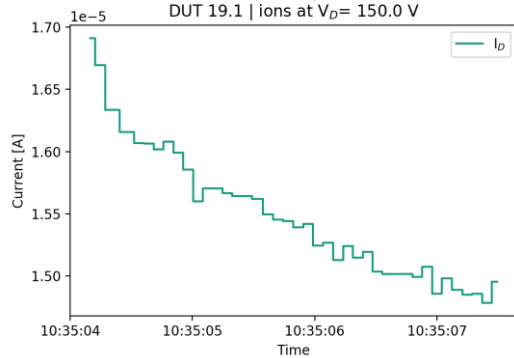
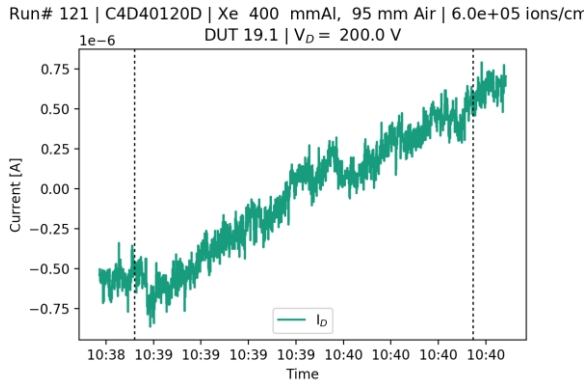


Figure 62: Run# 121, C4D40120D, Xe 400 mmAl, 95 mm Air, 6.0e+05 ions/cm², DUT 19.1, V_D= 200.0 V



Run# 121 | C4D40120D | Xe 400 mmAl, 95 mm Air | 6.0e+05 ions/crr
DUT 19.1 | V_D = 200.0 V

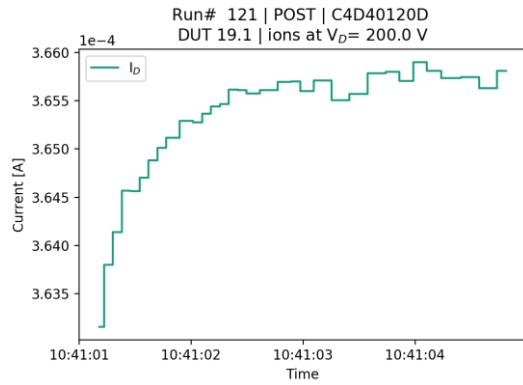
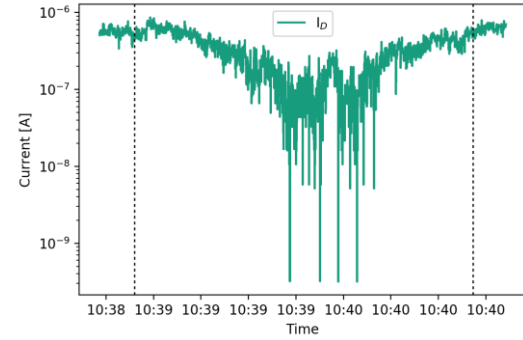
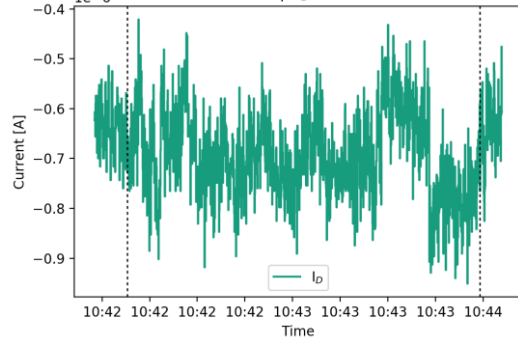


Figure 63: Run# 122, C4D40120D, Xe 400 mmAl, 95 mm Air, 6.0e+05 ions/cm², DUT 19.2, V_D= 175.0 V

Run# 122 | C4D40120D | Xe 400 mmAl, 95 mm Air | 6.0e+05 ions/crr
DUT 19.2 | V_D = 175.0 V



Run# 122 | C4D40120D | Xe 400 mmAl, 95 mm Air | 6.0e+05 ions/crr
DUT 19.2 | V_D = 175.0 V

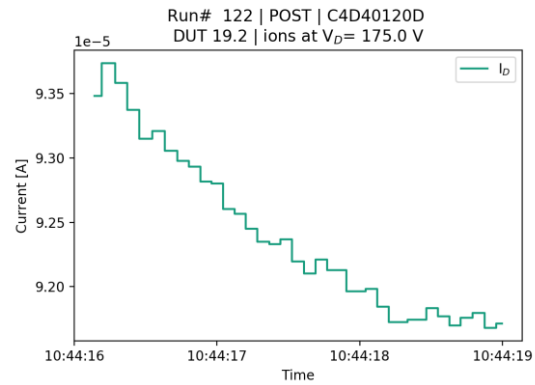
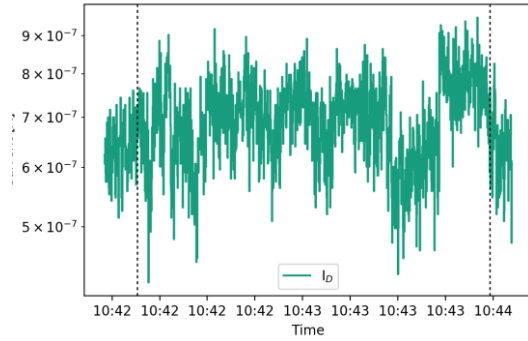
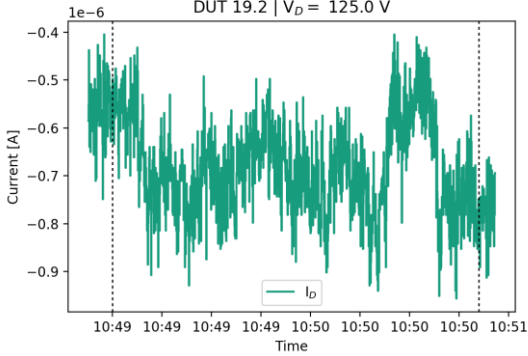


Figure 64: Run# 123, C4D40120D, Xe 500 mmAl, 180 mm Air, 6.0e+05 ions/cm², DUT 19.2, VD= 125.0 V

Run# 123 | C4D40120D | Xe 500 mmAl, 180 mm Air | 6.0e+05 ions/cr
DUT 19.2 | VD= 125.0 V



Run# 123 | C4D40120D | Xe 500 mmAl, 180 mm Air | 6.0e+05 ions/cr
DUT 19.2 | VD= 125.0 V

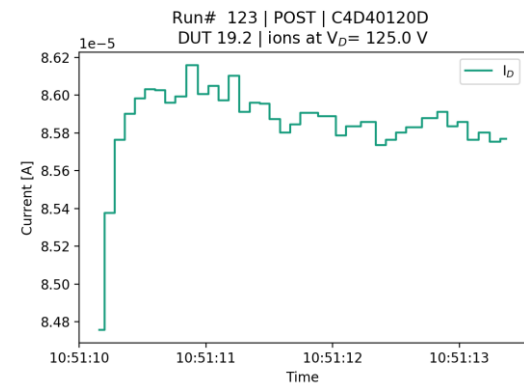
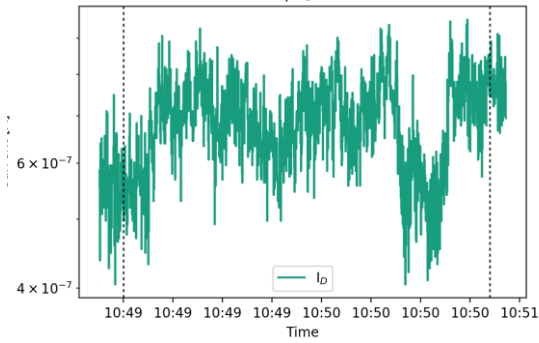
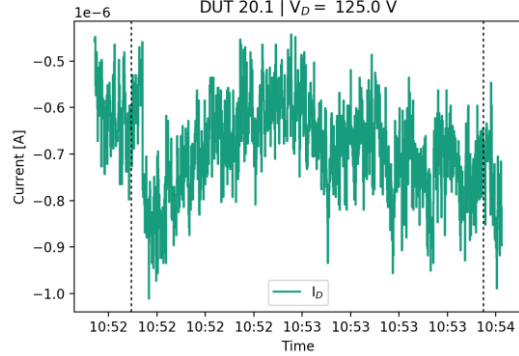
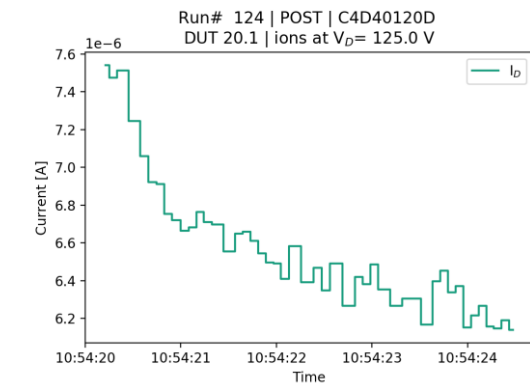
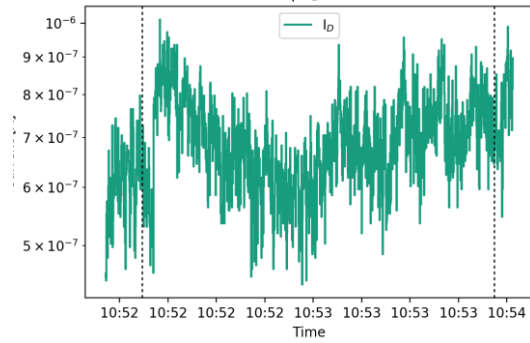


Figure 65: Run# 124, C4D40120D, Xe 500 mmAl, 180 mm Air, 6.0e+05 ions/cm², DUT 20.1, VD= 125.0 V

Run# 124 | C4D40120D | Xe 500 mmAl, 180 mm Air | 6.0e+05 ions/cr
DUT 20.1 | VD= 125.0 V



Run# 124 | C4D40120D | Xe 500 mmAl, 180 mm Air | 6.0e+05 ions/cr
DUT 20.1 | VD= 125.0 V



E Appendix: Tests at CERN

E.1. LET estimation

During the experiments (2017-11-30 – 2017-12-01) at the H8 beam line at CERN, the beam energy was set to 40 GeV/n. The calculation of the LET for particles of the energies cannot be done easily e.g. with SRIM. SRIM does not cover all interactions with matter at these energies and has a built-in limitation to ion energies of 10 GeV/n. Thus a realistic LET cannot be determined using SRIM.

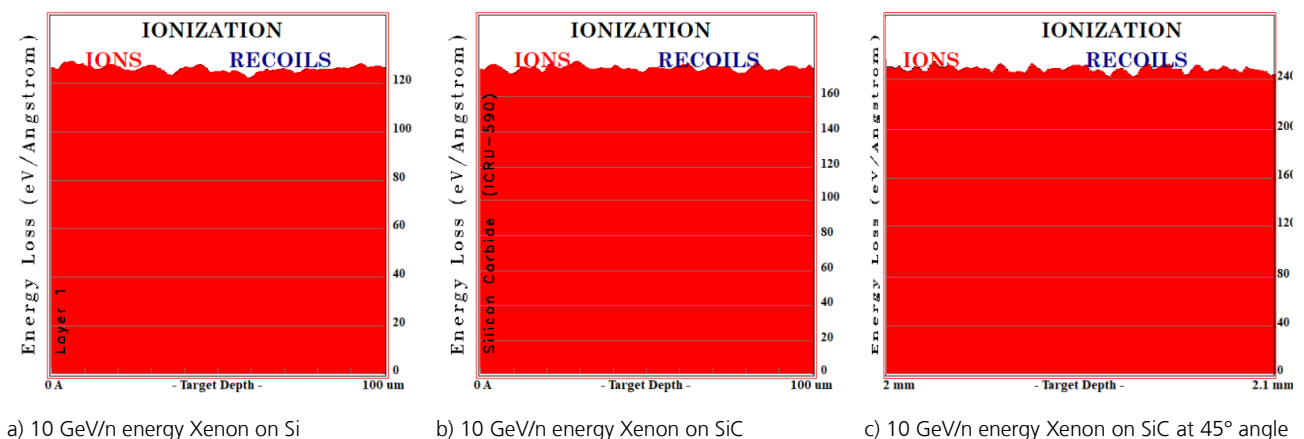
The LET values for silicon were simulated with FLUKA up to energies > 100 GeV/n and with SRIM up to 10 GeV/n by Rubén García Alía et al. and reported in [14]. There different LET values were considered, one unrestricted value taking into account all ionization caused by the beam (approx. 6.3 MeV cm²/mg) and a volume-restricted value covering the area of a 9.3 MeV/n Silicon particle track (approx. 3.7 MeV cm²/mg).

Up to energies of 10 GeV/n, the SRIM results closely follow the volume-unrestricted simulations in FLUKA. However, comparisons with the ESA SEU monitor in [14] indicate that the volume-restricted LET is a more proper expression for the particle LET in Silicon.

We will give only an approximation of the LET in SiC by looking at the similarity of results in Si and SiC with SRIM at 10 GeV/n energy. After that we compare simulations with and without a plastic package at that energy. Any air gap or beam exit window is ignored in these simulations, so the particles enter either the target material or a package immediately.

Figure 66 shows a constant ionization profile in a 100 μm layer of Si (left side) and SiC (right side). Taking the target density and the statistical fluctuations into account, the LETs amount to (5.43 ± 0.06) MeV cm²/mg for Si and (5.47 ± 0.05) MeV cm²/mg for SiC. Introducing a 2 mm plastic package (S11-O2-C1-H1 as defined in Appendix C) in front of the SiC does not alter the LET at all and again gives (5.47 ± 0.05) MeV cm²/mg (image not shown).

Figure 66: SRIM2013 simulations of Xenon ions of 10 GeV/n energy on Si and SiC



The Silicon LETs are in the same range as the SRIM-simulated ones from [14] and the unrestricted LETs simulated with FLUKA.

Finally we make two assumptions, both of which cannot be validated here:

1. If Si and SiC still yield the same results at 40 GeV/n, the LET would then be approx. 6.3 MeV cm²/mg.
2. As mentioned above, measurements in Silicon showed that the volume-restricted LET is more representative for the particle LET in Silicon, however we have no indication about that in SiC. Assuming similar behaviour, then the more proper LET of the 40 GeV/n in SiC would still be identical to the value of approx. 3.7 MeV cm²/mg in Silicon.

Thus in the end we assume the 40 GeV/m Xenon LET in SiC to be identical with the LET in Si based on the SRIM simulation results with Si and SiC at 10 GeV/n energy and assuming similarity at higher energies.

Additional simulations were performed with the ion beam directed under 45° angle to the SiC (tests were done at 42°). The SRIM results give an LET of (7.72 ± 0.07) MeV cm²/mg, which follows the rule of effective LET proportional to 1/cos(Θ). However in general the concept of effective LET is not valid for power devices [3] and all data collected at these settings further implicate that assuming a larger LET is invalid.

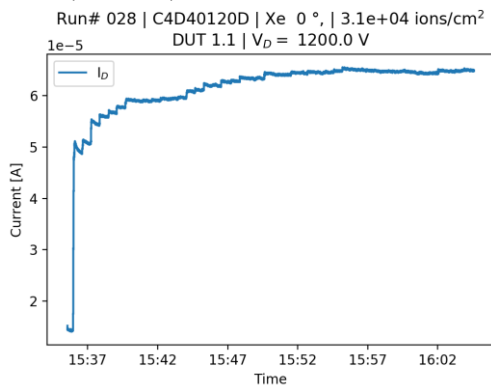
E.2. Logfile / Test steps

#	Date	Time	Ion	Tilt [°]	Device Type	Device	DUT #	V_DS, V	beam time [s]	fluence [cm ⁻²]
028	01.12.	15:35	Xe	0	Schottky	C4D40120D	1.1	1200	1.18E+03	3.14E+04
029	01.12.	16:05	Xe	0	Schottky	C4D40120D	1.2	1000	3.01E+02	8.03E+03
030	01.12.	16:11	Xe	0	Schottky	C4D40120D	1.2	1100	3.02E+02	8.05E+03
031	01.12.	16:16	Xe	0	Schottky	C4D40120D	1.2	1150	3.00E+02	8.00E+03
032	01.12.	16:21	Xe	0	Schottky	C4D40120D	1.2	1200	6.02E+02	1.61E+04
033	01.12.	16:32	Xe	0	Schottky	C4D40120D	1.2	1300	3.01E+02	8.03E+03
034	01.12.	16:37	Xe	0	Schottky	C4D40120D	2.1	1250	1.04E+02	2.77E+03
035	01.12.	16:40	Xe	0	Schottky	C4D40120D	2.2	1200	5.79E+02	1.54E+04
050	01.12.	18:13	Xe	42	Schottky	C4D40120D	3.1	1150	1.12E+02	2.99E+03
051	01.12.	18:15	Xe	42	Schottky	C4D40120D	3.1	1200	1.01E+02	2.69E+03
052	01.12.	18:17	Xe	42	Schottky	C4D40120D	3.1	1250	1.03E+02	2.75E+03
053	01.12.	18:19	Xe	42	Schottky	C4D40120D	3.1	1300	1.02E+02	2.72E+03
054	01.12.	18:21	Xe	42	Schottky	C4D40120D	3.1	1350	9.90E+01	2.64E+03
055	01.12.	18:23	Xe	42	Schottky	C4D40120D	3.1	1400	1.03E+02	2.75E+03
056	01.12.	18:24	Xe	42	Schottky	C4D40120D	3.1	1450	1.02E+02	2.72E+03
057	01.12.	18:26	Xe	42	Schottky	C4D40120D	3.1	1500	1.02E+02	2.74E+03
058	01.12.	18:29	Xe	42	Schottky	C4D40120D	3.2	1200	1.09E+02	2.94E+03

059	01.12.	18:31	Xe	42	Schottky	C4D40120D	3.2	1250	1.00E+02	2.72E+03
060	01.12.	18:33	Xe	42	Schottky	C4D40120D	3.2	1300	1.01E+02	2.76E+03
061	01.12.	18:34	Xe	42	Schottky	C4D40120D	3.2	1350	1.03E+02	2.83E+03
062	01.12.	18:36	Xe	42	Schottky	C4D40120D	3.2	1400	1.03E+02	2.85E+03
063	01.12.	18:38	Xe	42	Schottky	C4D40120D	3.2	1450	1.03E+02	2.87E+03
064	01.12.	18:40	Xe	42	Schottky	C4D40120D	3.2	1500	1.97E+02	5.52E+03

E.3. Measurement

Figure 67: Run# 028, C4D40120D, Xe 0°, 3.1e+04 ions/cm², DUT 1.1, V_D= 1200.0 V



Run# 028 | C4D40120D | Xe 0°, | 3.1e+04 ions/cm²
DUT 1.1 | V_D = 1200.0 V

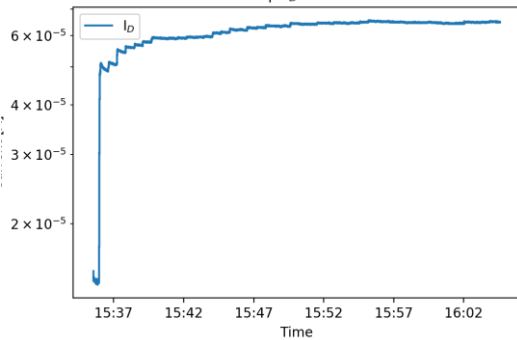
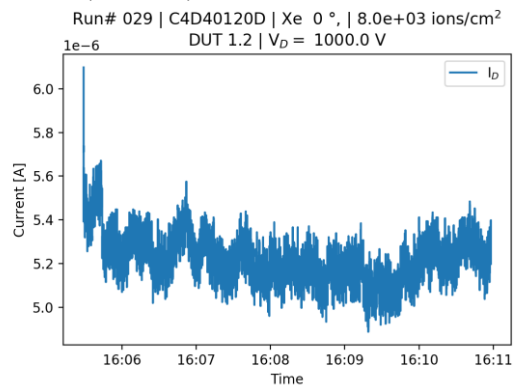


Figure 68: Run# 029, C4D40120D, Xe 0°, 8.0e+03 ions/cm², DUT 1.2, V_D= 1000.0 V



Run# 029 | C4D40120D | Xe 0°, | 8.0e+03 ions/cm²
DUT 1.2 | V_D = 1000.0 V

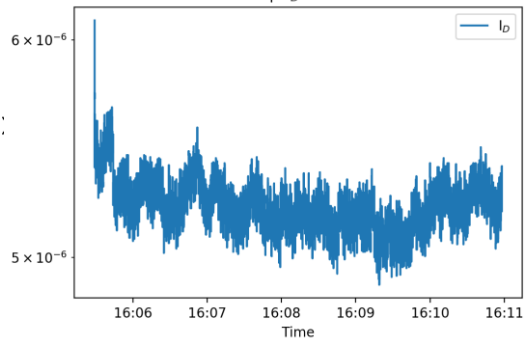


Figure 69: Run# 030, C4D40120D, Xe 0°, 8.1e+03 ions/cm², DUT 1.2, VD= 1100.0 V

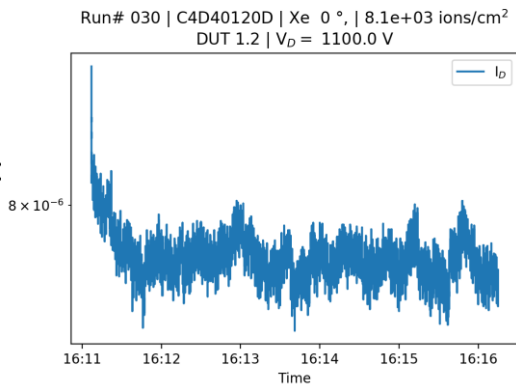
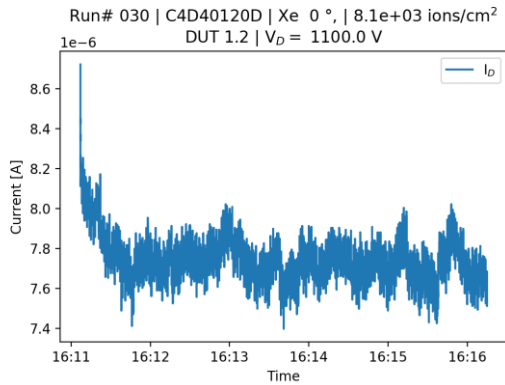


Figure 70: Run# 031, C4D40120D, Xe 0°, 8.0e+03 ions/cm², DUT 1.2, VD= 1150.0 V

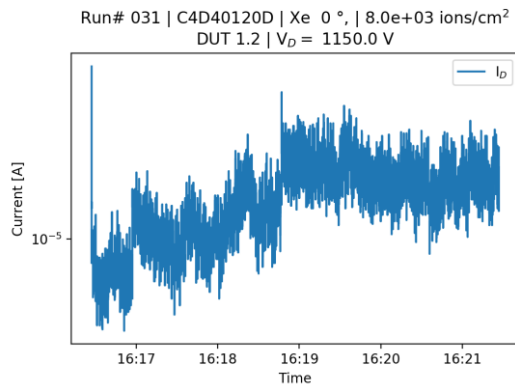
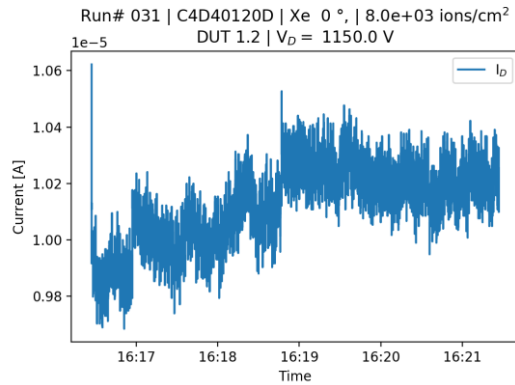


Figure 71: Run# 032, C4D40120D, Xe 0°, 1.6e+04 ions/cm², DUT 1.2, VD= 1200.0 V

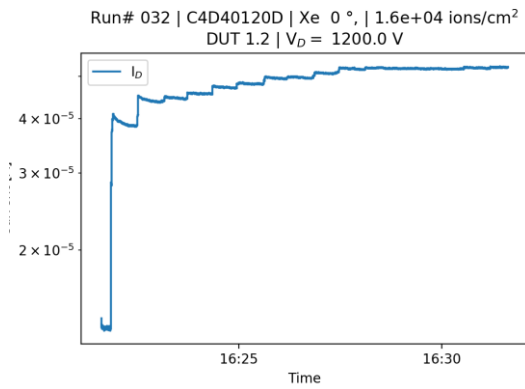
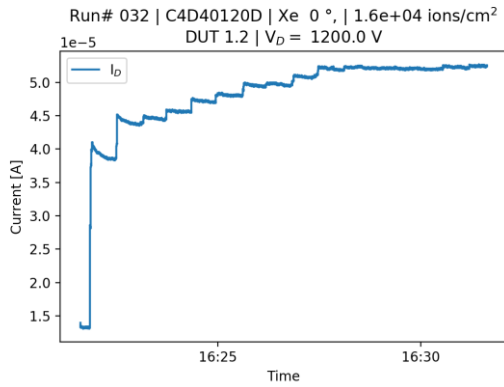


Figure 72: Run# 033, C4D40120D, Xe 0°, 8.0e+03 ions/cm², DUT 1.2, VD= 1300.0 V

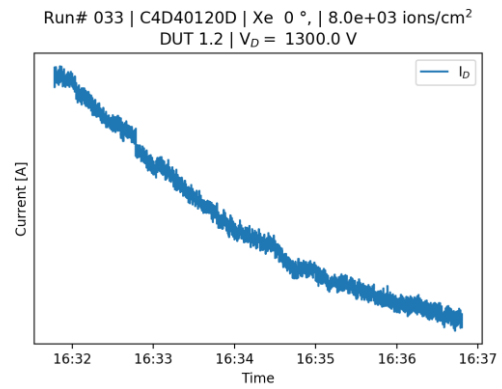
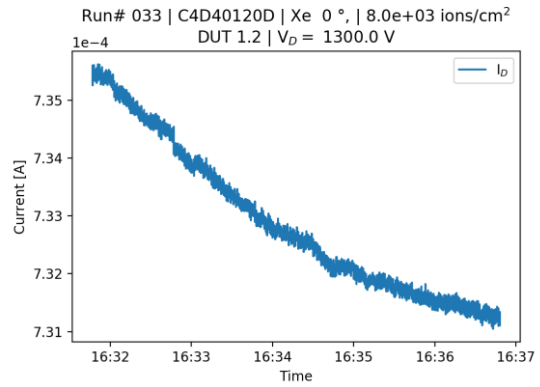


Figure 73: Run# 034, C4D40120D, Xe 0°, 2.8e+03 ions/cm², DUT 2.1, V_D= 1250.0 V

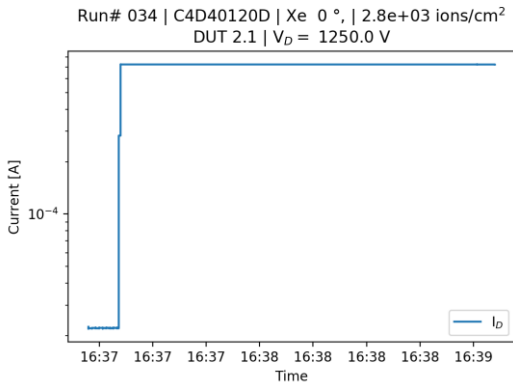
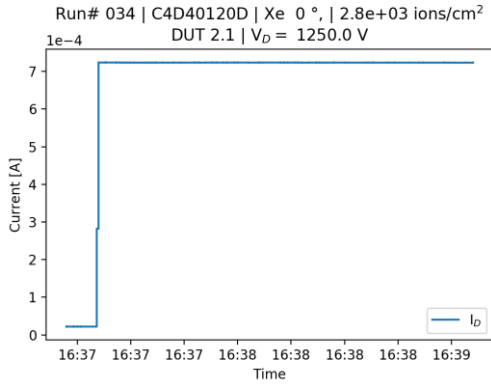


Figure 74: Run# 035, C4D40120D, Xe 0°, 1.5e+04 ions/cm², DUT 2.2, V_D= 1200.0 V

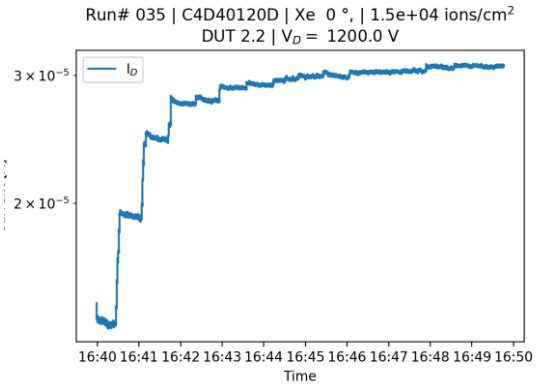
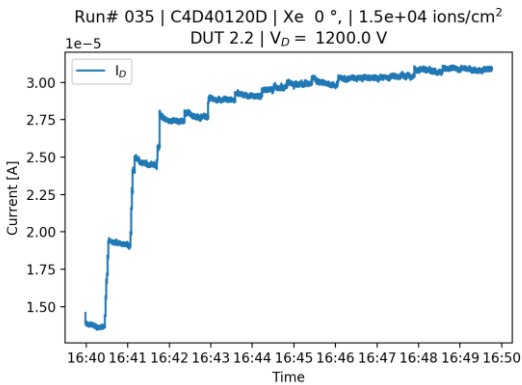
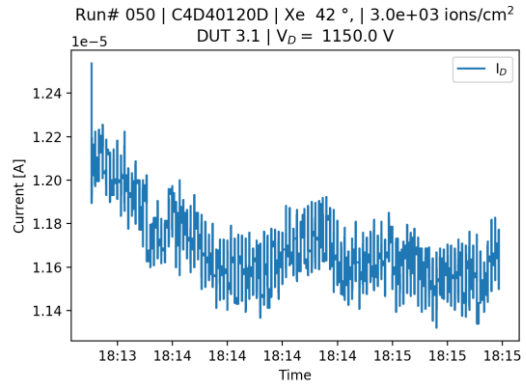


Figure 75: Run# 050, C4D40120D, Xe 42°, 3.0e+03 ions/cm², DUT 3.1, V_D= 1150.0 V



Run# 050 | C4D40120D | Xe 42°, | 3.0e+03 ions/cm²
DUT 3.1 | V_D = 1150.0 V

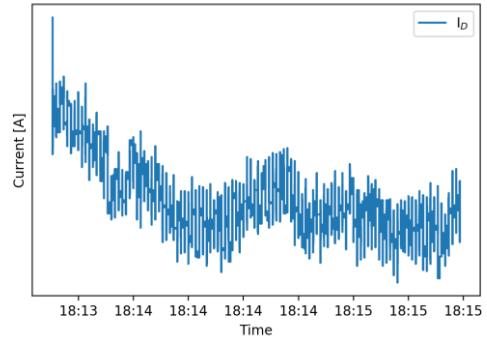
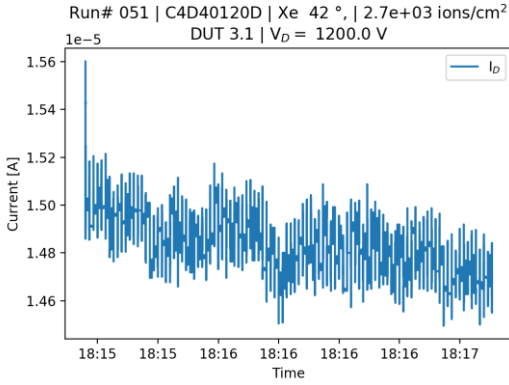
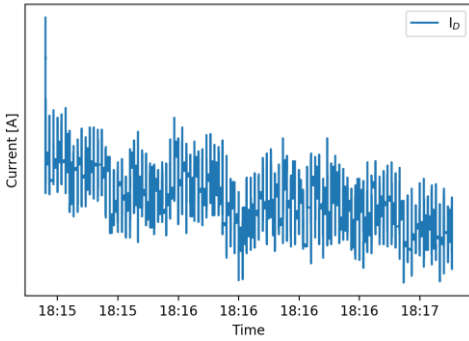


Figure 76: Run# 051, C4D40120D, Xe 42 °, 2.7e+03 ions/cm², DUT 3.1, V_D= 1200.0 V



Run# 051 | C4D40120D | Xe 42 °, | 2.7e+03 ions/cm²
DUT 3.1 | V_D = 1200.0 V



Run# 052 | C4D40120D | Xe 42 °, | 2.7e+03 ions/cm²
DUT 3.1 | V_D = 1250.0 V

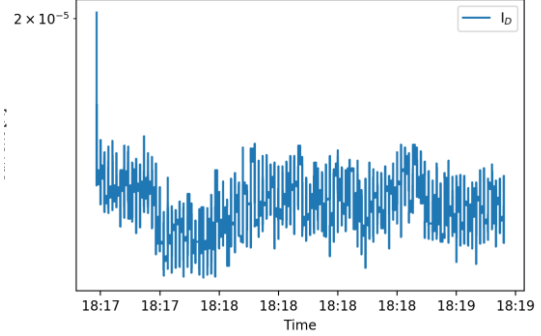


Figure 78: Run# 053, C4D40120D, Xe 42 °, 2.7e+03 ions/cm², DUT 3.1, V_D= 1300.0 V

Run# 053 | C4D40120D | Xe 42 °, | 2.7e+03 ions/cm²
DUT 3.1 | V_D = 1300.0 V

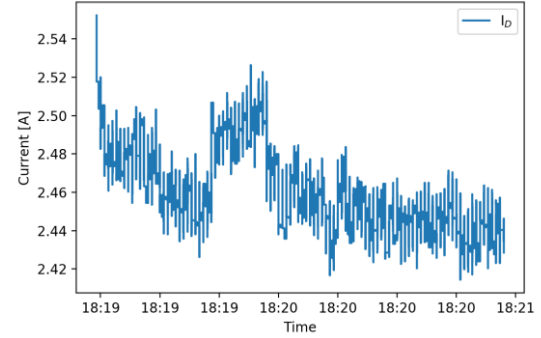
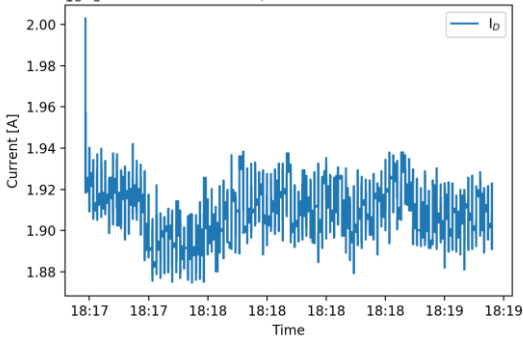


Figure 77: Run# 052, C4D40120D, Xe 42 °, 2.7e+03 ions/cm², DUT 3.1, V_D= 1250.0 V

Run# 052 | C4D40120D | Xe 42 °, | 2.7e+03 ions/cm²
DUT 3.1 | V_D = 1250.0 V



Run# 053 | C4D40120D | Xe 42 °, | 2.7e+03 ions/cm²
DUT 3.1 | V_D = 1300.0 V

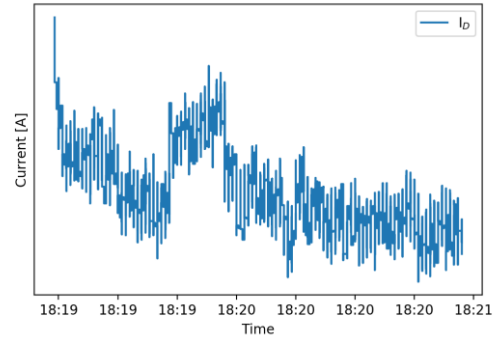
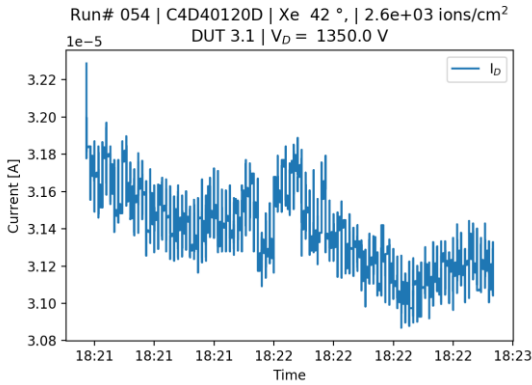
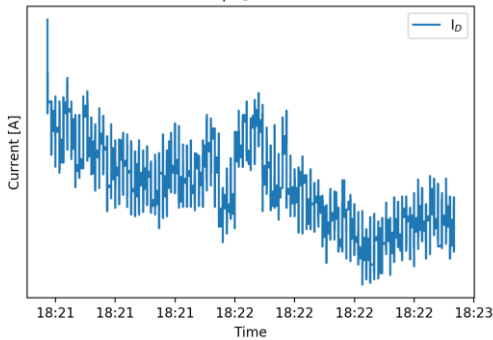


Figure 79: Run# 054, C4D40120D, Xe 42 °, 2.6e+03 ions/cm², DUT 3.1, V_D= 1350.0 V



Run# 054 | C4D40120D | Xe 42 °, | 2.6e+03 ions/cm²
DUT 3.1 | V_D = 1350.0 V



Run# 055 | C4D40120D | Xe 42 °, | 2.7e+03 ions/cm²
DUT 3.1 | V_D = 1400.0 V

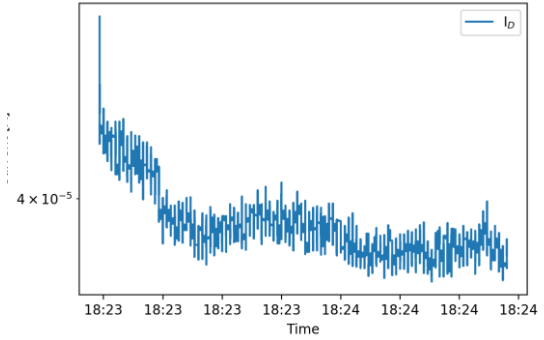


Figure 81: Run# 056, C4D40120D, Xe 42 °, 2.7e+03 ions/cm², DUT 3.1, V_D= 1450.0 V

Run# 056 | C4D40120D | Xe 42 °, | 2.7e+03 ions/cm²
DUT 3.1 | V_D = 1450.0 V

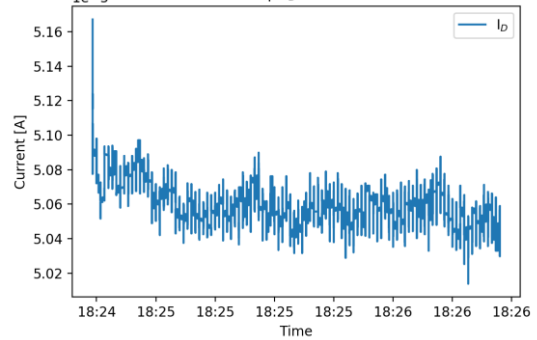
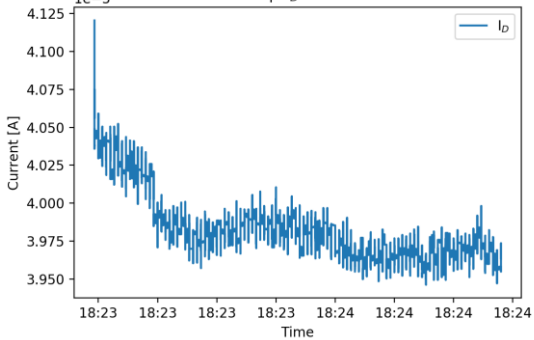


Figure 80: Run# 055, C4D40120D, Xe 42 °, 2.7e+03 ions/cm², DUT 3.1, V_D= 1400.0 V

Run# 055 | C4D40120D | Xe 42 °, | 2.7e+03 ions/cm²
DUT 3.1 | V_D = 1400.0 V



Run# 056 | C4D40120D | Xe 42 °, | 2.7e+03 ions/cm²
DUT 3.1 | V_D = 1450.0 V

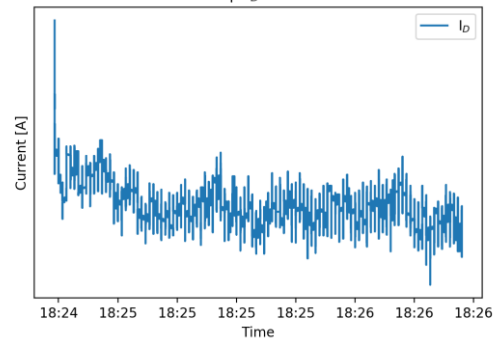
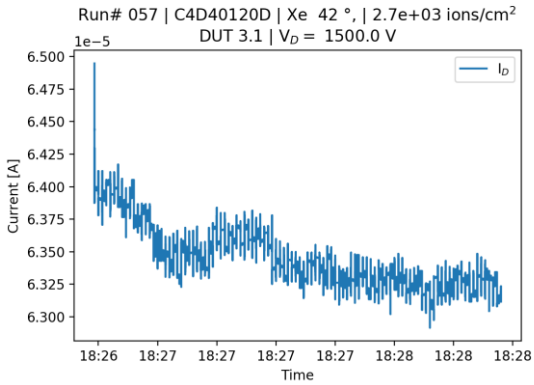
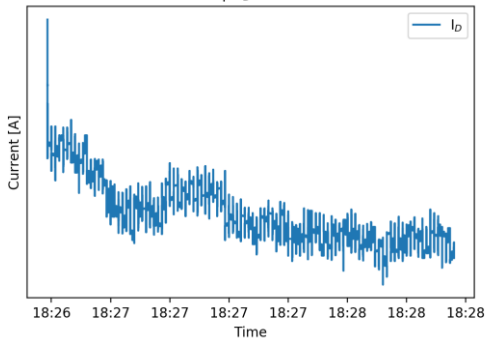


Figure 82: Run# 057, C4D40120D, Xe 42 °, 2.7e+03 ions/cm², DUT 3.1, V_D= 1500.0 V



Run# 057 | C4D40120D | Xe 42 °, | 2.7e+03 ions/cm²
DUT 3.1 | V_D = 1500.0 V



Run# 058 | C4D40120D | Xe 42 °, | 2.9e+03 ions/cm²
DUT 3.2 | V_D = 1200.0 V

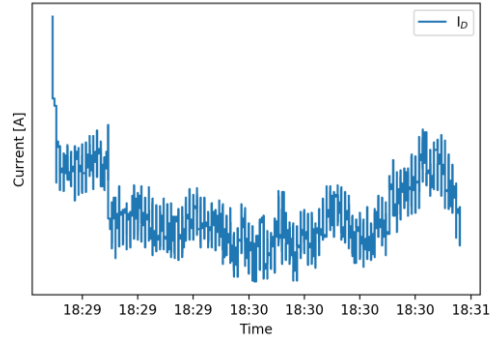


Figure 84: Run# 059, C4D40120D, Xe 42 °, 2.7e+03 ions/cm², DUT 3.2, V_D= 1250.0 V

Run# 059 | C4D40120D | Xe 42 °, | 2.7e+03 ions/cm²
DUT 3.2 | V_D = 1250.0 V

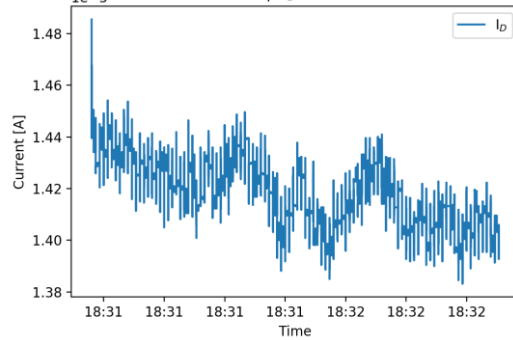
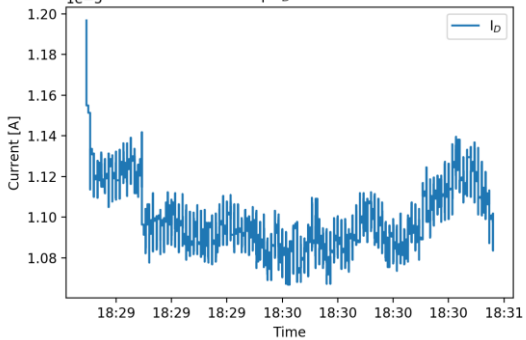


Figure 83: Run# 058, C4D40120D, Xe 42 °, 2.9e+03 ions/cm², DUT 3.2, V_D= 1200.0 V

Run# 058 | C4D40120D | Xe 42 °, | 2.9e+03 ions/cm²
DUT 3.2 | V_D = 1200.0 V



Run# 059 | C4D40120D | Xe 42 °, | 2.7e+03 ions/cm²
DUT 3.2 | V_D = 1250.0 V

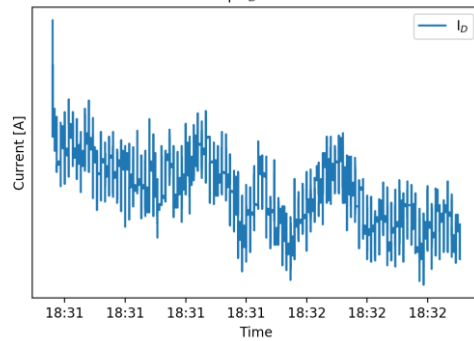
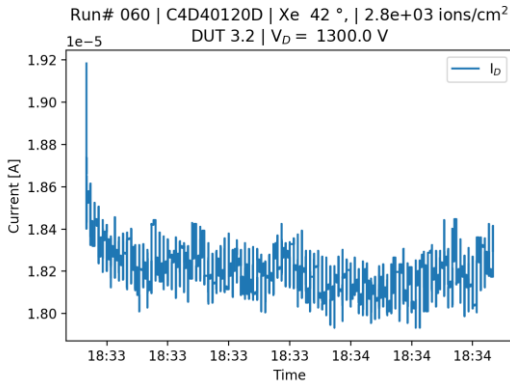


Figure 85: Run# 060, C4D40120D, Xe 42 °, 2.8e+03 ions/cm², DUT 3.2, V_D= 1300.0 V



Run# 061 | C4D40120D | Xe 42 °, | 2.8e+03 ions/cm²
DUT 3.2 | V_D = 1350.0 V

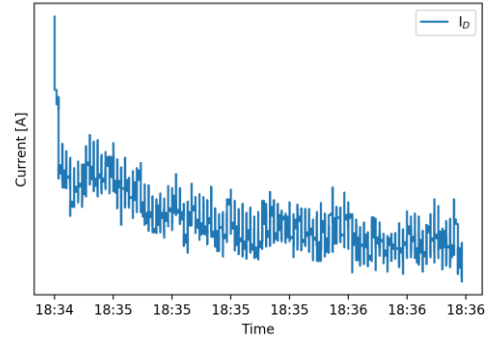


Figure 87: Run# 062, C4D40120D, Xe 42 °, 2.8e+03 ions/cm², DUT 3.2, V_D= 1400.0 V

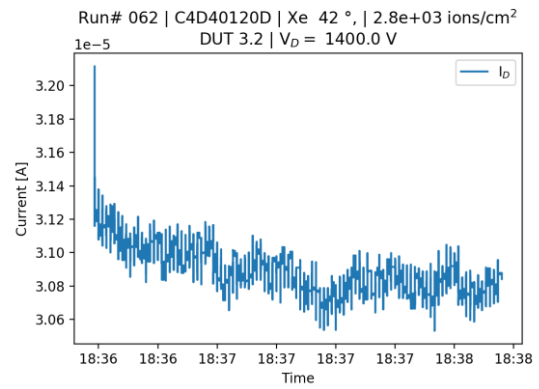
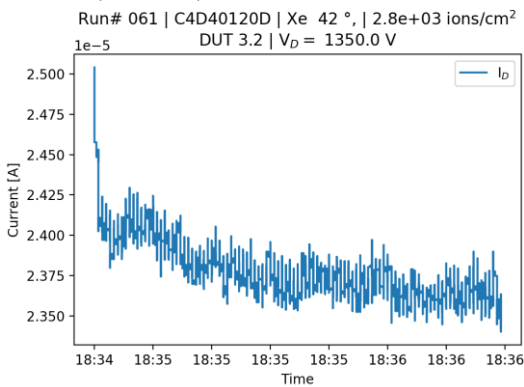


Figure 86: Run# 061, C4D40120D, Xe 42 °, 2.8e+03 ions/cm², DUT 3.2, V_D= 1350.0 V



Run# 062 | C4D40120D | Xe 42 °, | 2.8e+03 ions/cm²
DUT 3.2 | V_D = 1400.0 V

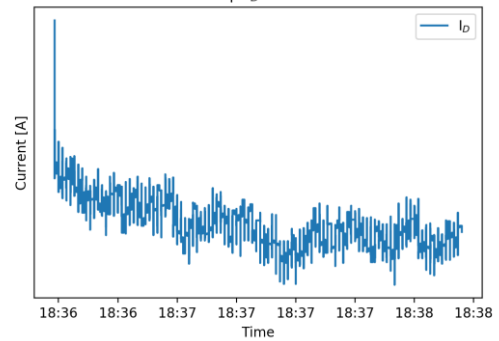
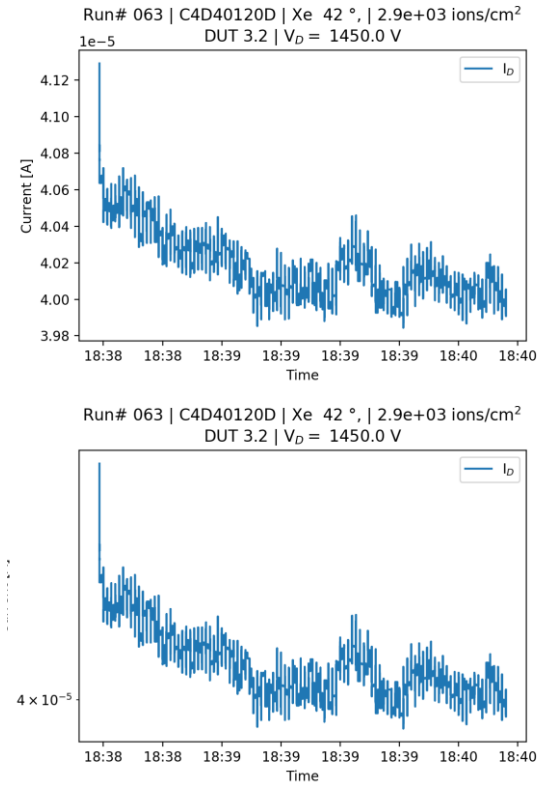


Figure 88: Run# 063, C4D40120D, Xe 42 °, 2.9e+03 ions/cm², DUT 3.2, V_D= 1450.0 V



Run# 064 | C4D40120D | Xe 42 °, | 5.5e+03 ions/cm²
DUT 3.2 | V_D = 1500.0 V

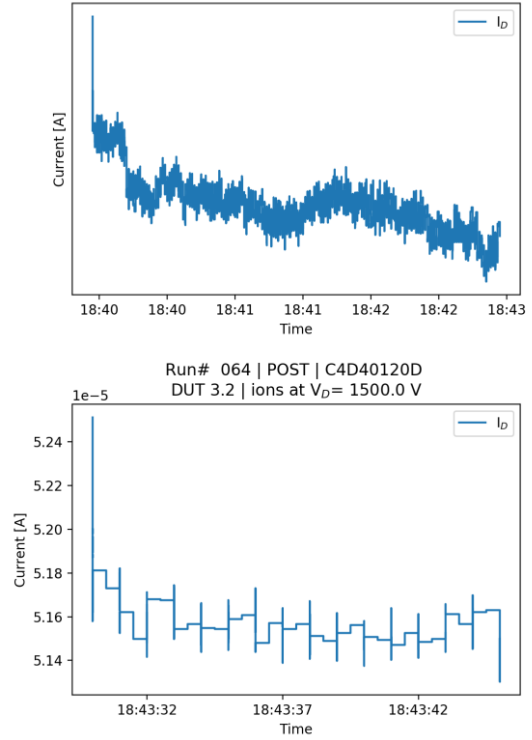


Figure 89: Run# 064, C4D40120D, Xe 42 °, 5.5e+03 ions/cm², DUT 3.2, V_D= 1500.0 V

